

Kristian Søbye Grønvold

Geoelectrical methods for mapping of quick clay in landslide area in Gjerdrum, Norway

Geoelektriske metoder for kvikkleire-kartlegging i et skredområde i Gjerdrum, Norge

Master's thesis in Geotechnical Engineering
Supervisor: Thi Minh Hue Le
Co-supervisor: Ana Priscilla Paniagua Lopez
June 2023



Christos Boufidis, Søren Bjørn

Kristian Søybye Grønvold

Geoelectrical methods for mapping of quick clay in landslide area in Gjerdrum, Norway

Geoelektriske metoder for kvikkleire-kartlegging i et skredområde i Gjerdrum, Norge

Master's thesis in Geotechnical Engineering
Supervisor: Thi Minh Hue Le
Co-supervisor: Ana Priscilla Paniagua Lopez
June 2023

Norwegian University of Science and Technology
Faculty of Engineering
Department of Civil and Environmental Engineering



Norwegian University of
Science and Technology

Abstract

Quick clay landslides can cause extensive devastation impacting human-life and critical infrastructure. This Master's thesis focuses on the investigation of the Gjerdrum area in Norway, following a catastrophic quick clay landslide that occurred in December 2020. A set of geophysical investigations, including Electrical Resistivity Tomography and towed Transient Electromagnetics is analyzed and compared to in situ geotechnical measurements (i.e., rotary pressure sounding, total soundings, and cone penetration test) as well as laboratory testing from a comprehensive collection of samples. The main aim is to establish local resistivity-thresholds for distinct soil materials (i.e., quick clay, unleached clay, landslide mass) in this area, while achieving an understanding of the various factors that influence this.

The results demonstrate a definitive threshold for non-quick behavior in clay when the resistivity measures fell below 10 Ωm . Quick clay was found in a threshold of 10-150 Ωm , while unleached, non-sensitive clay was located between 1-150 Ωm . It was found clear correlation between resistivity, remoulded shear strength and sensitivity. Clay content, bulk density, water content, and plasticity index were found to not have any clear affection on the resistivity of the samples.

A comparison was made between the geophysical methods, in order to assess the usefulness and dependability when applied to investigation of sensitive clays. The analysis revealed that the geophysical measurements exhibit consistent trends and values despite the challenging environment (e.g., noise-sources, landslide debris, and safety measures). Also, this combination of approaches has demonstrated the ability to mitigate certain limitations inherent in each approach. The methods exhibit a notable degree of reliability when their findings are concordant. This thesis also highlights tTEM as an efficient alternative, showing its potential in reducing the required number of geotechnical boreholes within a project or for mapping purposes.

Sammendrag

Kvikkleireskred kan føre til voldsom ødeleggelse som kan ha innvirkning både på menneskeliv og kritisk infrastruktur. Denne masteroppgaven tar for seg undersøkelsene som ble utført i Gjerdrumsområdet i Norge etter det katastrofale kvikkleireskredet i desember 2020. Geofysiske undersøkelser, henholdvis Electrical Resistivity Tomography and towed Transient Electromagnetics er analysert og sammenlignet mot geotekniske undersøkelser (dreietrykkssondering, totalsondering og cone penetration test), samt laboratorieundersøkelser fra en omfattende andel prøvetakninger. Avhandlingen har som mål å etablere lokale resistivitsintervaller for ulike jordmaterialer (kvikkleire, ikke-utvasket leire og skredmasser) i dette området, og forstå diverse faktorer som har innvirkning på dette.

Resultatene viser en definitiv grense for ikke-kvikk oppførsel i leiren når resistivitsmålingene er under $10 \Omega\text{m}$. Kvikkleire ble funnet mellom $10\text{-}150 \Omega\text{m}$, mens ikke-utvasket leire ble funnet mellom $1\text{-}150 \Omega\text{m}$. Det ble funnet tydelige sammenhenger mellom resistivitet, omrørt skjærstyrke og sensitivitet. Leirinnhold, tyngdetetthet, vanninnhold og plastisitetsindeks hadde ingen tydelig innvirkning på resistiviteten i prøvene.

For å vurdere nytteverdien og troverdigheten til de geofysiske undersøkelsene for lokalisering av sensitive leirer, er en sammenligningsstudie utført. Analysen avslørte at de geofysiske undersøkelsene viste sammenlignbare tendenser og verdier til tross for utfordrende forhold i skredområdet. I tillegg har kombinasjonen av metodene vist seg å kompensere for hverandres respektive begrensninger. Metodene har vist seg å ha troverdighet i de tilfeller der de samsvarer godt. Oppgaven trekker også frem mulighetene med tTEM som et effektivt alternativ med potensial til å redusere antall nødvendige borhull i prosjektsammenheng og for kartlegging av kvikkleire.

Preface

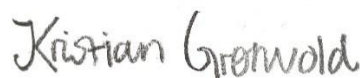
This Master's thesis have been conducted at the Norwegian University of Science and Technology (NTNU) in Trondheim. The thesis equals 30 ECTS and marks the end of the supplementary two years at the MSc programme in Civil and Environmental Engineering, with a course specialization in Geotechnical Engineering. The work was carried out during the spring semester in 2023 after completing a literature study in the autumn semester of 2022. The research has been part of the High resolution Geophysical mapping of the quick clays in Gjerdrum (HiGELIG) project, which is conducted in cooperation with NGI, Viken fylkeskommune, Aarhus Geoinstruments, Geomap Norge and Eskeland Electronics.

First of all, I would like to express my sincere gratitude to supervisor Thi Minh Hue Le at NGI Trondheim, for continued guidance and support throughout the thesis. Thank you for motivating and inspiring meetings and for always providing quick responses and valuable advice. Also, I would like to direct a great thanks to supervisor Ana Priscilla Paniagua Lopez, at NTNU and NGI, for sharing significant articles and for offering appreciated feedback.

A sincere thanks to Saman Tavakoli at NGI Oslo for facilitating the research in Gjerdrum as well as providing this thesis with exceptional insight within geophysical engineering. I would also like to thank Christos Boufidis at Aarhus Geoinstruments for interesting discussions and for contributing with precious knowledge. Many thanks to both of you, for being patient, educational, and competent. Without your contribution, the thesis would have been very lacklustered in terms of the geophysical part. Also, I would like to thank Ragnar Moholdt at NGI for sharing his knowledge of the Gjerdrum area.

Lastly, I would like to thank the rest of the HiGELIG team for allowing me to take part in your research. You have provided me with innovative high-quality geophysical data which have formed a basis for this thesis. Also, I would like to thank the geotechnical personell involved from NGI and Multiconsult for publishing the work that was carried out after the landslide. Without that, this thesis would not have been possible.

Trondheim, 01.06.2023



Kristian Søybe Grønvold

Contents

Acknowledgements	vii
Figures	viii
Tables	ix
Abbreviations/symbols	x
1 Introduction	1
1.1 Background	1
1.2 Previous studies	2
1.3 Research questions and formulations	5
1.4 Scope	5
1.5 Structure of the thesis	5
2 Material & Method	6
2.1 Site description	6
2.1.1 Geological history in Romerike	7
2.1.2 The extent of Gjerdrum quick clay landslide	8
2.2 Geotechnical investigations	13
2.2.1 Boreholes	13
2.2.2 Laboratory	15
2.3 Geoelectrical field work	16
2.3.1 ERT	16
2.3.2 tTEM	18
3 Results	20
3.1 Profile D	20
3.1.1 Comparison between ERT and tTEM	22
3.1.2 Geotechnical interpretations	25
3.1.3 ERT-correlation	28
3.1.4 tTEM-correlation	30
3.2 Other tTEM-profiles	32
3.2.1 L1	33
3.2.2 L2	33
3.2.3 L5	34
3.2.4 L6	35
3.2.5 L7	36
3.3 Resistivity thresholds in Gjerdrum	37
3.3.1 Geotechnical certainty	37
3.3.2 Geoelectrical certainty	37

3.3.3	Predicting quick clay in profile 2 and 4 with geoelectrical data.....	39
3.4	Geotechnical correlation	42
3.4.1	Sensitivity	43
3.4.2	Remoulded shear strength	44
3.4.3	Clay content	46
3.4.4	Salt content.....	48
3.4.5	Other geotechnical parameters	49
4	Discussion.....	50
4.1	Comparison with previous studies.	50
4.1.1	Resistivity-threshold	50
4.1.2	Consistency of geoelectrical surveys	52
4.1.3	Correlation study	54
4.1.4	Reliability and relevance	57
4.1.5	Significance	57
4.2	Solving research questions	57
4.3	Impact of the proposed findings	58
4.4	Assess the study	59
4.4.1	What could have been better?	59
4.4.2	Strong and weak sides of the study	60
4.5	Conclusions and recommendations	61
References	62
Attachments	69
Appendix A:	Profile drawings.....	70
Appendix B:	CPTu-interpretation (Mayne)	71
Appendix C:	Other geotechnical parameters	75
Bulk density	75
Water content	75
Plasticity index	76
Appendix D:	Overview of interpreted boreholes	77

Acknowledgements

This Master thesis is carried out with support from project HIGELIG (project number 332792) financed by the Norwegian Regional Research Fund, Viken and project GEOLAB financed under the European Union's Horizon 2020 research and innovation program (Grant Agreement No. 101006512). Norwegian Geotechnical Institute (NGI) and project partners i.e., Geomap Norway, Eskeland Electronics, Aarhus Geoinstruments and Viken fylkeskommune, are thanked for helping with field work and data processing.

Figures

Figure 1. Development of landslide triggers, adapted from L'Heureux et al., (2018).....	1
Figure 2. Resistivity-threshold of geological targets (Palacky, 1988)	4
Figure 3. Location of Gjerdrum municipality, with respect to Oslo	6
Figure 4. Location of the Gjerdrum landslide area	6
Figure 5. Before the landslide, retrieved from [kart.finn.no], 2020.....	7
Figure 6. After the landslide, retrieved from [cloud.pix4d.com], 8/1/2021.	7
Figure 7. The Romerike area for 9500 ¹⁴ C-years ago (Bargel, 2005).	7
Figure 8. Glacial impact on deposits in the Romerike area (NGU, 2023).....	7
Figure 9. Dronephoto, 18.05.21. Picture credit: Gjerdrum kommune.....	9
Figure 10. Picture taken 11.08.21, Fjellinna. Picture credit: NGI	10
Figure 11. Dronephoto 28.06.21. Picture credit: Gjerdrum kommune.....	10
Figure 12. Dronephoto 29.08.21. Picture credit: Gjerdrum kommune.....	10
Figure 13. Dronephoto 02.09.21. Excavator at work relieving masses behind the kindergarden. Photocredit: Gjerdrum kommune.	11
Figure 14. Inspection 29.03.22. Terrain is smoothed out with gravel on top. Photocredit: NGI	11
Figure 15. Dronephoto 10.06.22. Vertical drainage installed for most of the area south of Fjellinna. Photocredit: Gjerdrum kommune	12
Figure 16. Dronephoto: 30.05.22. The terrain is relieved at the northern edges. Photocredit: Gjerdrum kommune.....	12
Figure 17. Inspection 27.10.22. Clay is filled on top of the layer of gravel. Photocredit: NGI	13
Figure 18. Overview of borehole-locations after the landslide (DiBiagio, 2021; Hovind, 2021; Reutz, 2022)	14
Figure 19. The gradient electrode configuration (Tavakoli, 2011)	16
Figure 20. ABEM LS 2 Terrameter used in Gjerdrum.....	17
Figure 21. The tTEM 3x3 system used in Gjerdrum (Aarhus GeoInstruments, 2022).	18
Figure 22. tTEM-equipment used in Gjerdrum. Photocredit: Christos Boufidis and Søren Bjørn	18
Figure 23. tTEM survey in the landslide area. Photocredit: Christos Boufidis and Søren Bjørn	19
Figure 24. tTEM surveys in zone 3. Photocredit: Christos Boufidis and Søren Bjørn	19
Figure 25. ERT- and tTEM data available in the landslide area	20
Figure 26. Profile D in whole length, with original color scheme and geotechnical layering	21
Figure 27. Profile D, divided into 4 smaller profiles, with a new color-scheme for differentiating layers	21
Figure 28. Profile D-1	22
Figure 29. Profile D-2.....	23
Figure 30. Profile D-3.....	24
Figure 31. Profile D-4.....	25
Figure 32. Profile D, with respect to the landslide area and available boreholes	26
Figure 33. Profile D-1, geotechnical interpretation	27
Figure 34. Profile D-3, geotechnical interpretation	27
Figure 35. Profile D-1, ERT data	28
Figure 36. Profile D-3, ERT data	29
Figure 37. Profile D-1, tTEM data.....	30

Figure 38. Profile D-3, tTEM data	31
Figure 39. Location of tTEM profiles in the landslide area. Green traces marks where tTEM data is available	32
Figure 40. Profile L1	33
Figure 41. Profile L2, 0-200m	33
Figure 42. Profile L2, 200-395m	34
Figure 43. Profile L5, 200-400m	34
Figure 44. Profile L5, 400-550m	35
Figure 45. Profile L6	35
Figure 46. Profile L7	36
Figure 47. Data residuals for tTEM in the landslide area	38
Figure 48. Profile D-2, tTEM data	39
Figure 49. Profile D-2, ERT data	40
Figure 50. Profile D-4, tTEM data	40
Figure 51. Profile D-4, ERT data	41
Figure 52. Overview of sampling locations in Gjerdrum	42
Figure 53. Sensitivity v. resistivity, all data	43
Figure 54. Sensitivity < 100	43
Figure 55. Remoulded shear strength v. resistivity, all data	44
Figure 56. Remoulded shear strength < 1.5 kPa	45
Figure 57. Clay content measurement locations	46
Figure 58. Clay content v. resistivity	46
Figure 59. Clay content < 40 %	47
Figure 60. Salt content measurement locations	48
Figure 61. Salt content v. resistivity	48

Tables

Table 1. Resolution for different geoelectrical methods, adapted from Grønvold, (2022) .	3
Table 2. Overview of geotechnical investigations after the landslide.	14
Table 3. Overview of laboratory testing after the landslide.	15
Table 4. Profile D-1, ERT data	28
Table 5. Profile D-3, ERT data	29
Table 6. Profile D-1, tTEM data	30
Table 7. Profile D-3, tTEM data	31
Table 8. Profile L1, resistivity-thresholds	33
Table 9. Profile L2, resistivity-thresholds	34
Table 10. Profile L5, resistivity-thresholds	35
Table 11. Profile L6, resistivity-thresholds	36
Table 12. Profile L7, resistivity-thresholds	36
Table 13. Overview of resistivity-thresholds	37
Table 14. Resistivity-thresholds in Norway proposed by previous studies.	50
Table 15. Resistivity-thresholds in Gjerdrum proposed by this study.	50
Table 16. Profile drawings	70
Table 17. List of interpreted boreholes	77
Table 18. Simplified layering	77

Abbreviations/symbols

ERT	Electrical Resistivity Tomography
AEM	Airborne Transient Electromagnetics
RCPTU	Cone Penetration Test with Resistivity measurement
tTEM	towed Transient Electromagnetics
DCIP	Direct Current with Induced Polarization
RPS	Rotary Pressure Sounding
TOT	Total Sounding
CPTU	Cone Penetration Test with pore pressure measurement
GPR	Ground Penetrating Radar
RMT	Radio-Magnetotellurics
NIFS	Natural hazards, Infrastructure, Floodings and Slides

1 Introduction

1.1 Background

Quick clay landslides represent a major risk in northern countries, e.g., Norway, Sweden, Canada. In Norway, there has been many catastrophic quick clay landslides, e.g., Rissa 1978, Finneidfjord 1996, Gjerdrum 2020. A profound comprehension of ground conditions, coupled with enhanced precision in the mapping of sensitive materials, is imperative to ensure the safety and stability of areas encompassing sea- and fjord deposits. Figure 1 illustrates the temporal progression of man-made triggers and natural triggers of quick clay landslides over the past decades. The prevalence of quick clay landslides instigated by human activities exhibits a pronounced escalation, particularly during recent years, as substantiated by empirical evidence presented by L'Heureux et al., (2018). Also important seasonal changes in temperature, precipitation, heavy rainfall and flood frequency are expected due to climate change (L'Heureux et al., 2018). The alterations in the environment will lead to increased water infiltration in the ground, increased pore pressure, and increased erosion. Interaction of these factors collectively contributes to reducing the safety factor in natural slopes, giving a greater probability of impending quick clay landslides.

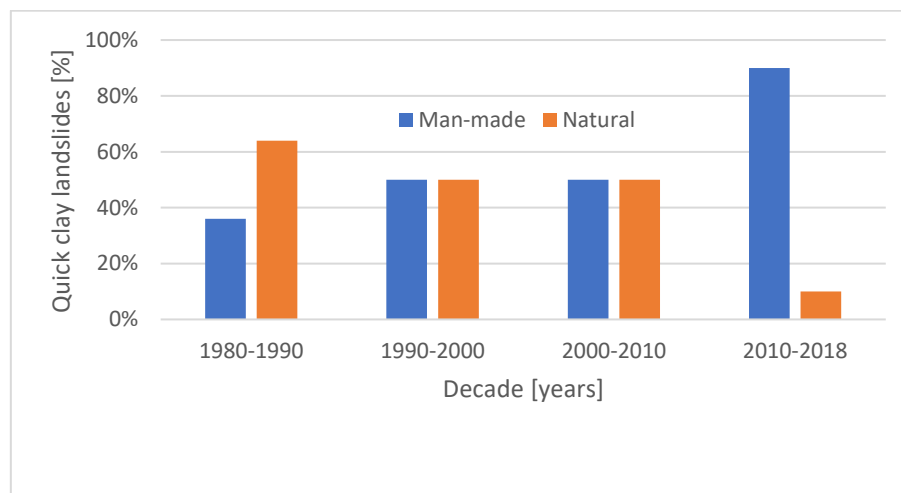


Figure 1. Development of landslide triggers, adapted from L'Heureux et al., (2018)

Regardless of whether it pertains deliberate interventions for constructional projects, or the inherent perils posed by natural hazards compromising stability, it is imperative to undertake comprehensive subsurface mapping to effectively mitigate the risk of quick clay landslides.

The northern regions of the world underwent a significant geological event known as the ice age approximately 20,000 years ago. After being heavily compacted, these areas have been undergoing a gradual process of post-glacial rebound, leading to the formation of clay deposits above the present-day sea levels. These deposits, commonly known as marine clays, exhibit distinct characteristics and can be classified as quick clay based on their leaching history. Leaching is a process in which involves the removal of minerals and other soluble components from the clay through groundwater flow, either by upward

artesian pressure or downward infiltration (Sauvin, 2014). When the salt content in the porewater of marine clay falls below 2 grams per liter, a transformation occurs within the clay structure, leading to the development of a sensitive state characterized by flocculated clay minerals (L'Heureux et al., 2018). Under excessive loading conditions, the sensitive structure of marine clay is disrupted, leading to the transformation of the clay into a fluid-like material.

Traditionally, quick clay areas are mapped using boreholes and sampling. Sounding methods, namely rotary pressure sounding (RPS), total sounding (TOT), and cone penetration test (CPTU), have emerged as prominent geotechnical techniques for gathering necessary geotechnical information. Nonetheless, the verification of quick clay necessitates the essential step of obtaining representative samples from the field and subjecting them to comprehensive laboratory testing to confirm the presence and characteristics of quick clay (see Grønvold, 2022). Although boreholes offer valuable information at specific locations, their extensive cost and time requirements render them impractical for comprehensive projects, often resulting in a limited number of boreholes (Grønvold, 2022). Interpolating between boreholes over greater distances can lead to incorrect or overconservative assumptions about layering, which can be dangerous in potentially unstable terrain. Geophysical methods present a valuable approach for mitigating the uncertainty associated with borehole interpolations. These methods measure resistivity which has previously proven to be a valuable parameter to locate quick clay within the subsurface. Resistivity refers to the inherent property of a material to impede the flow of electrical current (Sandven et al., 2015). Because the resistivity of the soil is highly dependent on the salt content in the pore water, this parameter has the potential of differentiating leached from unleached clay.

In addition to being expensive and time-consuming, geotechnical boreholes are difficult to conduct in demanding terrains (Tavakoli et al., 2022), e.g. sloping or area with restricted access for the drill rig. The search for alternatives that can address the existing gap in quick clay mapping while simultaneously offering non-intrusive, cost-effective, and highly efficient solutions is of utmost importance. Therefore, it is worthwhile to pursue further research on the reliability of geophysical methods to locate or disprove the presence of quick clay deposits.

1.2 Previous studies

Geophysical methods are used in a variety of fields, e.g., environmental studies, mining, geology and civil engineering (Sharma, 1997). In Norway and Sweden, geophysical methods have in the last decade risen in popularity when studying properties and extent of quick clay. Prior research studies concur on the general efficacy of these surveys for the purpose of mapping quick clay deposits. However, most studies highlight the persistent requirement for geotechnical data.

The most used resistivity-measurement is the resistivity cone penetration test (RCPT), see Rømoen et al., (2010), which provides one-dimensional resistivity data in a borehole. Electrical resistivity tomography (ERT) is also frequently used, see Donohue et al., (2012); Lundstrøm et al., (2009); Rankka et al., (2004); Solberg et al., (2012), which measures resistivity in a two-dimensional profile. These two methods are often used in combination, and numerous studies have explored the consistency of these two measurements for the purpose of quick clay mapping (Bazin & Pfaffhuber, 2013; Dahlin et al., 2013; Kalscheuer et al., 2013; Long et al., 2012; Salas-Romero et al., 2016). Mostly, these studies show good agreement between ERT- and RCPT data. A method that have seen increasing use in

later years is airborne transient electromagnetics (ATEM), see Anschütz et al., (2015); Baranwal et al., (2017); Bastani et al., (2017); Lysdahl et al., (2017). In accordance with these prior studies, the ATEM exhibits relatively favorable consistency with both RCPT and ERT. Resistivity-measurements with electromagnetics can also be conducted using a ground-based system. The towed transient electromagnetic (tTEM) system, presented in Auken et al., (2019), is a newer, ground-based method that provides higher resolution than the ATEM. Rydman, (2021) has demonstrated that tTEM can be a useful tool for quick clay mapping in Sweden. In Norway, tTEM was used for the first time in the HiGELIG project (NGI et al., 2022). This Master’s thesis utilizes selected data from this project to investigate its research questions.

Table 1. Resolution for different geoelectrical methods, adapted from Grønvold, (2022)

Method	Resolution [m]	Resolution controlled by:	Source
RCPT	0.01 – 0.10	-	(Sandven et al., 2015)
ERT	1 – 2.5	Electrode spacing: 2m spacing = 1m resolution	(Personal com. Tavakoli, 2022)
tTEM	4 – 10	Higher resolution when subsurface has frequent change in conductivity	(Personal com. Boufidis, 2023)
ATEM	10 – 100	Highly dependent on equipment	(Sandven et al., 2015)

The geophysical methods differ in terms of costs, resolution, accuracy and effectiveness. RCPT data are only given in a singular point; however, it provides exceptional resolution and accuracy in resistivity. This measurement requires a borehole and cannot be considered non-intrusive like other geophysical methods. Boreholes are expensive and should not be considered effective or cheap compared with other methods. Based on several previous studies (Bazin & Pfaffhuber, 2013; Long et al., 2012; Solberg et al., 2016), RCPT data show good coherence with other geophysical methods. For two-dimensional geophysical mapping, the ERT usually provides the best resolution. The tTEM have slightly lower resolution, but is a decent alternative compared to ATEM, see Table 1. There are limited number of studies comparing the accuracy between ERT- and tTEM data. However, in some studies, ERT-profiles have been directly compared to ATEM data, see e.g. Solberg et al., (2016); With et al., (2022). Based on these studies, ATEM derived data appear to exhibit comparable values to ERT in a majority of cases. Anschütz et al., (2015) found that ATEM clearly were able to separate leached from unleached deposits. However, ATEM data have a disadvantage in detecting leached clay deposits situated in proximity to high resistivity materials, such as bedrock or moraine (Sandven et al., 2015). In such instances, the method may be unable to discern the transition due to its low resolution. tTEM and ERT provide greater resolution than the ATEM and should have clear advantages when dealing with these issues, while still providing two-dimensional profiles. In terms of effectiveness and costs, ATEM should be considered the most effective for mapping greater areas. Christensen et al., (2021) demonstrated how ATEM data combined with a reduced amount of geotechnical data and machine learning can provide a useful geotechnical basis in big projects. Rydman, (2021) showcased the capability of ATEM data to offer a preliminary overview of large areas, while tTEM data can be employed in areas where enhanced resolution is required for more detailed subsurface investigations. tTEM is anticipated to offer notable advantages in terms of efficiency, particularly when compared to ERT, for survey areas exceeding a few hectares (Auken et al., 2019). This is primarily

attributed to the necessity of frequent movement of ground electrodes during data collection using ERT, in order to obtain reliable and high-quality data for larger areas.

As elucidated earlier, there is typically a strong agreement and consistency observed among the resistivity values obtained from various geoelectrical methods. However, extensive research has demonstrated that resistivity values exhibit geographical variations across different locations. The general consensus in Norway is that leached, possible quick clay is located between 10-100 Ωm , see e.g. Anschütz et al., (2015); Baranwal et al., (2017); Long et al., (2012); Sauvin et al., (2014). Other studies propose a slightly lower threshold of 10-80 Ωm (Donohue et al., 2012; Kalscheuer et al., 2013; Lysdahl et al., 2017; Pfaffhuber et al., 2014; Solberg et al., 2008). Some studies also show an even narrower range of resistivity-values when using RCPT. Solberg et al., (2012) observed a range of 15-60 Ωm , while Bazin & Pfaffhuber, (2013) proposed quick clay between 10-65 Ωm . Most of the studies agree that unleached marine clay is located below this limit, between 1-10 Ωm . Dry crust clay deposits and coarse sediments will possess values above 100 Ωm (Shan et al., 2014; Solberg et al., 2012).

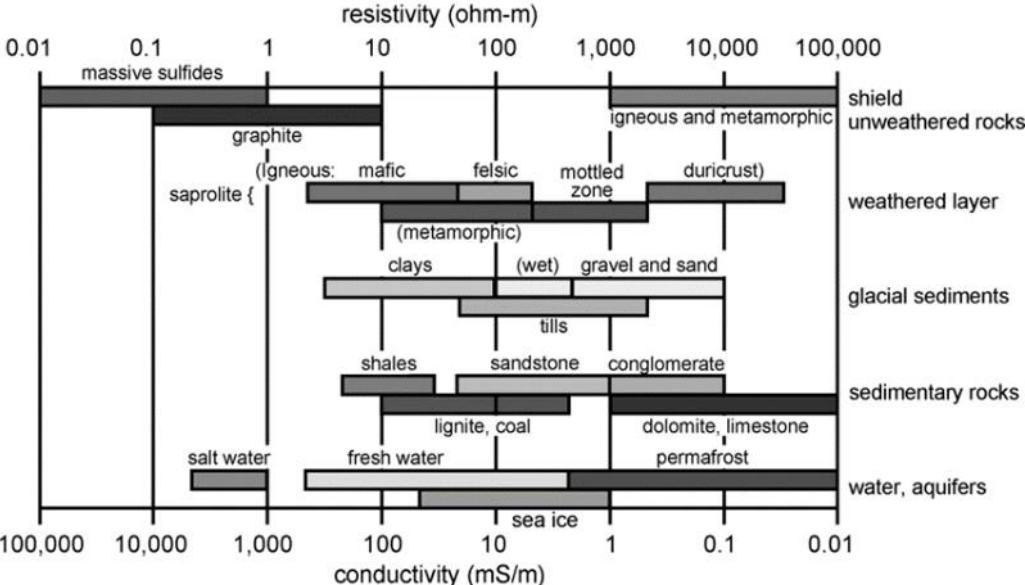


Figure 2. Resistivity-threshold of geological targets (Palacky, 1988)

In Sweden, With et al., (2022) have located quick clay for resistivity-values as low as 3 Ωm . However, the majority of studies ultimately arrive at the conclusion that quick clay deposits are situated beneath the proposed 10 Ωm -limit in Norway (Dahlin et al., 2013; Löfroth et al., 2017; Rankka et al., 2004). Three studies from Fråstad agree on the 10-80 Ωm -interval (Rydman, 2021; Salas-Romero et al., 2016; Shan et al., 2014). The difference in this lower limit between Norwegian and Swedish clay can be attributed to a higher proportion of clay content in certain Swedish quick clay deposits (Dahlin et al., 2013; Sandven et al., 2015). As these intervals vary a lot, multiple studies recommend to establish local resistivity-thresholds for different sites (Löfroth et al., 2017; Pfaffhuber et al., 2014; Rømoen et al., 2010b).

The integration of geotechnical and geophysical data is a well-established approach in the field of quick clay mapping. Mostly, the previous studies conclude that geophysical methods can contribute to limit the necessity of boreholes, while making the mapping more precise and effective (Baranwal et al., 2017). Geophysical methods are attractive to implement within quick clay mapping because they offer compelling advantages, primarily due to their

potential to enhance cost-efficiency, effectiveness, and safety. While being non-intrusive and non-destructive they allow for continuous acquisition of 2D or 3D information over large areas (Tavakoli et al., 2022). The HIGELIG project aims to explore the value of a well-constrained 3D model of the subsurface. This will reduce uncertainty associated with unconstrained 2D data. The HIGELIG project also proposes an innovative element of the tTEM within geophysical quick clay mapping. ERT profiles are also available for comparative analysis with the tTEM-derived data in specific areas. Integration of these two high-resolution methods will provide a comprehensive dataset which hopefully can contribute to increase the accuracy of quick clay mapping.

1.3 Research questions and formulations

The main aim of this study is to investigate resistivity-values for known quick clay zones in Gjerdrum, using innovative methods. To acquire this information, the following tasks are proposed:

- Provide resistivity-thresholds for non-leached clay, leached clay, and dry crust clay in the area, based on geotechnical boreholes.
- Explore geophysical method tTEM's ability to differentiate between leached and unleached clay.
- Assess the effectiveness of tTEM in conjunction with the geophysical method ERT to explore its utility for mapping of quick clay.

The second aim of this study is to achieve a better understanding of the geotechnical parameters that affect resistivity in clay. The study will mainly focus on these parameters:

- Salt content
- Clay content
- Sensitivity
- Remoulded shear strength

The third aim is to investigate the correlation between the Mayne-approach (Mayne et al., 2019) and soundings and samplings conducted in Gjerdrum.

1.4 Scope

Multiple geophysical methods exist that possess potential for quick clay mapping, e.g., seismic refraction, magnetometry. Some of these methods were also included in the HIGELIG project. This study is limited to evaluation of geophysical methods that measure resistivity using current injection or potential difference. These are often referred to as "geoelectrical" methods (Personal com. Tavakoli 2022).

1.5 Structure of the thesis

This thesis consists of 4 chapters and is structured using the IMRoD-model. Chapter 2 provides an exposition on the study's location and methodology for obtaining the results. In chapter 3, the results are presented objectively and uncertainty in the different data is shortly accounted for. In chapter 4, the results are thoroughly discussed. First, they are compared to various previous studies. Then, the significance, relevance and reliability of the results are considered. The research questions proposed in 1.3 are answered and the impact of this is debated. Lastly, the study is assessed before final conclusions and recommendations are made.

2 Material & Method

2.1 Site description

The study area for this thesis is Gjerdrum, a municipality in Norway, located about 30km northeast of Norway's capital Oslo, see Figure 3. Gjerdrum has about 7000 residents (OED, 2021), and has in recent decades been marked by population growth. The administrative center, Ask, has emerged as a focal point for prioritized constructional projects aimed at accommodating the expanding population (OED, 2021). The natural environment is characterized by fertile clay soil areas located below the marine limit, as well as extensive forested regions.

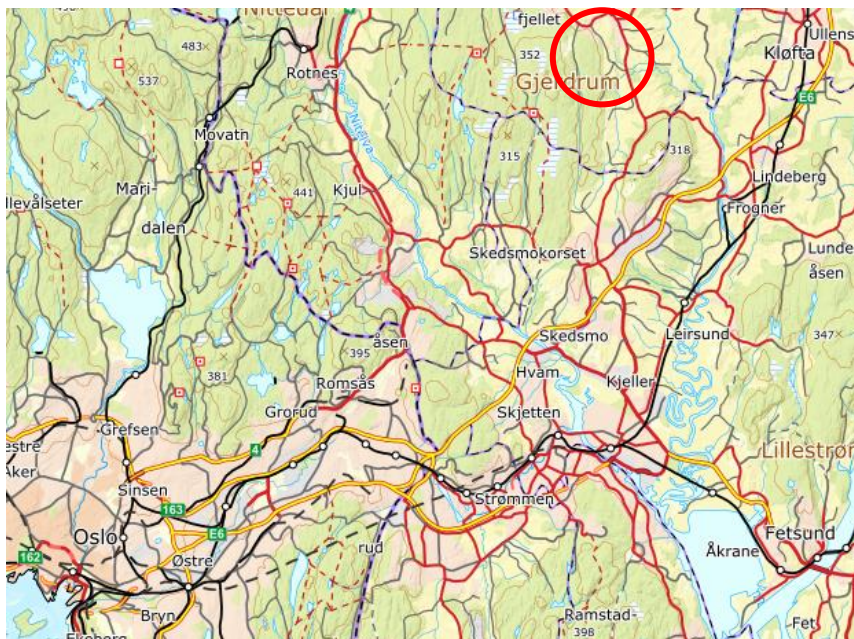


Figure 3. Location of Gjerdrum municipality, with respect to Oslo

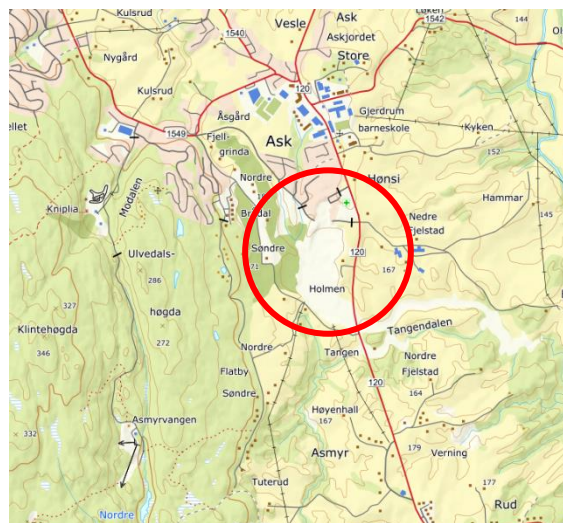


Figure 4. Location of the Gjerdrum landslide area

On December 30, 2020, a devastating quick clay landslide occurred near the administrative center of Ask in Gjerdrum, as depicted in Figure 4. This catastrophic event resulted in the tragic loss of eleven lives, including an unborn baby, necessitated the evacuation of over 1600 individuals, and caused extensive damage to both property and the environment (Grønvold, 2022). Following the landslide, the topography of the affected area underwent significant transformations, as illustrated in Figure 5 and Figure 6.

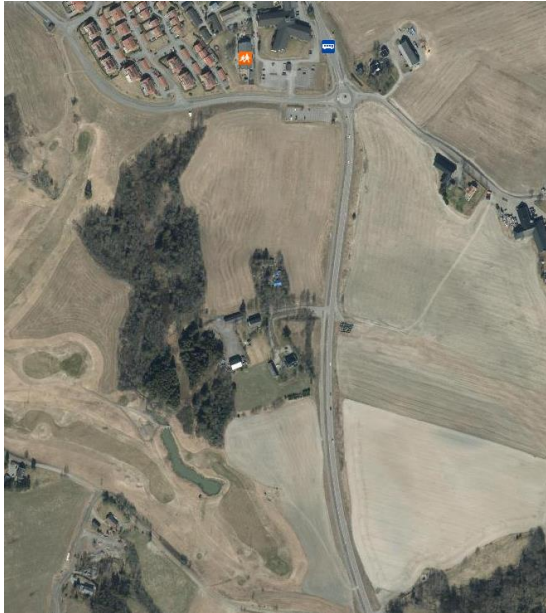


Figure 5. Before the landslide, retrieved from [kart.finn.no], 2020.

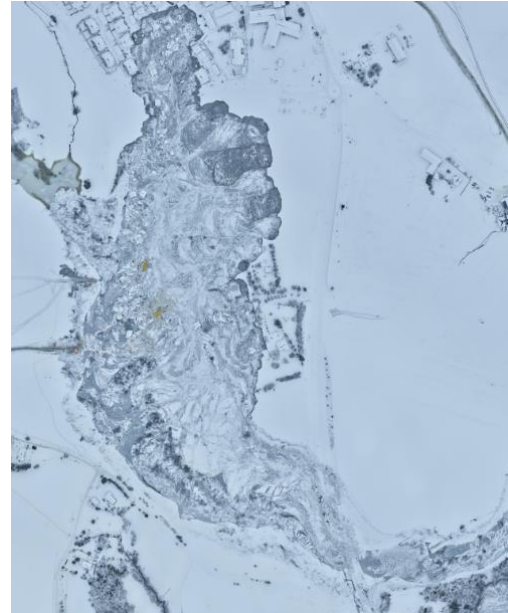


Figure 6. After the landslide, retrieved from [cloud.pix4d.com], 8/1/2021.

2.1.1 Geological history in Romerike

The marine deposits found in Gjerdrum are largely attributed to the melting of glacial ice, which happened in this area (locally denoted Romerike) for 9500¹⁴C-years ago (Bargel, 2005). This process had significant impact on the formation of these deposits, resulting in distinct characteristics in the grain distribution and layering of soil materials (OED, 2021).

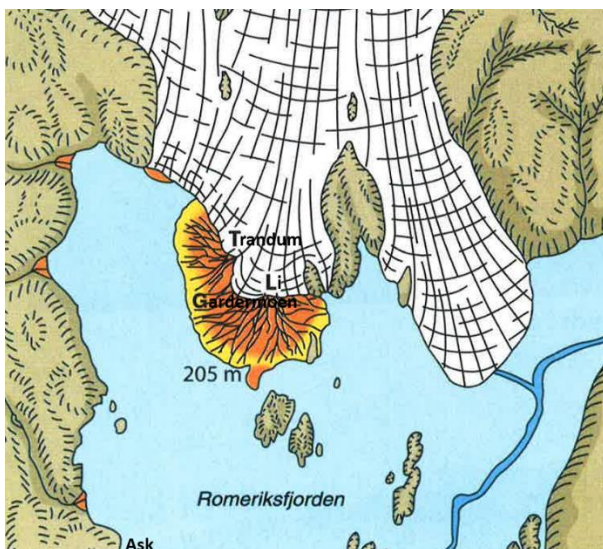


Figure 7. The Romerike area for 9500 ¹⁴C-years ago (Bargel, 2005).

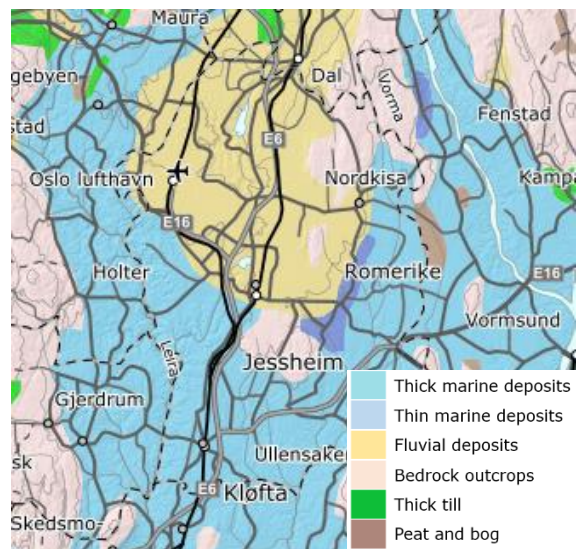


Figure 8. Glacial impact on deposits in the Romerike area (NGU, 2023).

The deglaciation process occurred in multiple stages, during which the glacier remained stationary and deposited substantial quantities of coarse materials in certain regions (Bargel, 2005). The primary stage of deglaciation led to the significant accumulation of fluvial deposits situated in the Gardermoen region, see Figure 8. In this area, an outwash plain, see the orange area in Figure 7, was formed by the convergence of two glacial deltas, namely Trandum and Li. This outwash plain rose 17 meters above the sea level of Romeriksfjorden, and is often referred to as Hauersetersanduren (Bargel, 2005). This became a delta that deposited finer materials like silt and clay, into Romeriksfjorden. In Figure 7 and Figure 8, one may see how Hauersetersanduren has formed the fluvial deposits of the Gardermoen region. One may also see how the present exposure of the thick marine deposits in Romeriksfjorden is a direct result of the postglacial rebound, which refers to the uplift of land after the retreat of the glacier.

After the land rose above the sea-level, rivers and streams started to slowly erode deeper into the sediments (OED, 2021). Due to erosion as well as gradual quick clay formation, due to leaching of minerals, Romerike is characterized by numerous ravines and traces of hundreds of greater and lesser quick clay landslides (Bargel, 2005). In the studied region, the marine limit is situated at an elevation of approximately 180 meters above sea level. Currently, the sea- and fjord deposits are found at an elevation of 160-170 meters above sea level, which is approximately 10-20 meters lower than the marine limit in this particular area. Since the sea- and fjord depositions were formed during the melting of the ice, the silty clay or clayey silt may also contain significant amounts of sand, gravel and stones. Romerike is consequently characterized by a pattern of alternating layers of clay, silt and coarser materials, which is likely a result of complex geological processes that have occurred in the region over time. Generally, quick clay is often formed in pockets or layers in the ground and in slopes towards rivers or lakes (OED, 2021). If the clay contains thin layers of coarser materials such as silt or sand, the leaching process may occur faster. Through further leaching, more stabilizing ions can be added to the quick clay through groundwater to make the clay more stable. In this case it is considered that the clay has passed its quick state. Near the ground surface, a thick dry crust often develops which is not quick. The dry crust clay is usually much firmer than the deeper loose deposits.

Moraine can also be found below the marine deposits (OED, 2021). In several places moraine lays exposed in canyons and landslide pits and along river cuts. The moraine in the area is mostly sandy (Longva, 1987), while the bedrock outcrops consist mainly of gneiss (Olerud, 1982). Previous geotechnical data in the Romerike region indicate significant variations in the rock surface, and the depth to the bedrock in the area can reach up to 110 meters (NGU, 2023). Areas near bedrock will often exhibit quick clay.

2.1.2 The extent of Gjerdrum quick clay landslide

The detachment area of the Gjerdrum quick clay landslide was around 120 000 m² (OED, 2021). The length of the landslide pit from the release area in the south, to Nystulia in the north was around 630 meters. The width of the pit was 240 meters at the widest. The bottom of the pit was around 22 meter below original terrain at the deepest. The volume of the masses that was released during the landslide was around 1.35 million m³. The volume the of displaced material that remained in the landslide pit was around 0.47 million m³ (Penna & Solberg, 2021).

The outlet area was around 260 000 m² (OED, 2021). The length from the bottom of the outlet area to where the landslide mass stopped, was around 2 km. Here, the landslide mass was up to 11 meters above original terrain. Volume of displaced material in the outlet area amounted to around 0.93 million m³.

On May 16th, 2021 a smaller landslide on the eastside of the landslide-pit destroyed an additional two houses that were standing on the landslide edge, see Figure 9 (Moholdt & DiBiagio, 2021b).



Figure 9. Dronephoto, 18.05.21. Picture credit: Gjerdrum kommune

After this, there have been multiple smaller slides at the edge near Fjellinna, mainly smaller peelings in July, and bigger slides in August, 2021.



Figure 10. Picture taken 11.08.21, Fjellinna. Picture credit: NGI

Figure 11 and Figure 12 shows the development of the landslide in Fjellinna through the summer of 2021 (Moholdt & DiBiagio, 2021b).



Figure 11. Dronephoto 28.06.21. Picture credit: Gjerdrum kommune



Figure 12. Dronephoto 29.08.21. Picture credit: Gjerdrum kommune

To stop further landslides, about 2.5 meters of mass was removed from the top of the edges in these areas. First, a wide trench was dug out some meters away from the edge, see Figure 13. Then, masses were relieved at the edge of the landslide pit (Moholdt & DiBiagio, 2021b).



Figure 13. Dronephoto 02.09.21. Excavator at work relieving masses behind the kindergarden. Photocredit: Gjerdrum kommune.



Figure 14. Inspection 29.03.22. Terrain is smoothed out with gravel on top. Photocredit: NGI

Vertical drains were installed in the landslide area to ensure that the filled masses consolidated faster. To install the vertical drains the apparent obstacles like asphalt and concrete were removed from the pit and the terrain of the pit was then leveled. This was done using clay from relieved areas. After smoothing out the pit, a layer of permeable masses was added to ensure drainage of the area (Bache, 2021), see Figure 14. The length of the vertical drains varies with depth to bedrock, from 4 to 24 meters.



Figure 15. Dronephoto 10.06.22. Vertical drainage installed for most of the area south of Fjellinna. Photocredit: Gjerdrum kommune

Also in the northern areas of the landslide pit, about 2 meters of mass was removed at the landslide edge to make sure that the slope was not steeper than 1:4 (Moholdt & DiBiagio, 2021a).



Figure 16. Dronephoto: 30.05.22. The terrain is relieved at the northern edges. Photocredit: Gjerdrum kommune

Further, clay-mass was added on top of the gravel. Counterfillings have been established at the edges south of Fjellinna, and all around the northern edge of the landslide, because of the low safety factor in these areas (DiBiagio & Heyerdahl, 2022).



Figure 17. Inspection 27.10.22. Clay is filled on top of the layer of gravel. Photocredit: NGI

These interventions were done in the area, from when the landslide occurred until all the geotechnical and geoelectrical investigations were finished. This must be born in mind when comparing the data. Due to the prolonged duration of the investigations, it is possible that the study area is not entirely consistent between the different phases of the research.

2.2 Geotechnical investigations

2.2.1 Boreholes

Prior to the quick clay landslide in the Gjerdrum area, approximately 200 boreholes had been drilled as part of various projects in the region. Following the occurrence of the landslide, two rounds of geotechnical investigations were carried out in the area. The initial investigations were conducted as emergency assistance to identify the cause of the landslide, to review the evacuation plan and to develop mitigation measures. These investigations were carried out from 30.12.20 to 02.02.21 by NGI and Multiconsult (DiBiagio, 2021; Hovind, 2021). The geotechnical drilling rigs used was GM 85GT and Geotech 605. During the initial investigations, NGI conducted geotechnical surveys to the north of Fjellinna and west of the landslide area, see DiBiagio, (2021). Multiconsult conducted investigations south of Fjellinna, see Hovind, (2021). Between 12.08.21 and 13.07.22, a second phase of geotechnical investigations was carried out by NGI to conduct a comprehensive evaluation of the stability and safety of the landslide area (Reutz, 2022).

Table 2. Overview of geotechnical investigations after the landslide.

Abbreviation	Report nr.	Time period		Rotary pressure sounding	Total sounding	Cone penetration test	Sampling
NGI-01	20200909-01-R	30.12.20-02.02.21		-	50	33	33
M-01	10223695-02-RIG-RAP-002	30.12.20-02.02.21		19	28	29	7
NGI-02	20200909-02-R	12.08.21-13.07.22		46	4	55	15
			Total	65	82	117	45

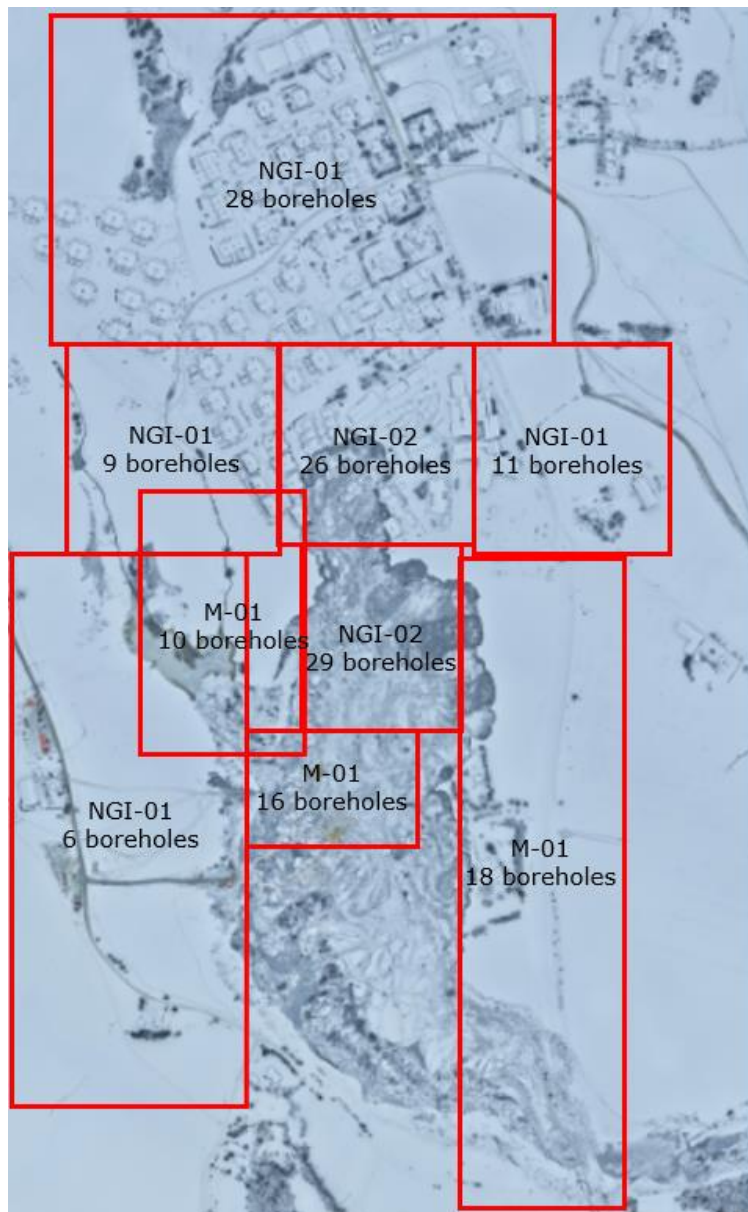


Figure 18. Overview of borehole-locations after the landslide (DiBiagio, 2021; Hovind, 2021; Reutz, 2022)

Through this study, 153 newer boreholes and 101 older boreholes have been interpreted to evaluate the ground conditions in the area, see Appendix D: Overview of interpreted

boreholes. These boreholes consist largely of either rotary pressure- or total soundings. One of these investigations is included in almost every borehole. Total sounding and rotary pressure sounding give indications on sensitive clay and can also provide a picture of the subsurface layering. An approximately steep or negative sounding curve indicate quick clay (Grønvold, 2022). Cone penetration test is also frequently used to investigate layering and geotechnical parameters. The CPTU measure pore pressure and sleeve friction as well as tip resistance and is well equipped to differentiate layers (Sandven et al., 2017). This is not a preferred investigation to indicate quick clay. However, methods have been proposed for this matter, e.g. Robertson charts (Robertson, 2010), NIFS classification parameters (Sandven et al., 2015), preconsolidation stress approach (Mayne et al., 2019), see Grønvold, (2022) for examples. Sampling and laboratory tests are necessary to confirm quick clay. The samples are collected using Ø54 mm and Ø72 mm piston samplers. Ø72 mm tends to give samples of higher quality than the Ø54 mm. Piezometers are also installed in Gjerdrum and are of type Geotech PVT with memory and Geokon 4500DP (DiBiagio, 2021; Hovind, 2021; Reutz, 2022). These instruments measure pore pressure which is useful in calculation of in-situ stresses and estimating the groundwater level.

2.2.2 Laboratory

The samples are examined in NGI- and Multiconsult's geotechnical laboratories in Oslo. Every sample is registered, opened, and visually classified. Index-testing includes measurements of bulk density (γ), water content (w), and undrained shear strength (S_u). Undrained shear strength is obtained using both the fall cone test and uniaxial equipment. Through the fall cone test, see NS 8015, (1988) the remoulded shear strength (S_{ur}) and sensitivity (S_t) are also obtained, as well as the fall-cone liquid limit (w_L), see NS 8002, (1982). The plastic limit is obtained in accordance with NS 8003, (1982). The Plasticity-index (I_p) is estimated using equation: $I_p = w_L - w_p$. Grain distribution is analyzed using the "Falling-Drop" method, see NS 8005, (1990). Determination of salinity is done by expelling pore water from a clay sample using a centrifuge (Hovind, 2021). Then the electrical conductivity of the pore water is measured using the Hanna HI 9835 equipment. The value is compared with empirical values, and the concentration of salt is found. The triaxial test provides estimates of shear strength and pore pressure parameters (Sandven et al., 2017). This test aims to determine development of stress-strain relation of the soil sample up to failure. Both passive extension tests, and active compression tests were performed on selected samples from Gjerdrum. Four direct shear tests were also carried out to decide shear strength under horizontal shearing, following the method proposed by Bjerrum & Landva, (1965). The samples were consolidated to assumed vertical in-situ stress before loaded to failure (Reutz, 2022). Oedometer-tests are also carried out to decide consolidation- and deformation properties, and to estimate the effective preconsolidation stress p_c' (DiBiagio, 2021).

Table 3. Overview of laboratory testing after the landslide.

Abbreviation	Report nr.	Index-testing	Triaxial	Oedometer	Grain distribution	Salinity	Plasticity-index	DSS
NGI-01	20200909-01-R	152	15	13	21	-	92	-
M-01	10223695-02-RIG-RAP-002	88	21	28	38	14	59	-
NGI-02	20200909-02-R	75	15	27	5	-	55	4

2.3 Geoelectrical field work

The multidisciplinary fieldwork of the HiGELIG project was carried out from 05.09.22 to 23.09.22 (NGI et al., 2022). For HiGELIG, ERT was conducted by NGI, Eskeland Electronics and Geomap Norway. The tTEM data was collected by Aarhus Geoinstruments. Both these investigations provide the resistivity of the subsurface by inducing different types of current, and then measure the potential difference. Resistivity is a measurement of the material's ability to resist flow of electricity (Sandven et al., 2015). To find the resistivity in the soil, the resistance R is first found from Ohm's Law (Tavakoli, 2011):

$$R = \frac{V}{I} [\Omega]$$

where V is the potential difference in volt, and I is the induced current in ampere. The resistivity (ρ), is calculated as an inherent property of the soil volume (Tavakoli, 2011):

$$\rho = R \frac{A}{L} [\Omega m]$$

where A is the cross section of the investigation area in m^2 , and L is the length of the cross section. The resistivity of the soil is given in Ωm , and varies primarily with salt content of the pore water within the material (Sauvin, 2014). This information is valuable in assessing the extent of leaching observed in a clay. Resistivity-values are also affected by water content, grain distribution, presence of organic fluids, temperature, etc. (Sandven et al., 2015; Sauvin, 2014).

2.3.1 ERT

The ERT uses direct currents to measure apparent resistivity in the subsurface (Tavakoli, 2011). A DCIP (Direct Current with Induced Polarization) profile was carried out close to the landslide area (NGI et al., 2022). In the HiGELIG project, this profile is referred to as Profile D. An ERT profile can be conducted using different array configurations. These configurations vary in how the I- and V-electrodes are organized along the profile. Each configuration has a geometrical factor K which is industry-standard and helps calculate the apparent resistivity in the profile (NGF, 2019; Tavakoli, 2011):

$$\rho_a = KR$$

The direct current measurement was carried out using the gradient electrode configuration, see Figure 19. This configuration uses multiple electrode combinations (Dahlin & Zhou, 2006), which drastically increases the survey-speed while allowing for larger survey areas, at the cost of minor resolution-loss (Personal com. Tavakoli, 2022).

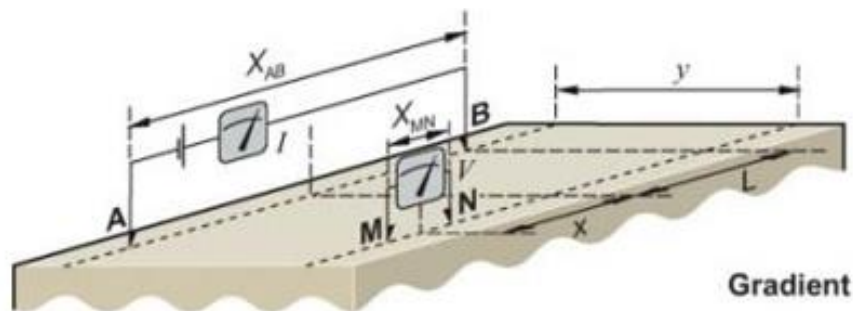


Figure 19. The gradient electrode configuration (Tavakoli, 2011)

For data acquisition, an ABEM LS 2 Terrameter was used with a spread of $n \times 21$ electrodes, where “ n ” is the number of cables used (NGI et al., 2022). The recommended cable layout was used with four cables of 21 take-outs (ABEM, 2016). By implementing this procedure, high near surface resolution was acquired as well as high resolution towards the end of the measured section. The Terrameter was powered from an external battery.



Figure 20. ABEM LS 2 Terrameter used in Gjerdrum

The chosen cable layout resulted in an electrode spacing of 5 meters. This setup gives an approximate vertical resolution of around 2.5 meters. Accordingly, the ERT should have the capability of distinguishing soil layers with thickness of at least 2.5 meters. The total length of the profile was 400 meters, which should be able to provide resistivity-values to approximately 60-70 meters depths. To generate a 2D resistivity distribution for a given profile, the measured apparent resistivity values are processed using inversion algorithms such as Res2DINV (Loke, 2013). For Gjerdrum, inversion of profile D was done using two different algorithms, Res2DINV and AarhusINV (NGI et al., 2022).

When inverting the data, it is important to account for noise (Personal com. Tavakoli, 2022). Common sources of noise that can affect ERT-measurements are pipelines, cables, or EM-coupling. The latter varies with array configuration and usually only contributes to minor noise. ERT-measurements are usually affected by some noise, and this was also the case for the measurements done in Gjerdrum (Personal com. Tavakoli, 2023). The origin of the noise or bad data in this profile has not been investigated but is probably highly influenced by the safety measures carried out in the landslide area, see 2.1.2. To account for noise, geophysicists define a preliminary noise level and apply it to the data, often as standard deviations plus a fixed value, e.g., 5% x minimum data. After this, several inversions are tested until the optimal model is acquired.

Induced polarization (IP) is often performed in combination with resistivity-measurement and measures the discharge in the subsurface after being subjected to a direct current (Tavakoli, 2011). IP measurements in this profile indicated a high signal-to-noise ratio, meaning that the data was highly affected by noise. Clay is expected to demonstrate high IP signature (Personal com. Tavakoli, 2023). However, this was not found for this profile for unknown reasons. The IP measurements also generate lesser depths and reached a maximum of 15 meters. This is ultimately not deep enough to locate quick clay for the entire profile.

2.3.2 tTEM

In Gjerdrum, the tTEM 3x3 system was used, see Figure 21. This system provides high-resolution data and is a ground based system that has operated at 15-20 km/h driving speed (NGI et al., 2022). Here, the TX-coil is located inside a frame with dimensions 3x3m. The TX- and RX-coils are installed on movable platforms and the coil centers are in this case positioned 9 meters apart from each other. This provides vertical resolution of about 4.5 meters (Personal com. Tavakoli, 2022). A GPS is located on the TX platform, while the transmitter electronics, receiver and power supply are placed in the back of the ATV (Aarhus GeoInstruments, 2022).

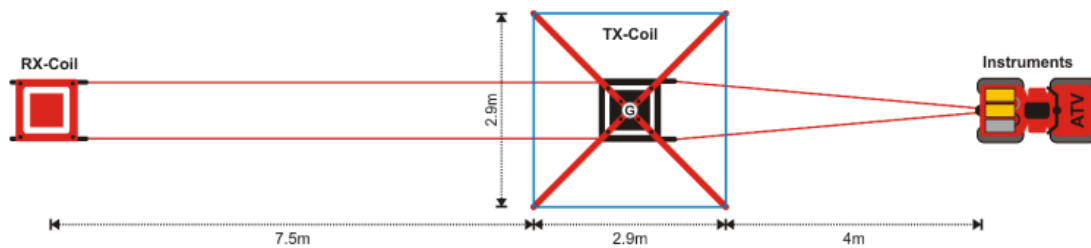


Figure 21. The tTEM 3x3 system used in Gjerdrum (Aarhus GeoInstruments, 2022).

The tTEM induces alternating currents to measure apparent resistivity (Tavakoli, 2011). The alternating currents are induced through the transmitter coil, also known as the TX-coil, and create a static primary magnetic field in the ground (Grønvold, 2022). The current is now abruptly shut off, creating eddy currents that circulates in the subsurface. From these currents, a secondary magnetic field is created. This field is continuously decaying as the resistance in the ground weakens the eddy currents. The receiver coil, also known as the RX-coil, measures the attenuation of these currents and provides information about the resistivity of the ground (Auken et al., 2019).



Figure 22. tTEM-equipment used in Gjerdrum. Photocredit: Christos Boufidis and Søren Bjørn

The measurements in Gjerdrum were conducted using two transmitter moments (NGI et al., 2022). A low (3A) and a high (30A) transmitter moment were applied sequentially, typically taking about 0.5 seconds per sequence. The lower moment is useful to receive shallow data, while the higher moment is able to reach deeper. During one sequence, several hundred transient measurements are recorded. The position of the TX-platform is also recorded through the GPS, as well as instrument parameters like temperature, current and voltage levels for quality control of data.



Figure 23. tTEM survey in the landslide area. Photocredit: Christos Boufidis and Søren Bjørn

Noise is also problematic for electromagnetic surveys. These surveys can be affected by either telluric noises (Personal com. Tavakoli, 2022), e.g., electrical flow in the subsurface, or human activity, e.g., instruments or metallic objects near the measurement area. It was observed that the noise level was high, leading to a limited penetration depth of the signal (Personal com. Boufidis, 2023). Moreover, due to the presence of numerous noise sources within the landslide area, significant data removal were necessary for the geophysicists to obtain reliable results. The reasons for this may be underground cables or metal that were broken in the landslide, and still lie in the subsurface. This, combined with a gravelly and uneven surface, see Figure 23, contributed to reducing the survey speed to about 3 km/h. In other areas, the data and the results were considered very good, due to a good signal-to-noise ratio and data residuals within an acceptable range.



Figure 24. tTEM surveys in zone 3. Photocredit: Christos Boufidis and Søren Bjørn

To assess the efficiency of the inversion, Aarhus Workbench operates with a parameter called "Data Residual" (Personal com. Boufidis, 2023). This parameter gives an idea of how well the data is fitted. In the landslide area, this parameter varies from 0 to 3.5. The data residual values are normalized with the standard deviation of the data. Here, values below 1 translate to a fit within one standard deviation. The higher the value, the further the data is from the standard deviation, which indicates that the inversion could not fit the data well. This ultimately means that the resulted inverted model differs from the resistivity that was recorded. Even though the resistivity might differ slightly, results with higher data residuals can still be considered reliable.

3 Results

3.1 Profile D

Resistivity measurements were conducted in profile D within the landslide area using ERT and tTEM. The ERT profile is depicted in Figure 25. Recorded tTEM data is displayed as green traces.

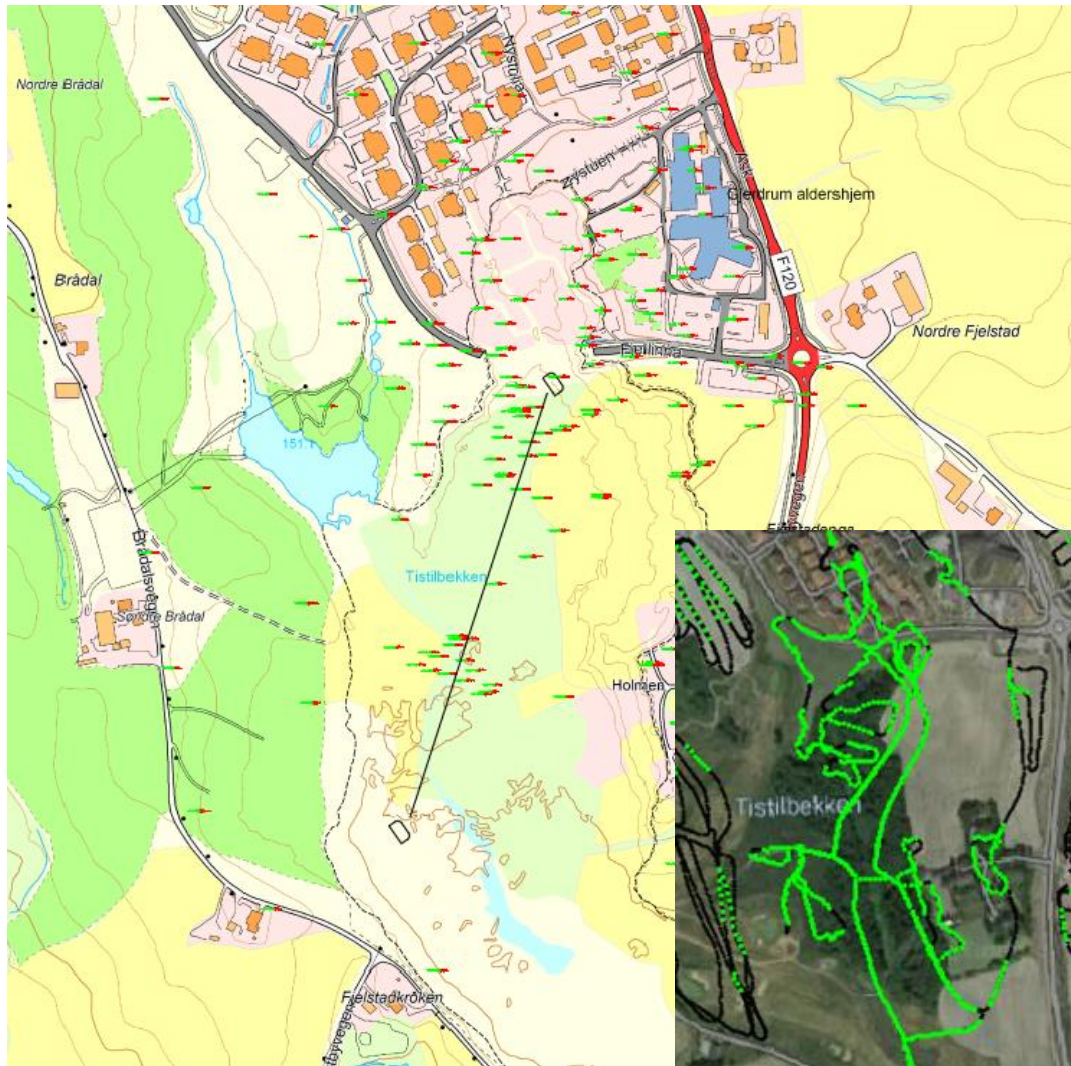


Figure 25. ERT- and tTEM data available in the landslide area

A color-scale with discrete range of the resistivity data has been developed to facilitate comparison with geotechnical interpretation, see Figure 27. This color-scale clearly separates soil material into smaller resistivity-intervals, enabling effective evaluation of the data in the stratigraphy. Profile D is also divided into 4 profiles of 100 meters each. Profile D-1 (0-100m) and D-3 (200-300m) have several geotechnical boreholes available in the area, while profile D-2 (100-200m) and D-4 (300-400m) have very limited geotechnical data available.

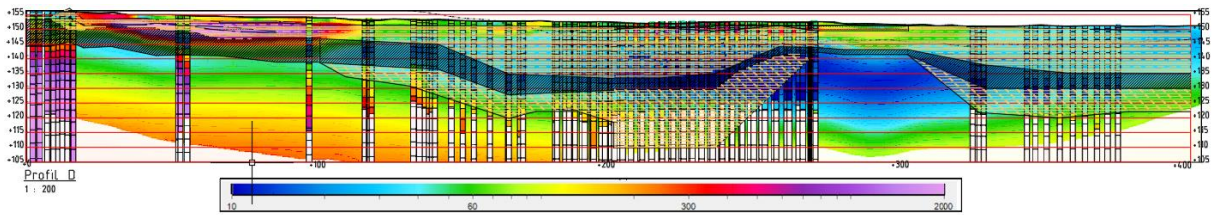


Figure 26. Profile D in whole length, with original color scheme and geotechnical layering

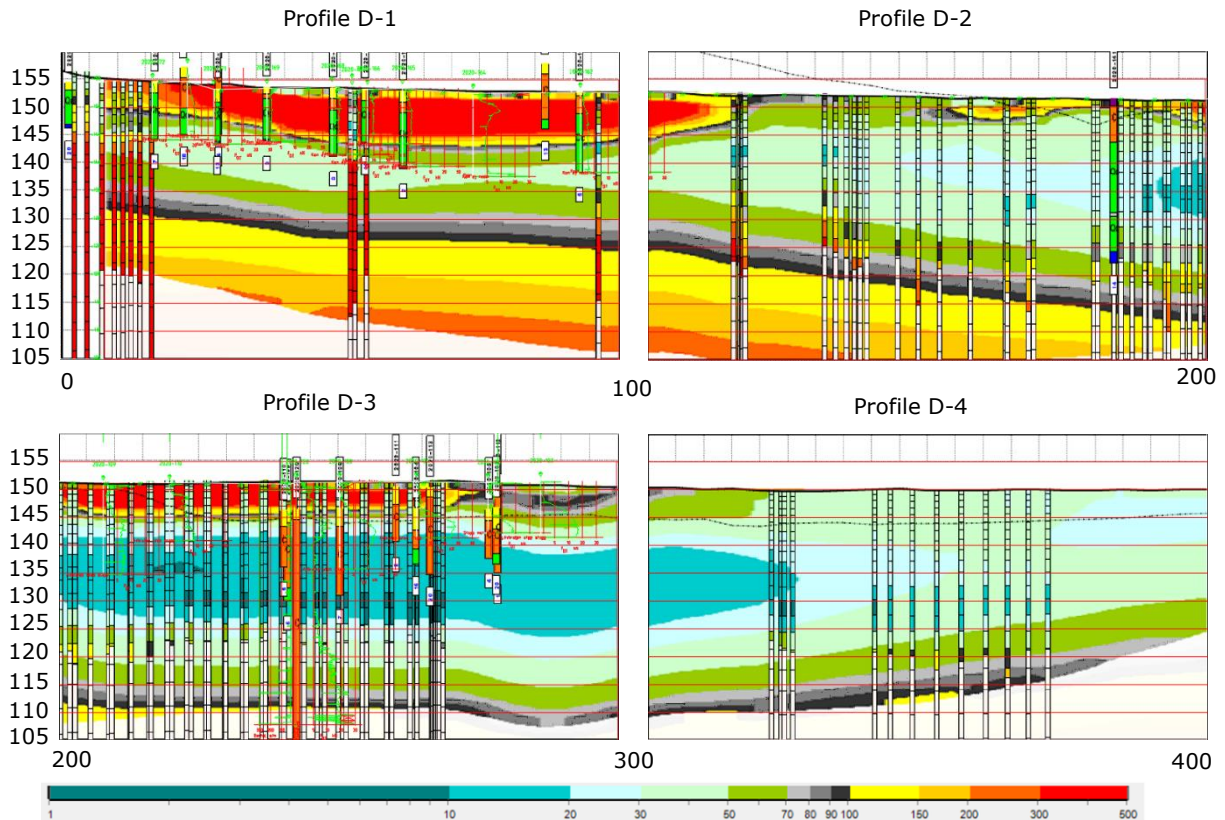


Figure 27. Profile D, divided into 4 smaller profiles, with a new color-scheme for differentiating layers

Resistivity is derived from 1 to 500 Ωm . The white areas in the bottom of the profiles mark the Depth of Investigation (DOI) for the geoelectrical surveys. In order to determine accurate DOI, a geoelectrical methodology has been employed (Vest Christiansen & Auken, 2012) which involves the utilization of observed data and inversion settings (constraints). The methodology takes into account the influence of the starting model and regularization specifications aiming to differentiate between information derived directly from the data and information influenced by these factors. The depth at which the signal penetrates is influenced by the resistivity characteristics of the above layers. When the soil material possesses low resistivity, it facilitates the penetration of the signal, whereas high resistivity layers may impede the signal from reaching greater depths. Consequently, the varying resistivity of the subsurface layers plays a crucial role in determining the DOI of the survey. However, an estimation of how much of the model that represents realistic response (data driven) or not (constraint driven) always needs to be considered (Personal com. Boufidis, 2023).

3.1.1 Comparison between ERT and tTEM

In this section the geoelectrical data sets will be compared.

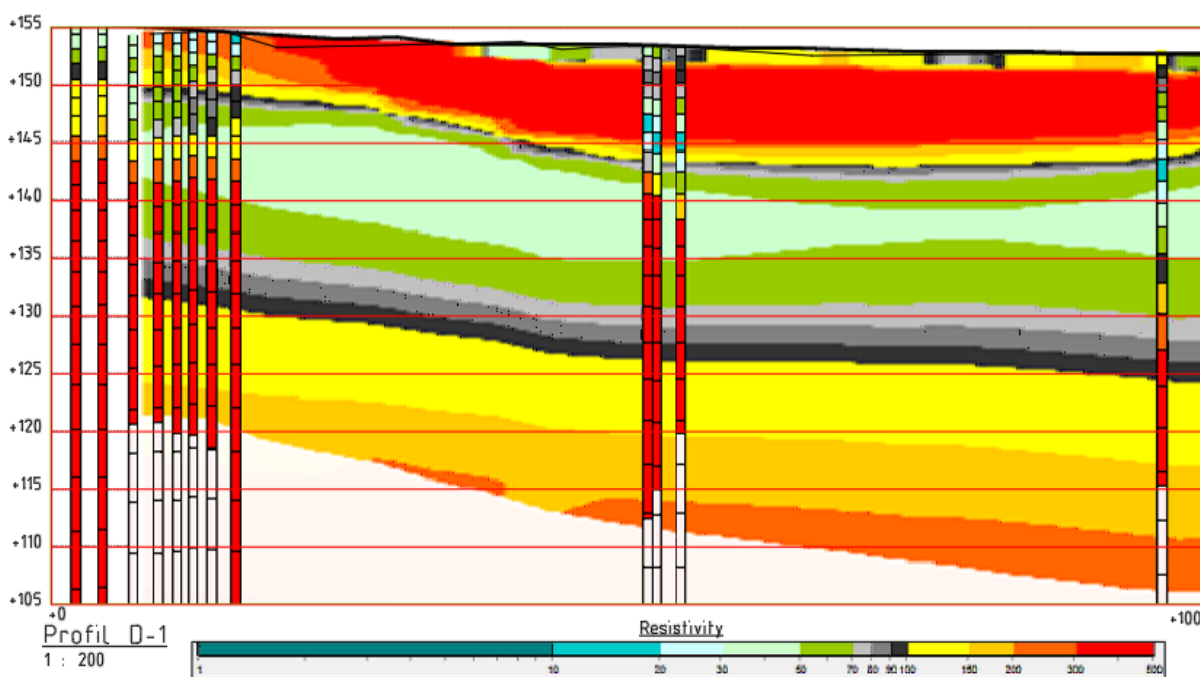


Figure 28. Profile D-1

The ERT and tTEM depict very different results for the measurements in profile D-1 (0-100 m), see Figure 28. Based on ERT results, the initial 7 meters of the profile exhibit significantly higher resistivity values. From a depth of 7 to 23 meters, the resistivity decreases to a range of 30-100 Ωm , suggesting the possible presence of leached clay in this region. Subsequently, at a depth of 23 meters, the resistivity begins to rise again, indicating the presence of coarser materials with resistivity values ranging from 150 to 500 Ωm .

The tTEM data indicates different stratigraphy along D-1. Within the top 10-20 meters of the profile, resistivity values ranging from 10 to 150 Ωm are observed. Notably, beyond the first 10 meters, resistivity already surpasses 200 Ωm and continues to increase with depth. Around the 50-60 meter mark, resistivity values exceed 300 Ωm at a depth of 13 meters. Around the 90-meter point, resistivity values surpass 200 Ωm at a depth of 23 meters.

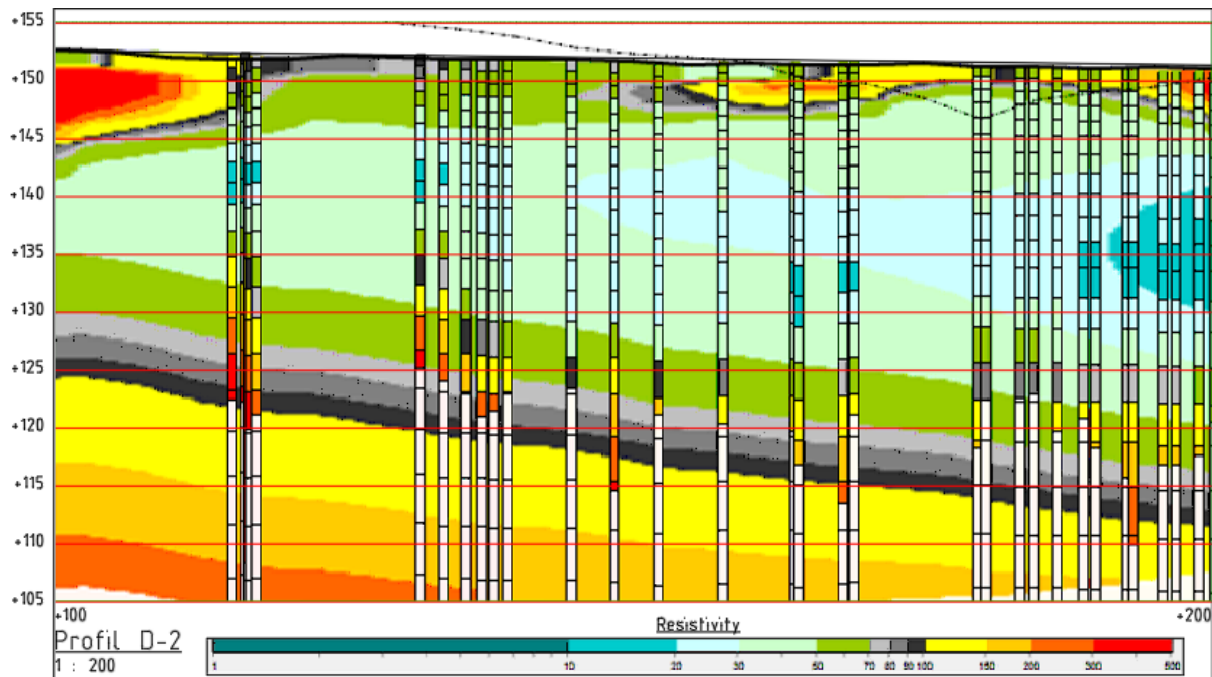


Figure 29. Profile D-2

The ERT data from profile D-2 (100-200 m), see Figure 29, reveals a broad spectrum of resistivity values within the uppermost 5 meters. This range varies from 30 to 500 Ωm . Moving deeper, the data indicates the presence of a thick layer, spanning 20 to 30 meters, with resistivity values ranging from 10 to 100 Ωm . Notably, at the beginning of the profile, resistivity exceeds 100 Ωm at a depth of 25 meters, while at the end of the profile, this threshold is surpassed at a depth of 35 meters.

ERT- and tTEM data are relatively comparable along this part. Between 100-140 meter-mark, the tTEM measurements display resistivity values ranging from 10 to 100 Ωm , extending down to a depth of 18 meters. Between 140 and 170 meters, the resistivity values surpass 100 Ωm at depths of 27 meters, as well as at the end of the profile at 30 meters depth. Notably, a discrepancy of approximately 5-7 meters is observed between the two survey methods in this section. The tTEM measurements in certain areas reach DOI already at 25 meters in depth.

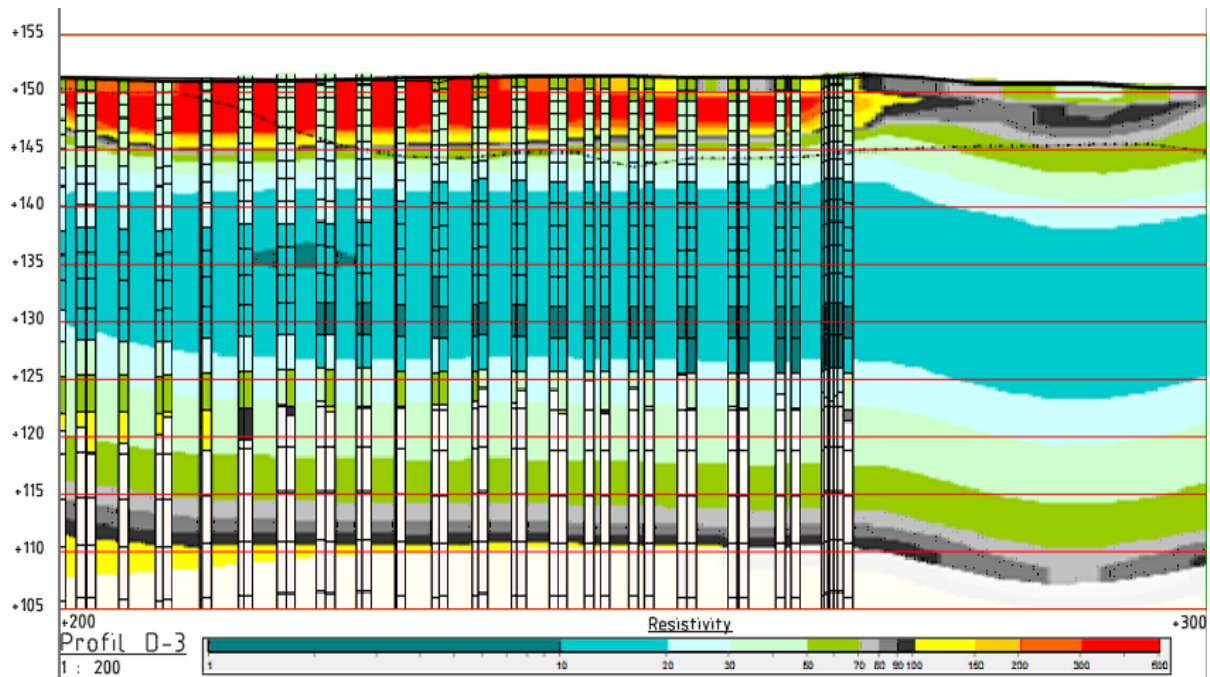


Figure 30. Profile D-3

The ERT has recorded very high resistivity values in the top 5 meters of profile D-3 (200-300 m), see Figure 30. Below this depth the resistivity drastically reduces and falls between 10 to 100 Ωm from 5 to 40 meters depths. There is a small patch of data below 10 Ωm at 15 meters depths.

The tTEM data shows values of 30 to 70 Ωm in the top 10 meters. Below this depth, a layer with thickness 15 meters has 1 to 20 Ωm . In the 200 to 210 meter-mark, the values rise to 30-150 Ωm over 5 meters before reaching DOI at 30 meters depth. At the 210 to 275 meter-mark, the tTEM reaches DOI at 25 meters depth. Here, the discrepancy in depth-resolution between ERT and tTEM data is 15 meters at the most.

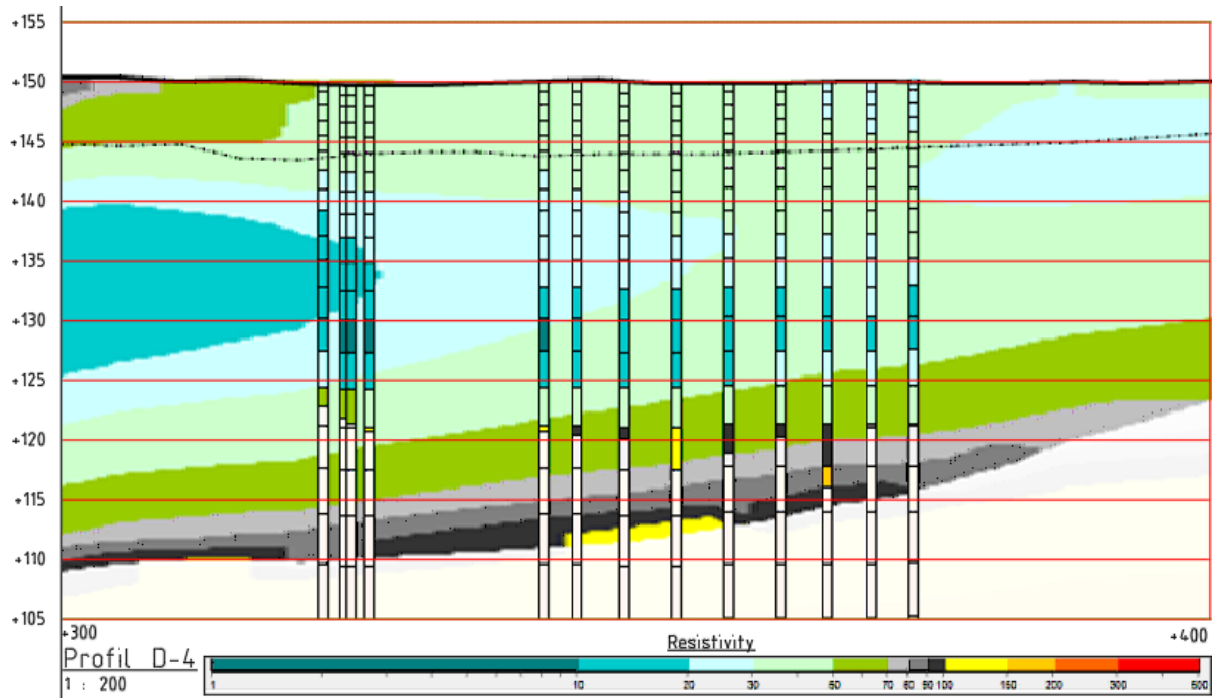


Figure 31. Profile D-4

In part 4 (between 300 and 400 m), see Figure 31, the ERT-profile demonstrates generally 10 to 70 Ωm for the entire profile down to 37 meters depth at the start, and 27 meters at the end of the profile. Below this, the ERT cannot resolve deeper layers.

The tTEM indicates a similar pattern. However, the tTEM locates resistivity below 10 Ωm in some patches at 20 meters depth. Furthermore, it is noteworthy that the tTEM reach DOI at approximately 27 meters depth. The discrepancy in signal penetration between the two methods is almost 10 meters in the start of the profile, while it is relatively accurate near the end.

In summary, the two methods exhibit significant discrepancies in the uppermost 5 meters of the subsurface. During this depth range, the ERT often recorded values reaching up to 500 Ωm , whereas the tTEM method never exceeded 100 Ωm . Beyond 5 meters, the two methods generally display similar resistivity patterns, with a variation range typically falling between 10 to 100 Ωm . Some localized areas exhibit resistivity values below 10 Ωm . Notably, the tTEM data consistently demonstrates a faster increase in resistivity with depth compared to the ERT data. The discrepancy in DOI between the two methods can reach up to 15 meters.

3.1.2 Geotechnical interpretations

Geotechnical boreholes within 10 meters distance of profile D are plotted on this profile using the Geosuite program. There are no boreholes available in profile D-2 and D-4. In D-1 and D-3, the boreholes indicate that the soil-layers in the area consist mostly of clay, quick clay, and silt. The terrain is generated from the elevation of where the boreholes are drilled and will therefore not replicate an exact match with current terrain in this area.

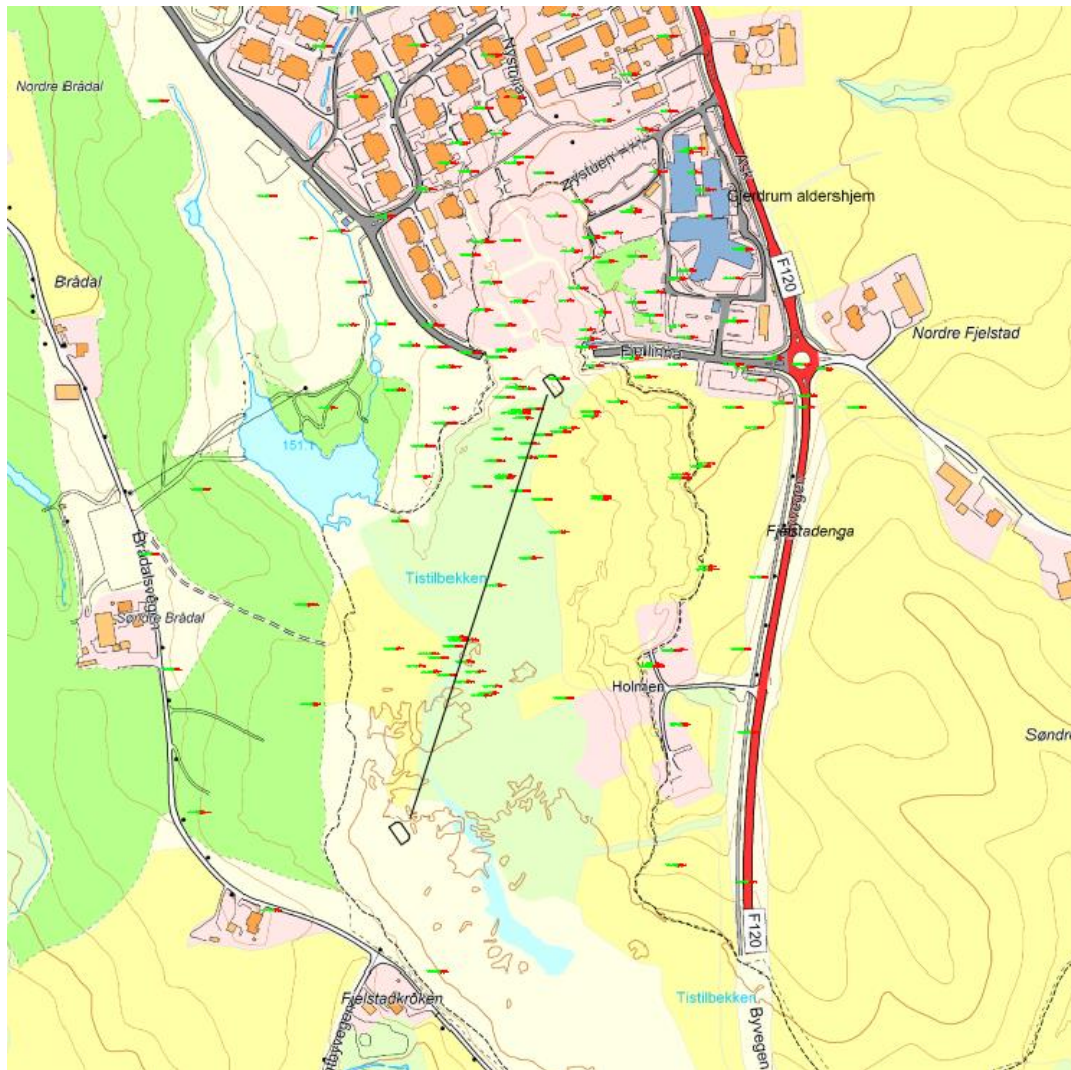


Figure 32. Profile D, with respect to the landslide area and available boreholes

The soil-layers in the area consist largely of unleached clay deposits and leached sensitive quick clay. Geological literature from the area suggests that the clay is largely influenced by silt fractions (see 2.1.1). Also, moraine should often be present below the clay/quick clay layers in this area. Reports revealed that much of the unleached clay mass from the landslide were used as fill in the landslide pit (see 2.1.2). It should therefore be expected that the top layer can consist of inhomogeneous mass that might hold a combination of unleached clay, coarse material and landslide debris. In this study, this layer will be defined as "landslide mass". A previous report (Bache, 2021) also describes gravel to be present in parts of the top layer from 29.03.22. Boreholes in the landslide pit were carried out between 12.08.21-13.07.22 and might therefore not include this gravel layer.

In the landslide area, piezometers are installed in 13 boreholes (Hovind, 2021; Reutz, 2022). The pore pressure data show that the gradient is drastically reduced from 19 kPa/m right after the landslide, to 10 kPa/m (hydrostatic conditions) after installing the vertical drains. The groundwater-table in the area is located about 1-2 meters below the bottom of the landslide pit, which means that this varies throughout the area. The vertical drains have contributed in counteracting excessive pore pressure while the fill mass consolidates.

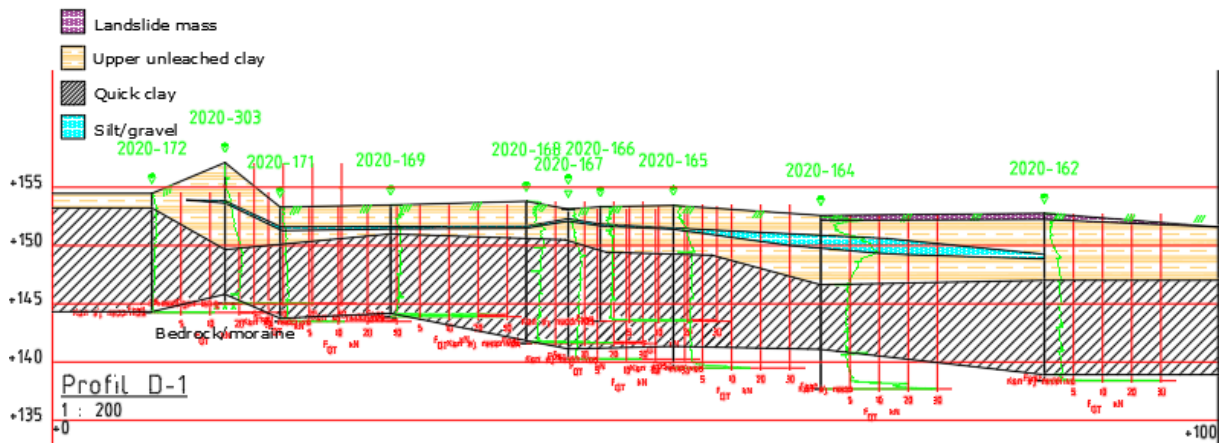


Figure 33. Profile D-1, geotechnical interpretation

In profile D-1, see Figure 33, there are quite a lot of boreholes in a small area, which give high certainty in the geotechnical interpretation. The boreholes consist of rotary pressure soundings and CPTU's. The CPTU's are removed from the profile drawing but are still considered in the interpretation. For this profile, the boreholes indicate that there is unleached clay in the top 2-7 meters. Further, we find a layer of silt that extends with a thickness from 0.5 to about 2 meters. The interpreted silt layer might instead be gravel from the vertical drains installed in the area. The quick clay layer is located below the upper unleached clay layer and has a thickness of about 8 meters throughout this profile. The boreholes in this area are quite shallow, which indicate coarser layers like moraine or bedrock underneath the quick clay layer. Based on drilling data from borehole 2020-303, it appears that bedrock or moraine may be present below. However, this cannot be proven using the rotary pressure sounding.

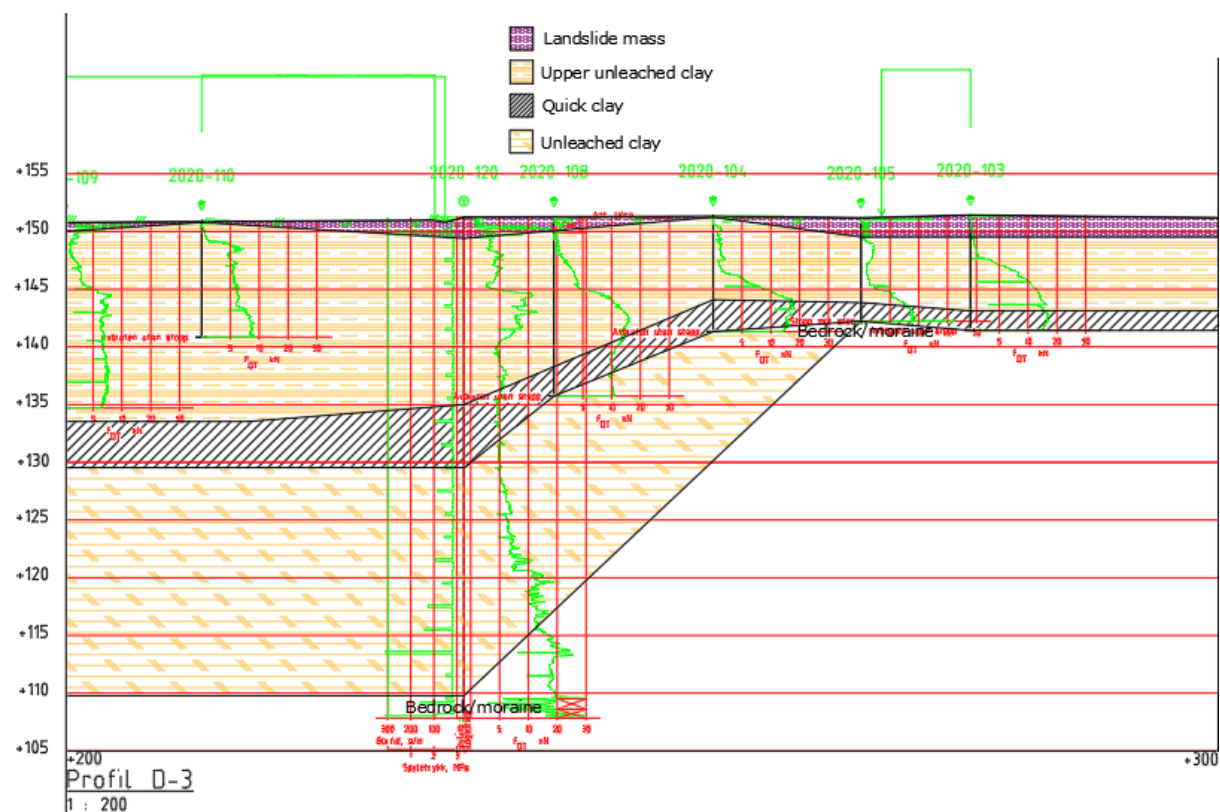


Figure 34. Profile D-3, geotechnical interpretation

In profile D-3, see Figure 34, there are 8 geotechnical boreholes. The interpreted part, from 2020-120 to 2020-103 should provide reasonable data for interpretation. The layering is interpreted to continue horizontally to the start and end of the profiles as is standard practice within geotechnical engineering. For this profile, there are landslide mass in the top 2 meters, followed by unleached clay with a thickness of 6-17 meters. Quick clay is located below these layers, and has a thickness of 2-5 meters. Unleached clay is then present down to assumed bedrock or moraine. In Figure 34, this is referred to as a new layer even though this is believed to be a similar soil material as the unleached clay above the quick clay layer. The total sounding in borehole 2020-120 suggests bedrock 40 meters depth, while a rotary pressure sounding in 2020-105 revealed indications at 8 meters depth.

3.1.3 ERT-correlation

Soil stratification from boreholes is superimposed on ERT-profile for comparison, see Figure 35.

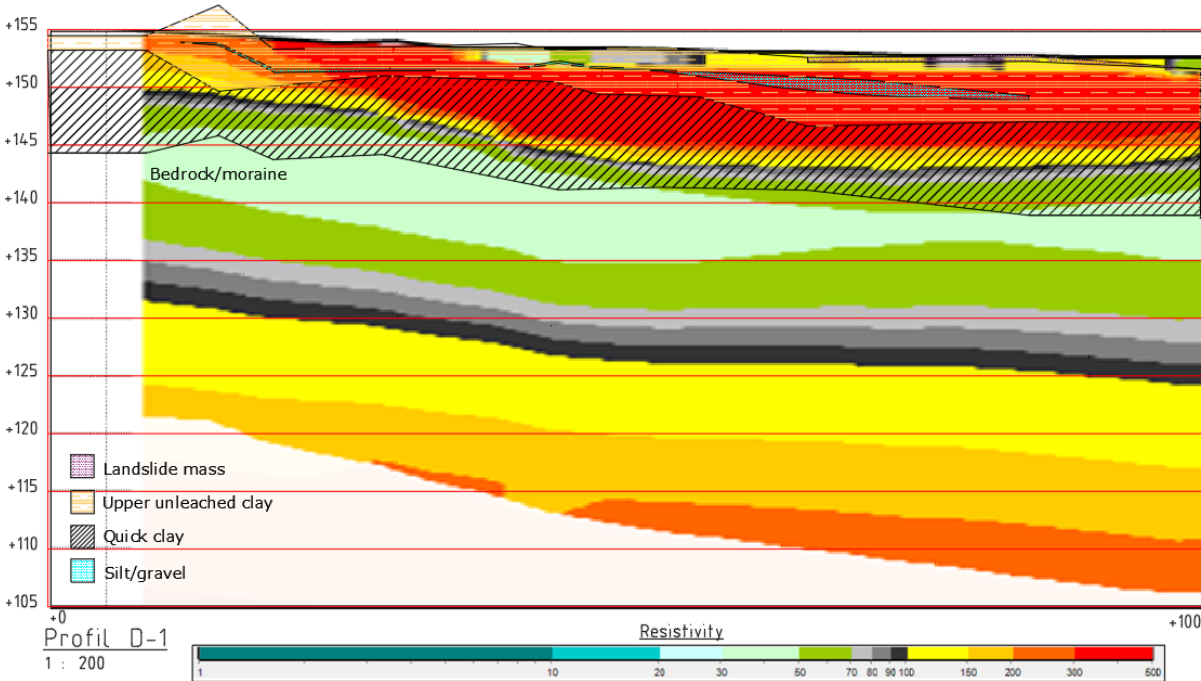


Figure 35. Profile D-1, ERT data

In areas with quick clay in part 1 (0-100 m), resistivity varies from 30-500 Ωm. The clay and silt layer generally have resistivity of 200-500 Ωm. However, the clay in the top 2 meters seems to have somewhat lower resistivity, about 20-100 Ωm.

Table 4. Profile D-1, ERT data

	Silt/gravel	Upper unleached clay	Quick clay	Bedrock/moraine
Resistivity[Ωm]	200-500	100-500	20-500	30

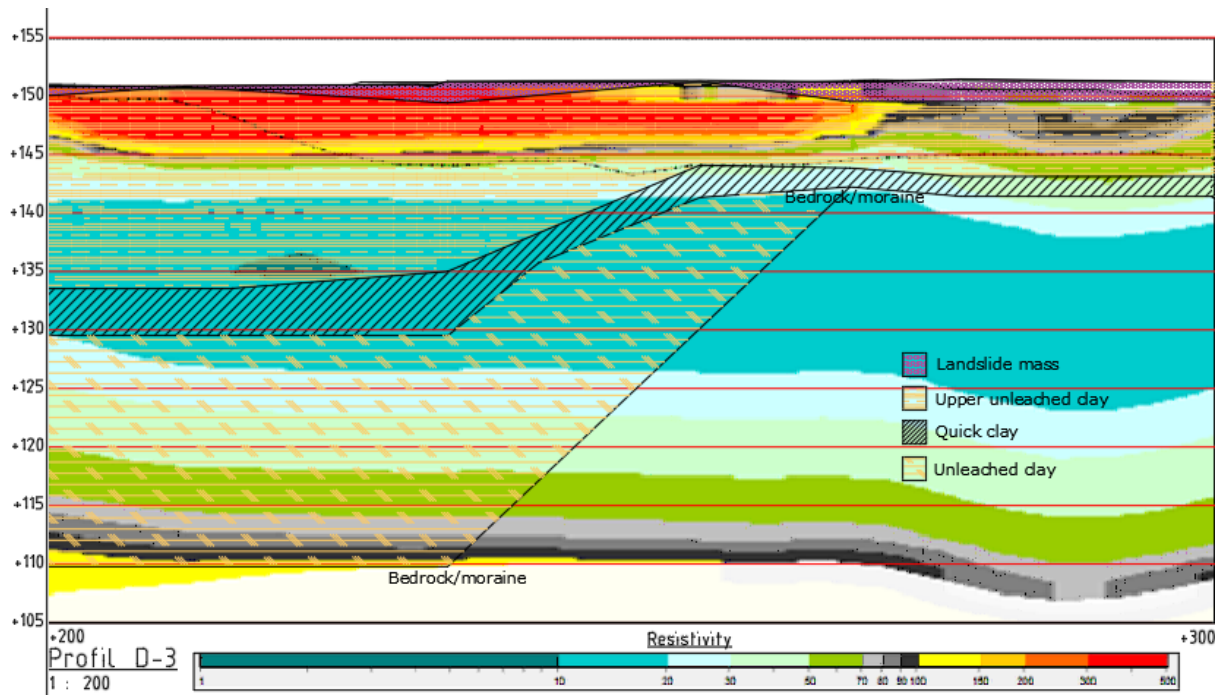


Figure 36. Profile D-3, ERT data

The resistivity range in areas of quick clay along D-3, see Figure 36, is between 10-50 Ωm , while the top unleached clays vary from 1-500 Ωm . Deeper unleached clay mostly displays values between 10-70 Ωm , but increases as it approaches bedrock. Landslide mass varies between 100-500 Ωm .

Table 5. Profile D-3, ERT data

	Landslide mass	Upper unleached clay	Unleached clay deposits	Quick clay	Bedrock/moraine
Resistivity [Ωm]	100-500	1-500	10-150	10-50	150, 10

3.1.4 tTEM-correlation

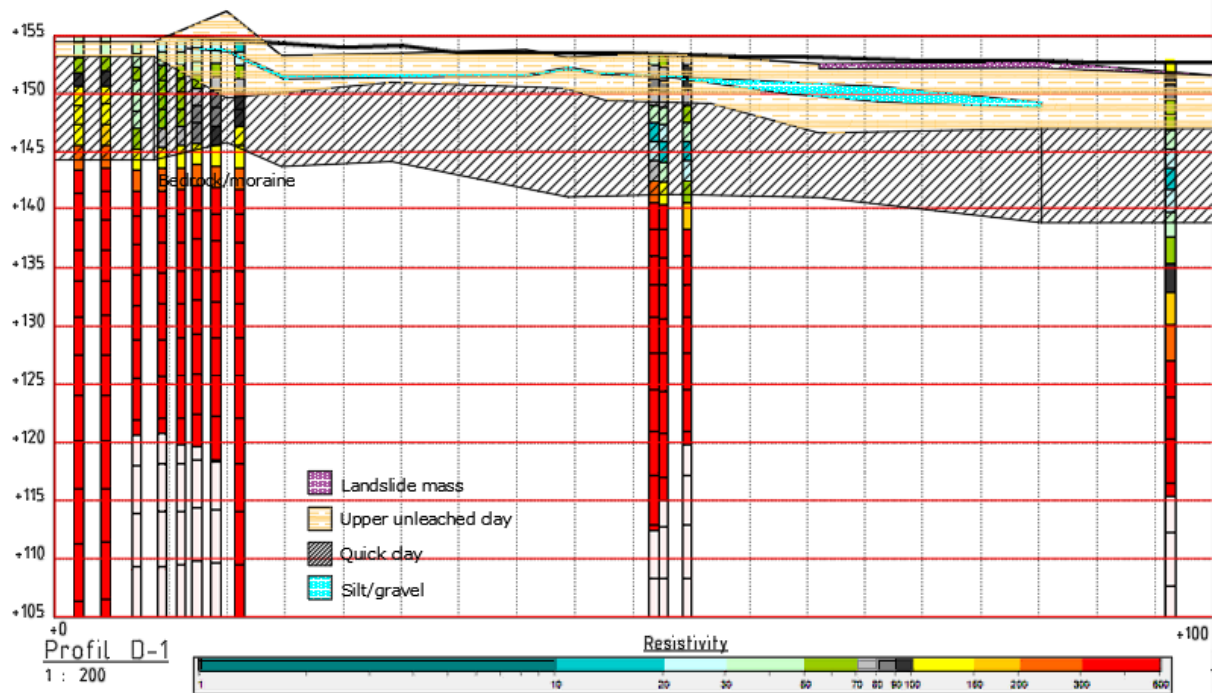


Figure 37. Profile D-1, tTEM data

In areas with quick clay along D-1, see Figure 37, resistivity varies from 10-150 Ωm . In clay and silt areas, the resistivity varies from 10-150 Ωm . Below the quick clay layer, the resistivity quickly increases to 300-500 Ωm , indicating coarser layers.

Table 6. Profile D-1, tTEM data

	Silt/gravel	Upper unleached clay	Quick clay	Bedrock/moraine
Resistivity[Ωm]	80-100	10-100	10-150	150-500

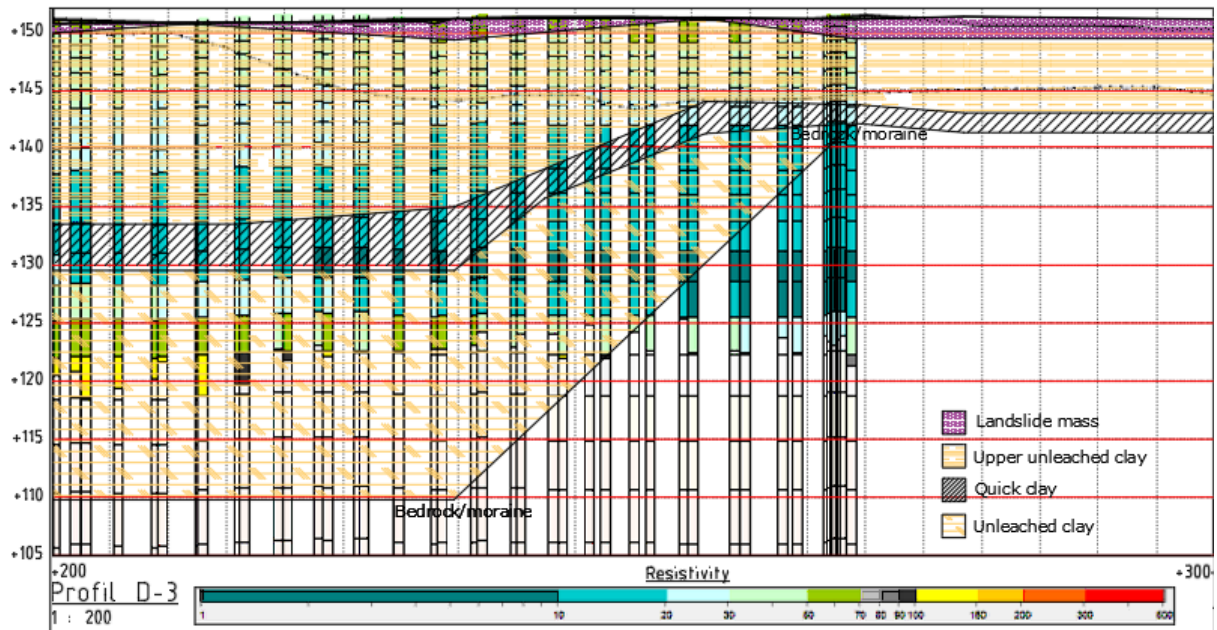


Figure 38. Profile D-3, tTEM data

The resistivity in areas along D-3, see Figure 38, containing quick clay fluctuates between 1-30 Ωm , while the values for the upper unleached clay areas range from 10-70 Ωm . In the deeper clay regions, resistivity varies between 1-150 Ωm . The tTEM signal does not reach deep enough to locate the bedrock/moraine at 40 meters depth.

Table 7. Profile D-3, tTEM data

	Landslide mass	Upper unleached clay	Deeper unleached clay	Quick clay	Bedrock/moraine
Resistivity [Ωm]	60-70	10-70	1-150	1-30	10

3.2 Other tTEM-profiles

To supplement the study in profile D, five more profiles are chosen to be analyzed using tTEM data. These profiles are also located in the landslide pit, and are interpreted utilizing boreholes within 10 meters of the profiles. The location of the profiles and the boreholes in the area are illustrated in Figure 39.

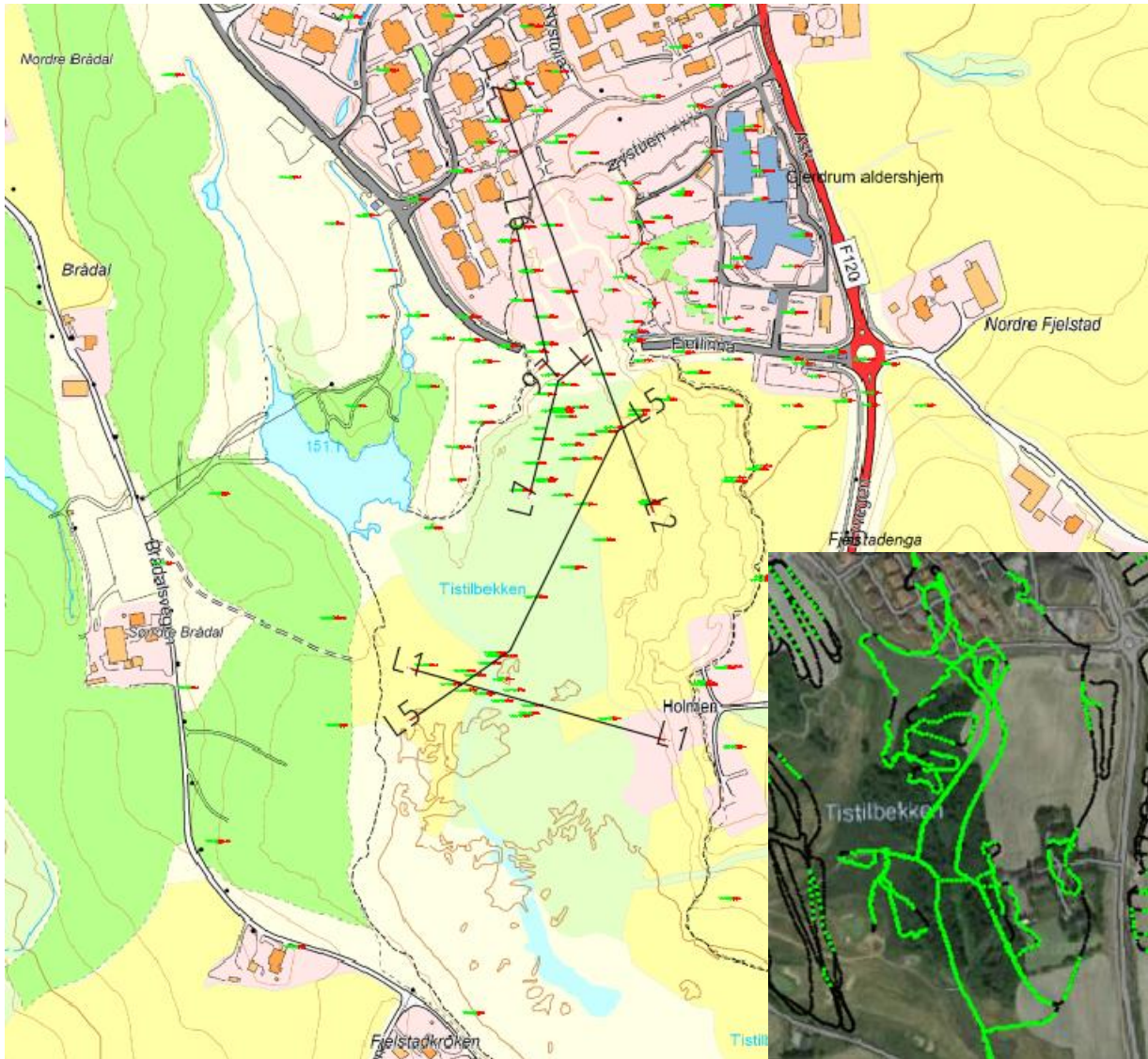


Figure 39. Location of tTEM profiles in the landslide area. Green traces marks where tTEM data is available

3.2.1 L1

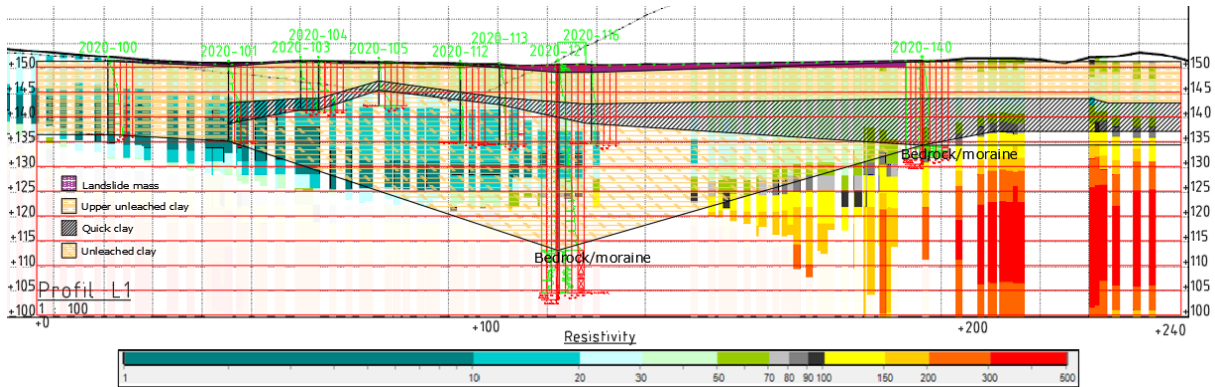


Figure 40. Profile L1

The layering of the L1-profile is interpreted based on 9 boreholes (from 2020-100 to 2020-116) and is relatively reliable. Here, quick clay layer corresponds to resistivity values of 10-50 Ωm . Unleached clay corresponds to resistivity varying from 1-70 Ωm . Between borehole 2020-116 and 2020-140, there are limited geotechnical data. In this area, landslide mass matches a resistivity of 30-70 Ωm . Quick clay is consistent with resistivity values of 20-100 Ωm . Unleached clay deposits correspond to 10-100 Ωm . Based on the total sounding in borehole 2020-140, bedrock or moraine is located at 16 meters depth, which aligns with resistivity values of 100-150 Ωm .

Table 8. Profile L1, resistivity-thresholds

	Landslide mass	Upper unleached clay	Unleached clay	Quick clay	Bedrock/moraine
Resisitivy[Ωm]	30-50	1-70	1-100	10-100	100

3.2.2 L2

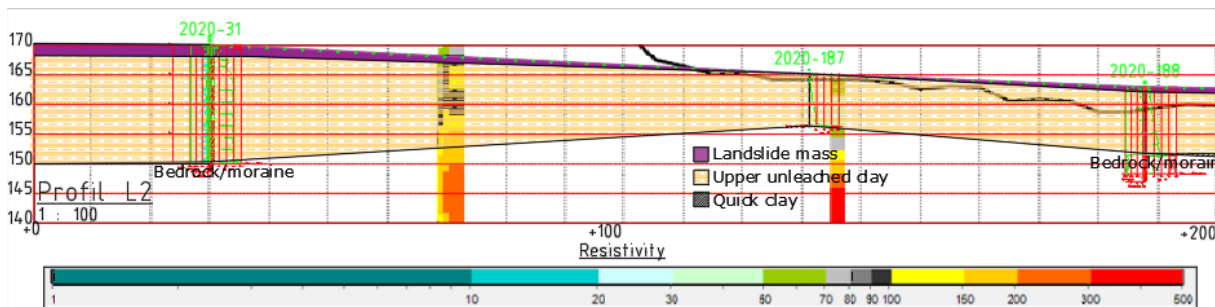


Figure 41. Profile L2, 0-200m

The first part of the L2 (0-200 m) profile does not include quick clay. The clay in this area corresponds to resistivity values of 20-150 Ωm . Landslide mass has resistivity range from 50-150 Ωm .

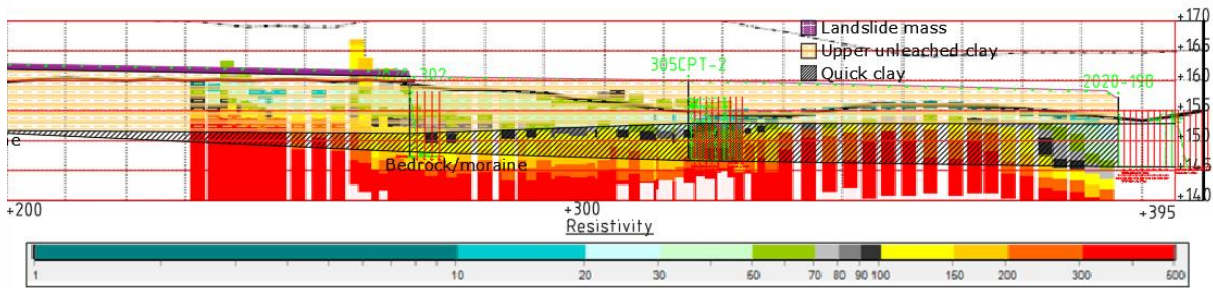


Figure 42. Profile L2, 200-395m

The second part (200-395 m) is interpreted using CPTU data in borehole 2020-305 and 2020-190. Here, the Mayne-approach (Agaiby & Mayne, 2021; Mayne et al., 2019) is utilized to indicate quick clay. This approach has been calibrated against other soundings and sampling in other boreholes and shows a reasonable match, this is discussed in Appendix B: CPTu-interpretation (Mayne). However, this slightly reduces the probability of the layering being realistic. Clay or landslide mass in this area matches values ranging from 1-150 Ωm . Quick clay corresponds to quite high values ranging mainly from 50-500. Based on rotary pressure, bedrock is indicated at 13 meters depth in borehole 2020-302, which agrees with 150-500 Ωm .

Table 9. Profile L2, resistivity-thresholds

	Landslide mass	Upper unleached clay	Quick clay	Bedrock/moraine
Resistivity [Ωm]	50-150	1-500	50-500	150

3.2.3 L5

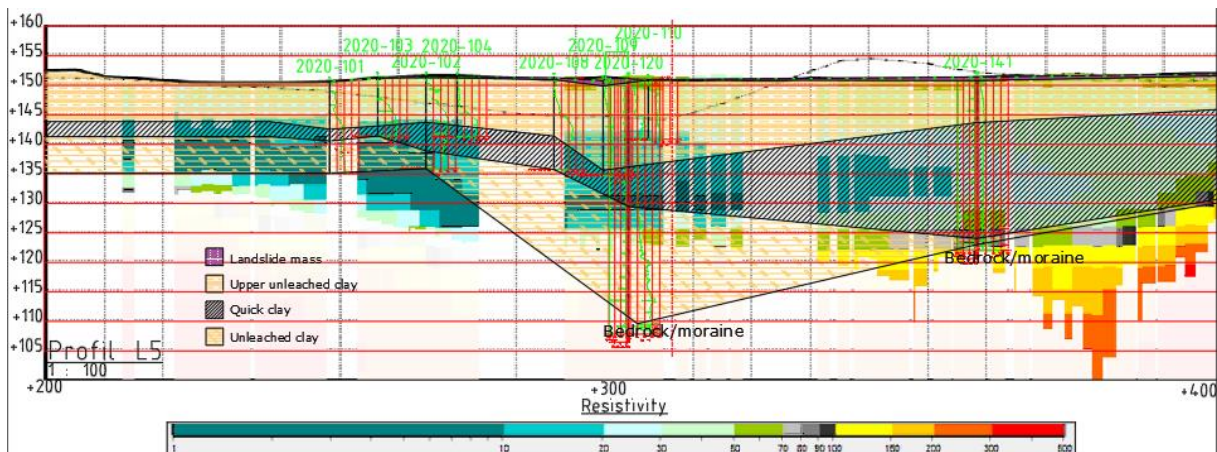


Figure 43. Profile L5, 200-400m

In the first part of the L5 profile (200-300m), there are several geotechnical boreholes from 2020-101 to 2020-141. Here, upper unleached clay matches resistivity of 10-70 Ωm . Quick clay aligns with values between 1-70 Ωm . A lot of the unleached clay lies below 10 Ωm . In the second part (300-400m), unleached clay varies between 1-150 Ωm . Based on a total sounding in borehole 2020-141, moraine or bedrock is indicated at roughly 28m depth. This agrees with resistivity values of 100-150 Ωm . In borehole 2020-120 a total sounding predict bedrock at about 45 meters depth. Here, the tTEM data show unresolvable data at 32 meters depth.

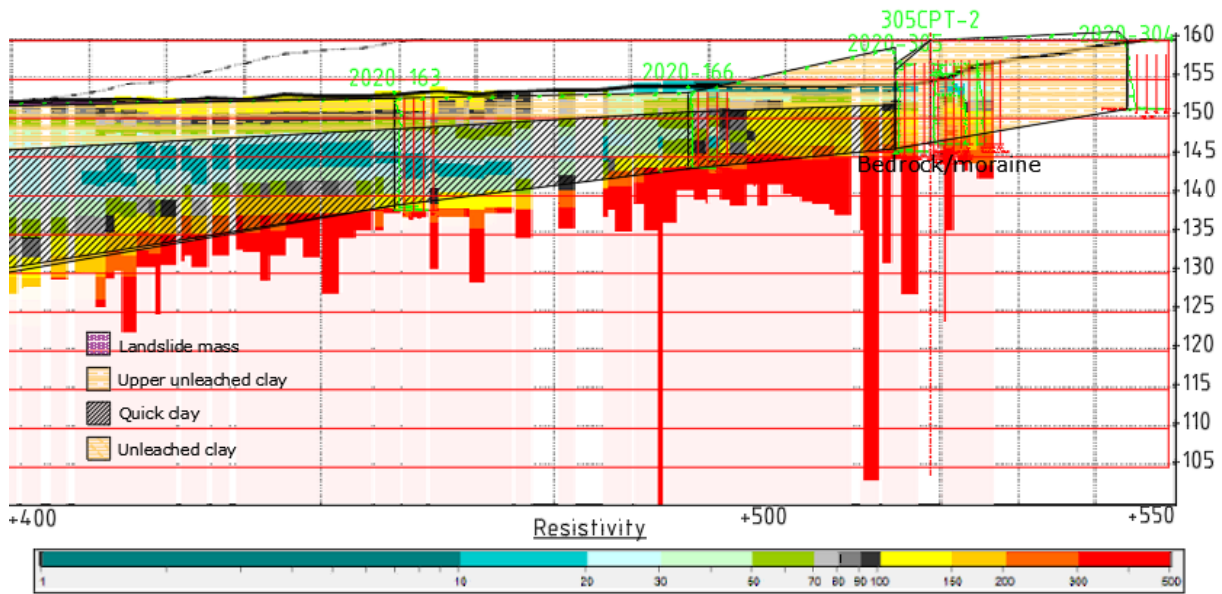


Figure 44. Profile L5, 400-550m

In the second part of the profile (400-550 m), unleached clay agrees with values ranging from 30-150 Ωm . Quick clay matches values from 10-150 Ωm . Bedrock is indicated through a rotary pressure sounding in borehole 2020-305, at 13 meters depth. This matches resistivity-values of 300-500 Ωm .

Table 10. Profile L5, resistivity-thresholds

	Landslide mass	Upper unleached clay	Unleached clay	Quick clay	Bedrock/moraine
Resistivity [Ωm]	50-70	10-70, 30-150	1-150	1-70, 10-150	100, 500

3.2.4 L6

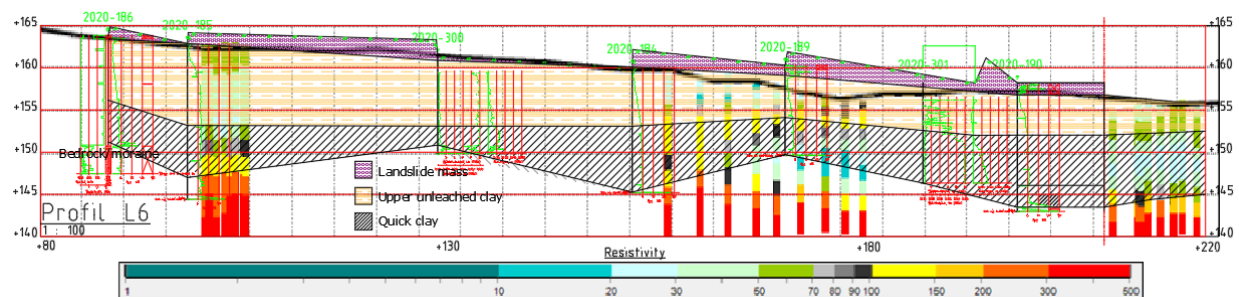


Figure 45. Profile L6

The L6 profile has a reasonable number of boreholes along the profile. In borehole 2020-306 and 2020-301, the Mayne-approach (Agaiby & Mayne, 2021; Mayne et al., 2019) is used to interpret the CPTU data. Landslide mass match values from 50-70 Ωm . Unleached clay corresponds to 10-150 Ωm . Quick clay in the area also compares to a range of 10-150 Ωm . In borehole 2020-186 a total sounding has proven bedrock at 14 meters depth.

There is no tTEM measurement in this exact point. However, this matches 300-500 Ωm about 10 meters to the right of the borehole.

Table 11. Profile L6, resistivity-thresholds

	Landslide mass	Upper unleached clay	Quick clay	Bedrock/moraine
Resistivity[Ωm]	50-70	10-150	10-150	300

3.2.5 L7

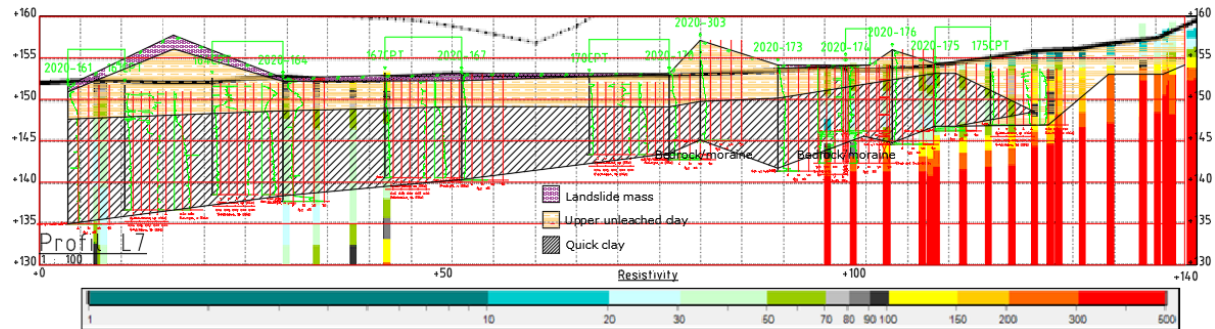


Figure 46. Profile L7

The L7 profile has a number of geotechnical boreholes located nearby which give higher certainty in the interpreted soil stratification. The upper unleached clay corresponds to 10-150 Ωm . Quick clay matches a lower range of 20-70 Ωm . Bedrock is indicated through a rotary pressure sounding in borehole 2020-176. This aligns with resistivity of 100-500 Ωm .

Table 12. Profile L7, resistivity-thresholds

	Landslide mass	Upper unleached clay	Quick clay	Bedrock/moraine
Resistivity[Ωm]	50-100	10-150	20-70	300

3.3 Resistivity thresholds in Gjerdrum

Table 13 gives a summary of resistivity-thresholds demonstrated from profiles in the landslide area. The silt or gravel layer from profile D-1 is not included here because of lack of data.

Table 13. Overview of resistivity-thresholds

Method	Profile	Landslide mass	Upper unleached clay	Unleached clay deposits	Quick clay	Bedrock/moraine	Geotechnical certainty	Geoelectrical certainty
ERT	D-1	-	100-500	-	20-500	30	High	Low
ERT	D-3	100-500	1-500	10-150	10-50	100	Medium	Medium
tTEM	D-1	-	10-100	-	10-150	150	High	Low
tTEM	D-3	60-70	10-70	1-150	1-30	-	Medium	High
tTEM	L1	30-50	1-70	1-100	10-100	100	High	High
tTEM	L2	50-150	1-500	-	50-500	150	Low	Low
tTEM	L5	50-70	10-150	1-150	1-150	100 500	Medium	High
tTEM	L6	50-70	10-150	-	10-150	300	Medium	Medium
tTEM	L7	50-100	10-150	-	20-70	300	High	Medium

This evaluation has demonstrated that quick clay generally lies between 10-150 Ω m. For some profiles, quick clay is located in tighter thresholds such as 10-70 Ω m. Unleached clay generally lies between 1-150 Ω m. Landslide mass resides between 50-150 Ω m. Bedrock or moraine is generally found where the geoelectrical surveys resolve values above 100 Ω m.

3.3.1 Geotechnical certainty

The certainty in the geotechnical interpretation is based on these factors:

- The number of boreholes available in the profile, and how these cover the length of the profile.
- How far the boreholes are located away from the profile (0-10 meters).
- The type of available geotechnical investigations. In this study, samples are considered the best, followed by RPS and TOT. CPTU is less certain in locating sensitive layers.

3.3.2 Geoelectrical certainty

The certainty in geoelectrical data is considered based on these factors:

For ERT:

- Highly resistive layering present in the top, will result in less reliable data deeper in the profile. The middle data, mostly consisting of upper unleached clay over quick clay over deeper unleached clay, should be considered most reliable.
- Closeness to infrastructure and noise-sources will reduce the certainty in the data, i.e., northern parts of the landslide area.

For tTEM:

- Areas with less "strings" of data available, will result in less reliable data when considering a profile.
- Highly resistive layering in the top will weaken the signal, resulting in less reliable data at lower depths.

- Lower "Data Residuals" indicate a higher certainty in the models.
- tTEM provides clearer data after the first 5-10 meters. Therefore, deeper data should prove more reliable than shallow data

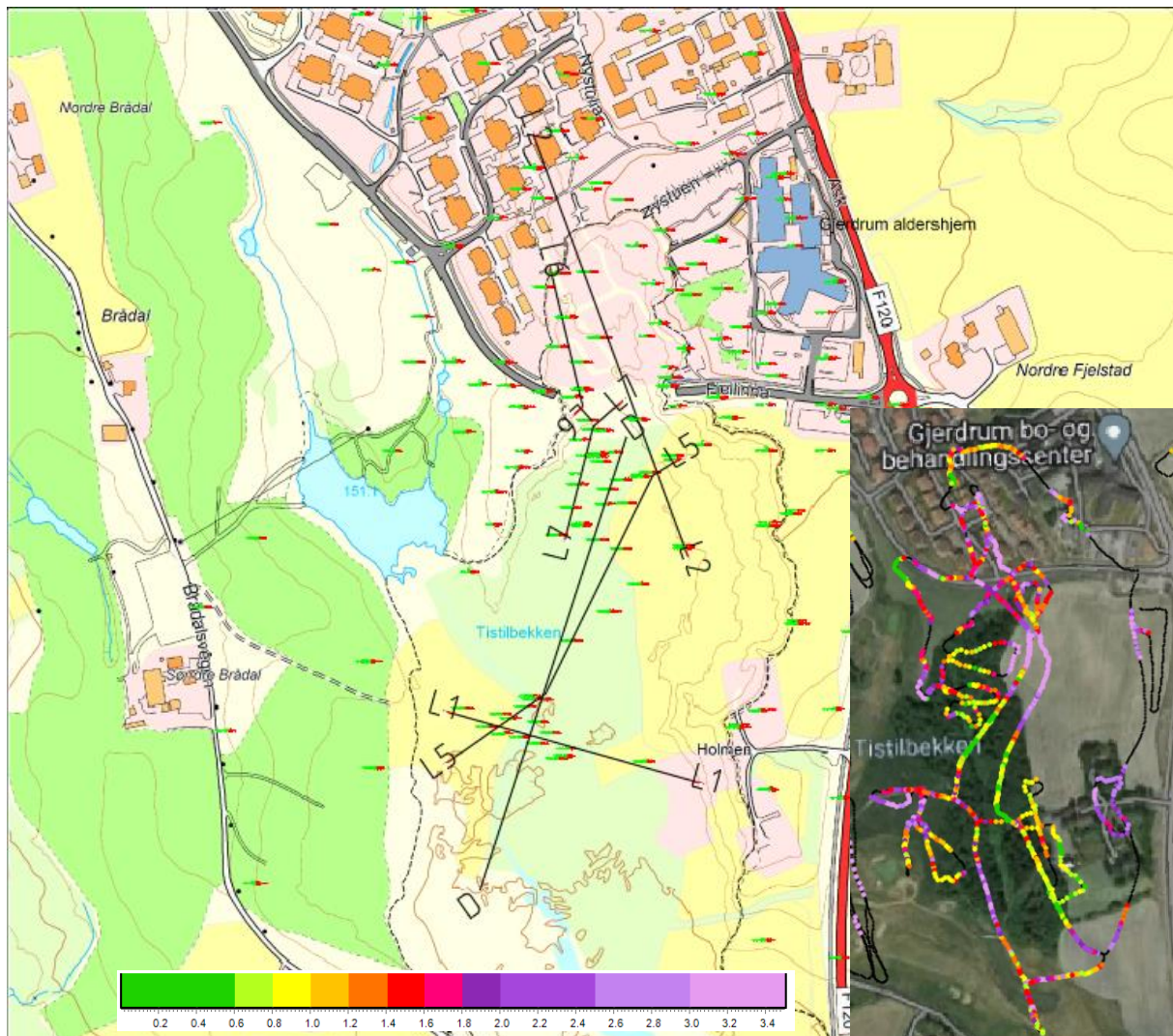


Figure 47. Data residuals for tTEM in the landslide area

3.3.3 Predicting quick clay in profile 2 and 4 with geoelectrical data

Establishing local thresholds for smaller areas can be useful if there is a high probability of proving different layers. For this evaluation 7 profiles have been analyzed with tTEM data. Two of these profiles have also been analyzed using ERT data.

An important objective for conducting geoelectrical surveys is to test their capabilities to predict layering in the subsurface and reduce the number of necessary geotechnical boreholes. In profile D-2 and D-4 there are no boreholes available. Based on the local thresholds proposed above, layering for these profiles are presented below.

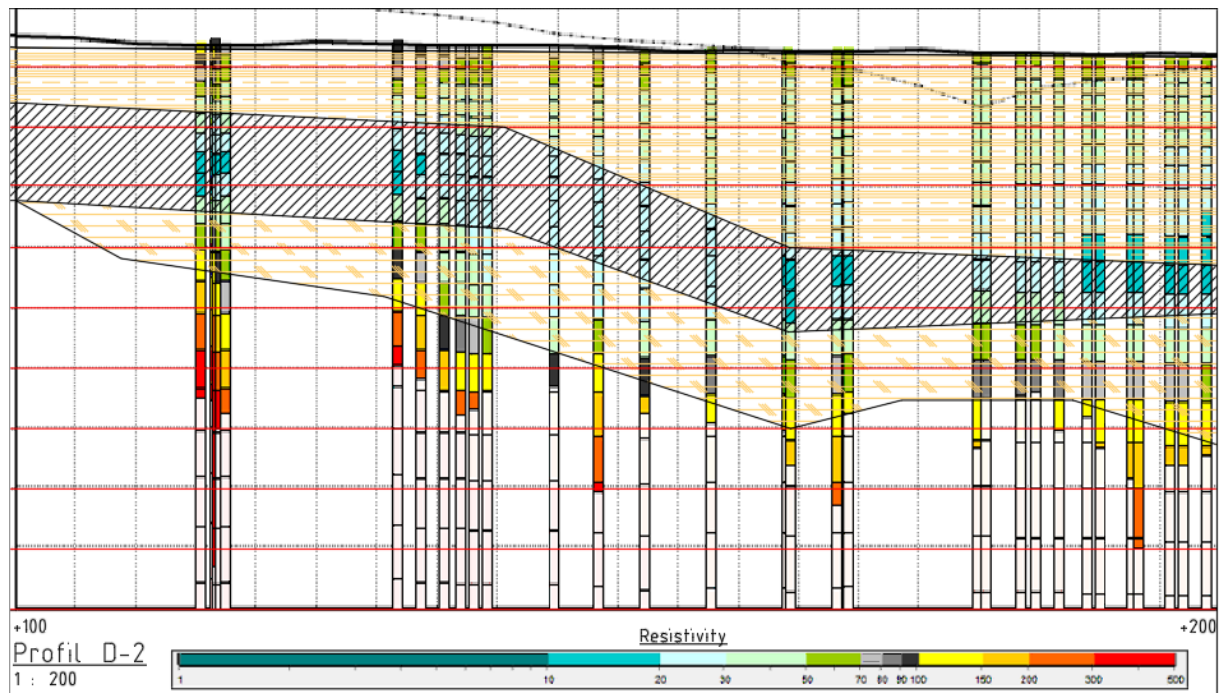


Figure 48. Profile D-2, tTEM data

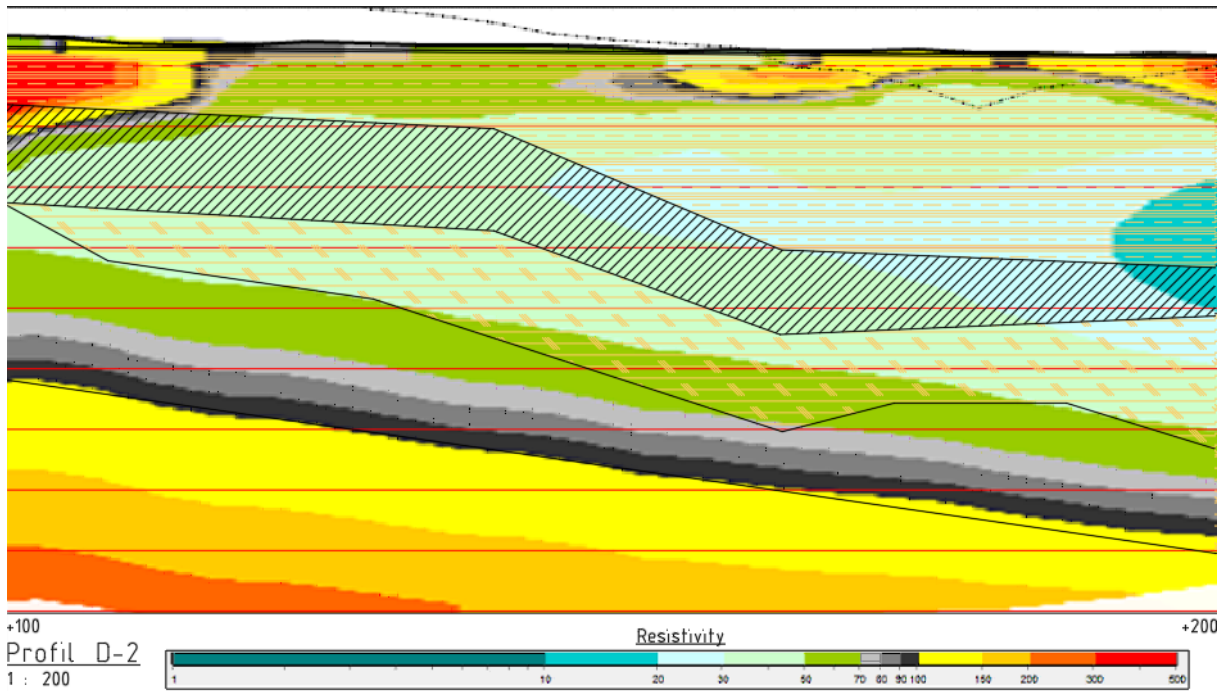


Figure 49. Profile D-2, ERT data

In Figure 48 and Figure 49 the soil stratigraphy is interpreted based on adjacent profiles, as well as tTEM and ERT data. The geoelectrical data agree well in this profile. It is observed that ERT data suggests unleached clay deposits some meters deeper. However, this example demonstrates how the two methods can provide an idea of the soil stratigraphy.

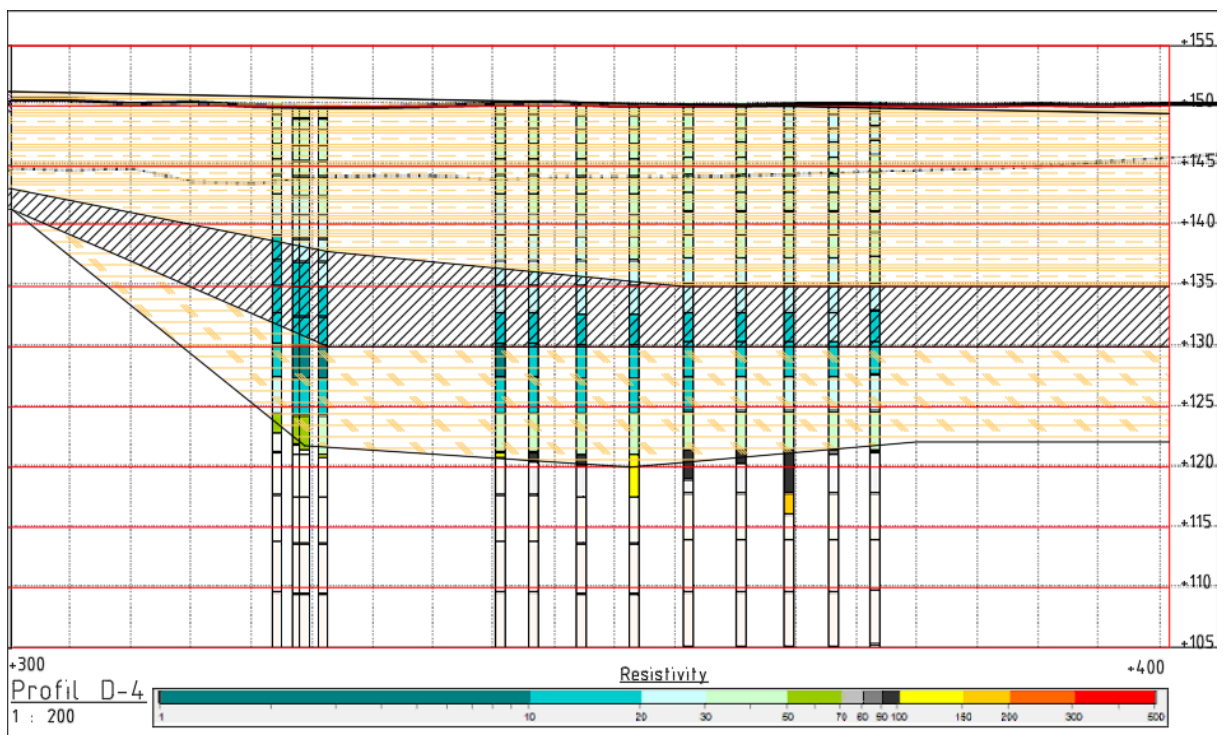


Figure 50. Profile D-4, tTEM data

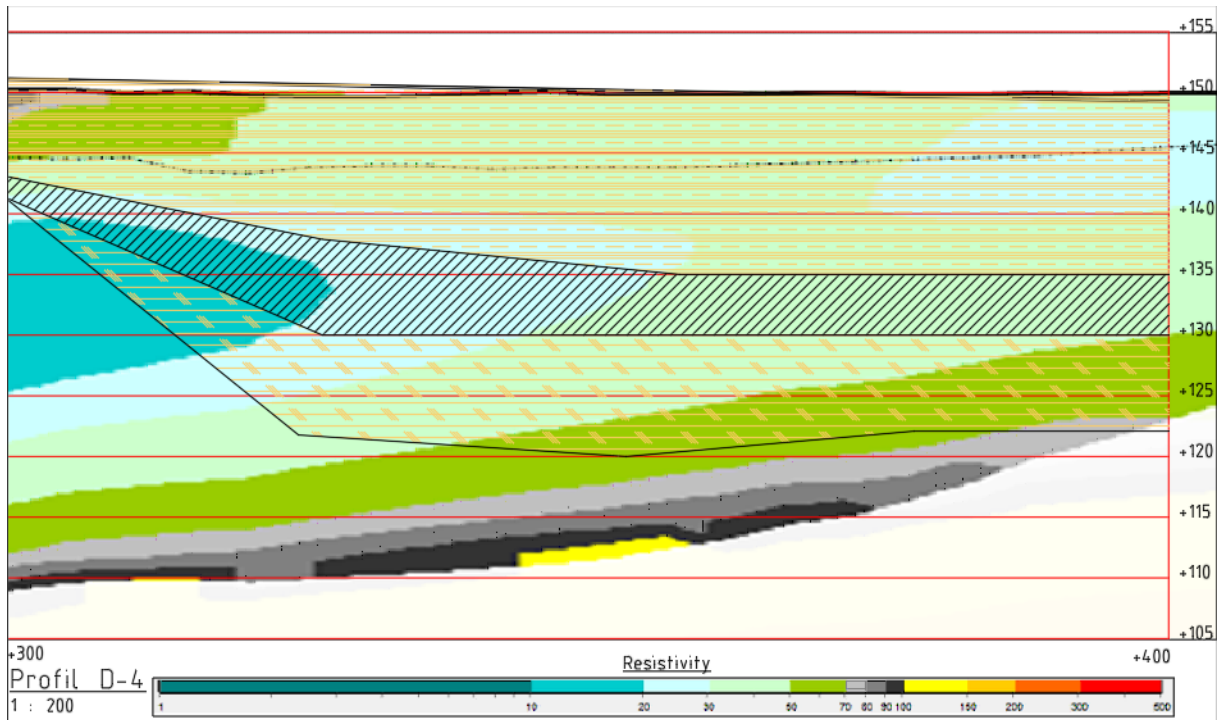


Figure 51. Profile D-4, ERT data

In Figure 50 and Figure 51 the soil stratigraphy is also interpreted based on geoelectrical data, as well as information at the start from profile D-3. It is apparent that the geoelectrical data agrees quite well, but the tendency of ERT data revealing deeper clay is consistent.

3.4 Geotechnical correlation

Results from the laboratory testing in Gjerdrum, see 2.2.2, have been plotted to examine potential correlations with resistivity. Based on the results from previous studies, see 1.2, and results acquired in this study, see 3.1 and 3.2, clay and quick clay in Gjerdrum will be studied within a range of 1-160 Ωm . Resistivity-readings above 160 Ωm will not be regarded as realistic values for unleached or leached Norwegian clays. The compared resistivity-readings were obtained using the tTEM-system. Through Aarhus Workbench, the closest reading to each sample was picked up using the function "Find Nearest". The depth of the sample is linked to the closest resistivity-reading in that depth. In situations where a sample was located between two readings, these are interpolated to acquire the most accurate value for the sample in that depth. The data residuals for the points analyzed in this evaluation reach a maximum value of 5.54. Aside from some outliers, the remaining data points exhibit values ranging between 1 and 2, indicating high quality readings. In order to increase the size of the dataset, all data points have been included, regardless of their residuals.

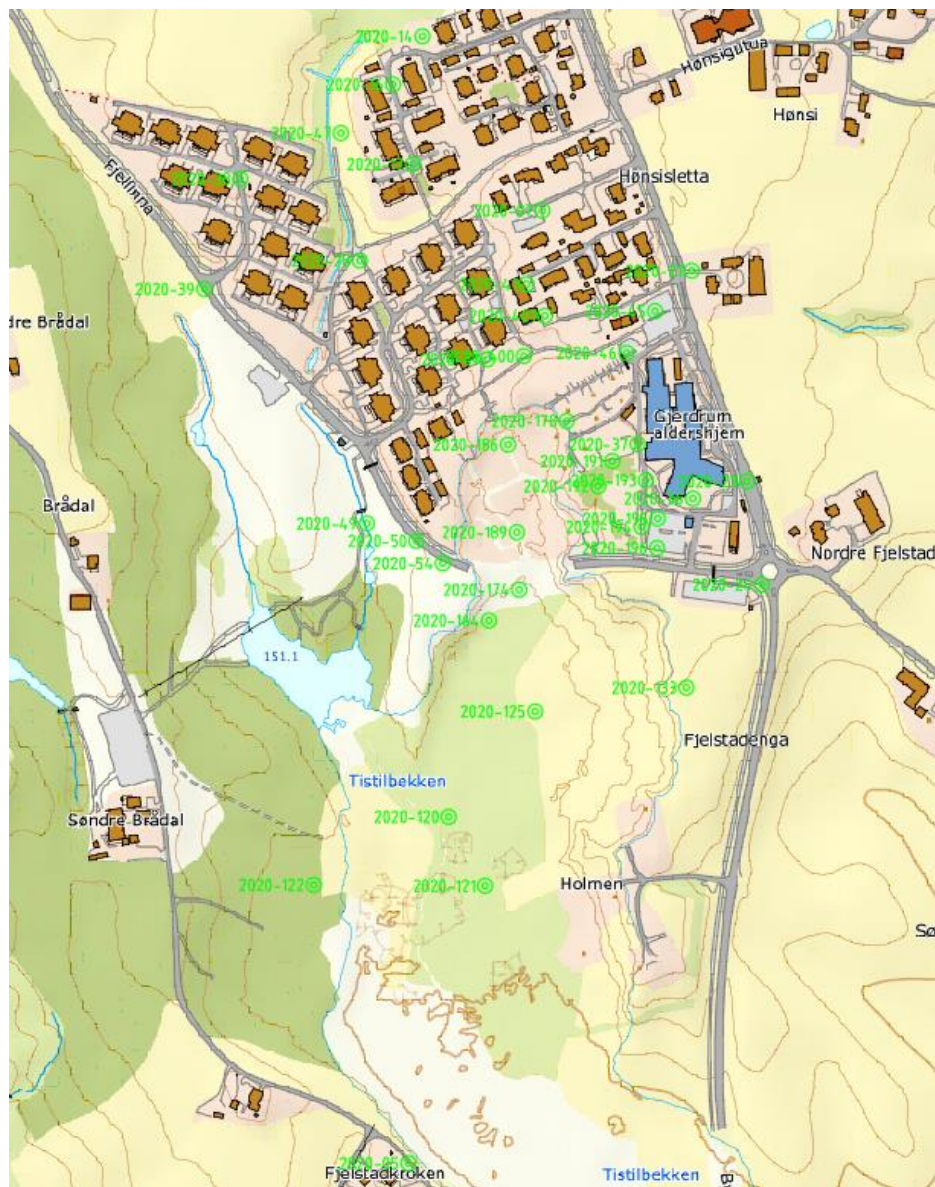


Figure 52. Overview of sampling locations in Gjerdrum

3.4.1 Sensitivity

Sensitivity is part of index-testing in the laboratory and is known by using the fall cone test, see NS 8015, (1988). NGF, (1982) propose quick clay for $S_t > 30$. This limit is marked with an orange line in Figure 53 and Figure 54. Gray lines mark a resistivity-limit between 20-100 Ωm . Sensitivity measurements is carried out for most of the samples from Gjerdrum, see Figure 52 for locations.

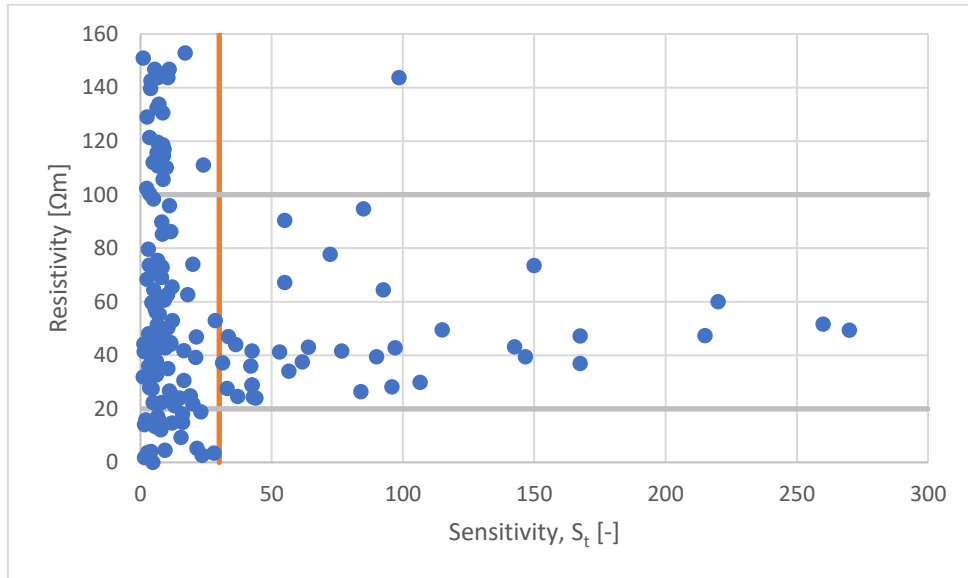


Figure 53. Sensitivity v. resistivity, all data

The majority of data points in this study are positioned below the sensitivity limit of 30, suggesting the presence of non-sensitive clay. Among the points that surpass this limit, indicating the occurrence of quick clay, nearly all of them exhibit resistivity values ranging from 20 to 100 Ωm .

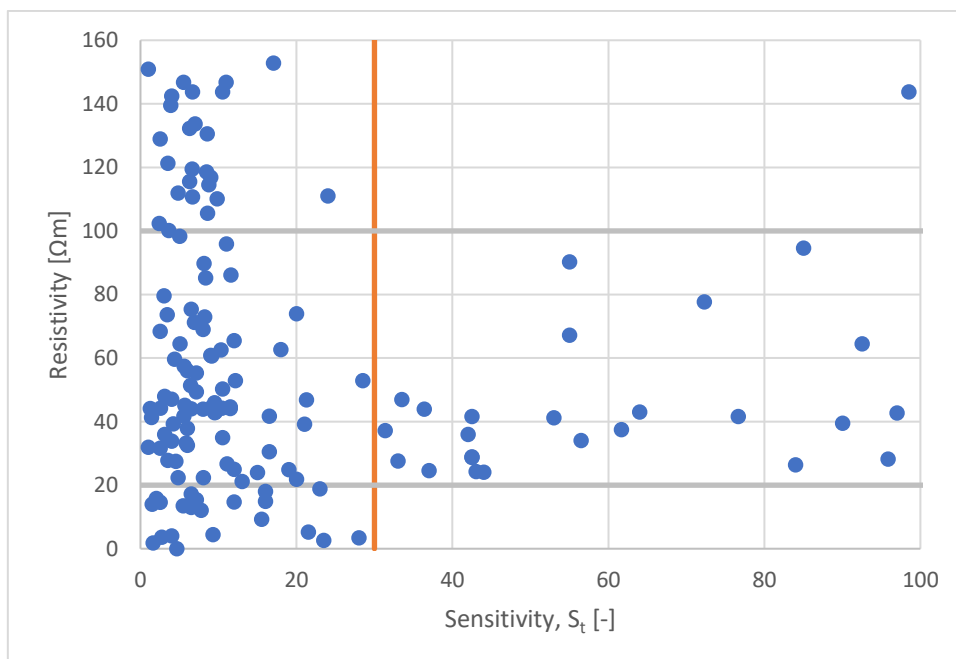


Figure 54. Sensitivity < 100

The examined data do not include any points with sensitivity values exceeding 30 while simultaneously exhibiting resistivity lower than 20 Ωm . This observation suggests that quick clay is not present for resistivity values below 20 Ωm in Gjerdrum. Additionally, the plot illustrates that sensitivity values below 30 can coexist with a wide range of resistivity values, spanning from 1 to 150 Ωm . Consequently, it is not possible to establish definitive threshold values based on these data. Both leached and unleached clay samples demonstrate considerable variation within the 20-100 Ωm resistivity range.

3.4.2 Remoulded shear strength

Remoulded shear strength is also part of index-testing in the laboratory and is known by using the fall cone test, see NS 8015, (1988). NGF, (1982) proposes quick clay for S_{ur} below 0.5 kPa, this limit is marked with an orange line in Figure 55 and Figure 56. Remoulded shear strength is also carried out for most of the samples in Gjerdrum, see Figure 52.

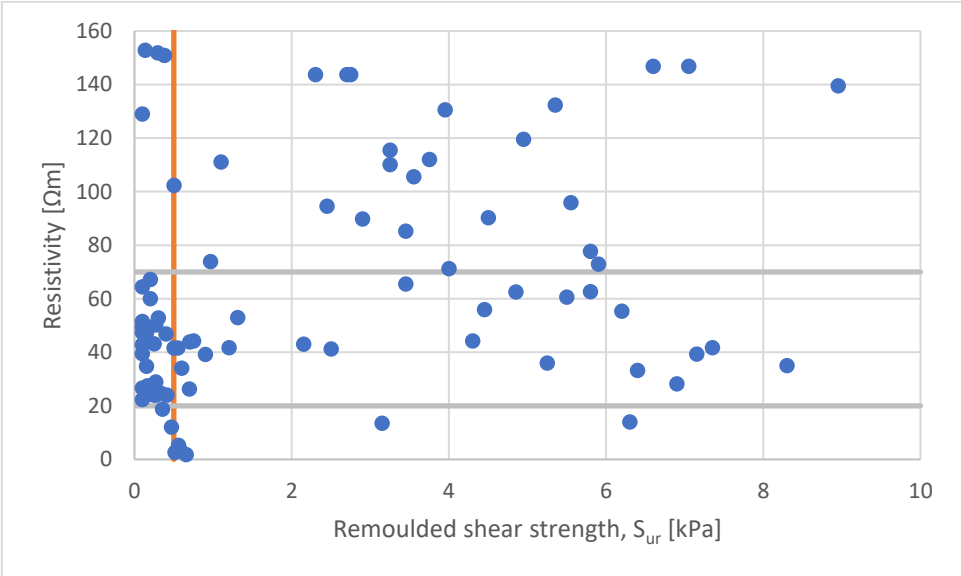


Figure 55. Remoulded shear strength v. resistivity, all data

The points exhibit considerable dispersion. Nevertheless, a distinct cluster of points is observed below the 0.5 line, indicating a concentration of data points with values falling below this threshold.

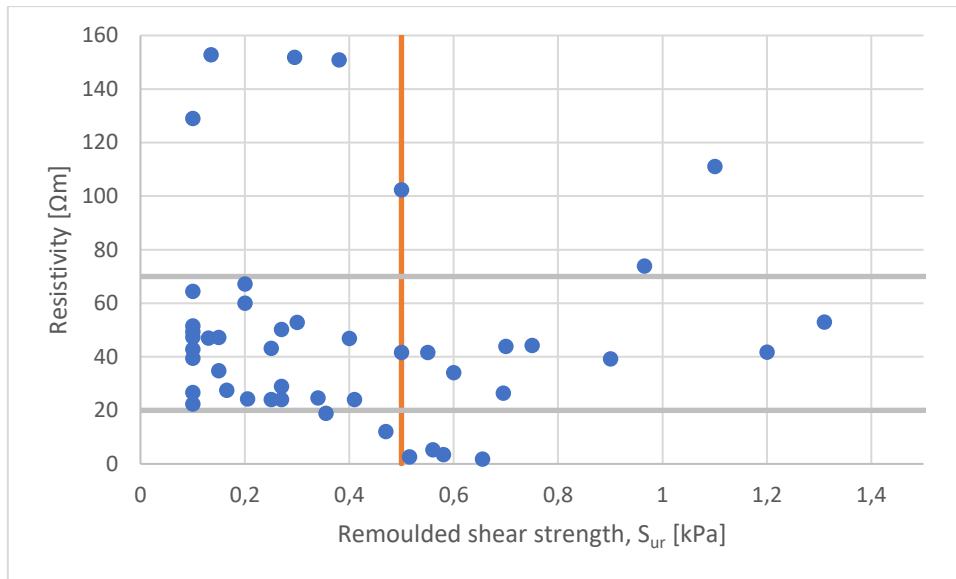


Figure 56. Remoulded shear strength < 1.5 kPa

Remoulded shear strength values below 0.5 kPa, which are indicative of quick clay, predominantly fall within the resistivity range of 20-70 Ωm . Additionally, the plot reveals the presence of several data points exceeding this limit, yet still positioned within this interval. Notably, only one data point exhibits shear strength lower than 0.5 kPa while simultaneously having resistivity lower than 20 Ωm . This finding supports the conclusion drawn from the sensitivity plot, indicating that quick clay in the Gjerdrum region tends to exhibit resistivity values above 20 Ωm .

Brittle soil material is indicated for samples with S_{ur} below 2 kPa (NS 8015, 1988). Within geotechnical engineering, brittle materials are treated with the same care as quick clay. The plot clearly illustrates that while no quick clay is observed below 10 Ωm , there are still multiple data points indicating the presence of brittle materials below this threshold.

3.4.3 Clay content

Clay content is found with the "Falling drop" method, see NS 8005, (1990). This measurement is carried out on a limited number of samples in Gjerdrum, see Figure 57.

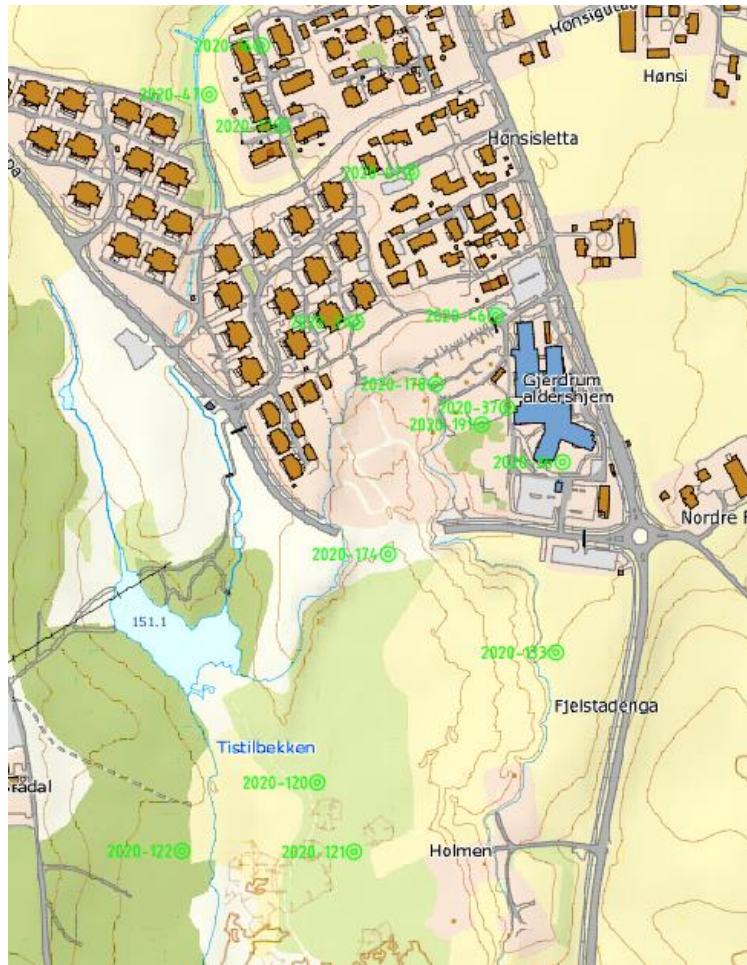


Figure 57. Clay content measurement locations

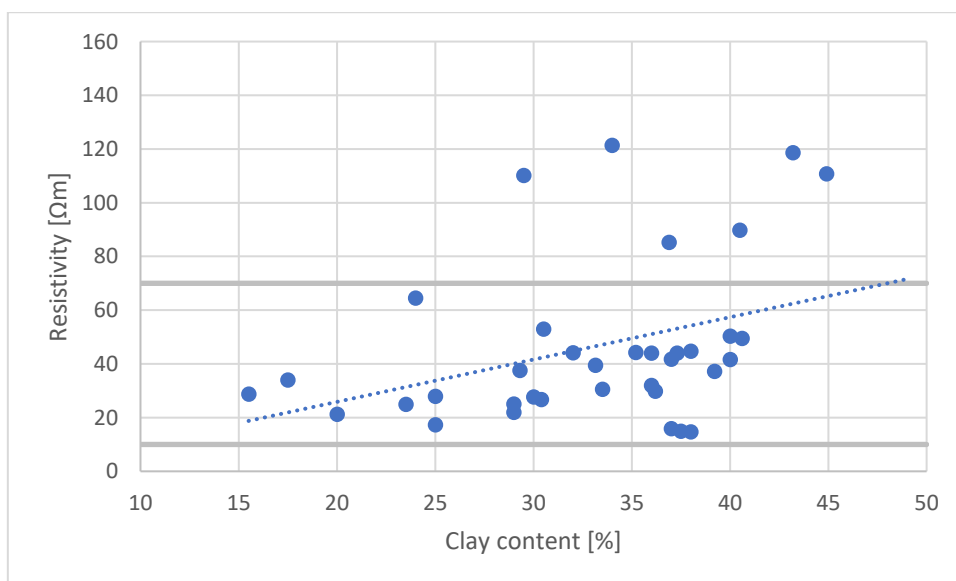


Figure 58. Clay content v. resistivity

The clay content in the Gjerdrum area varies between 15 % and 45 %. The majority of samples exhibit clay content in the range of approximately 30 % to 40 %. The plot visually demonstrates a subtle trend where the clay content tends to increase as resistivity values increase.

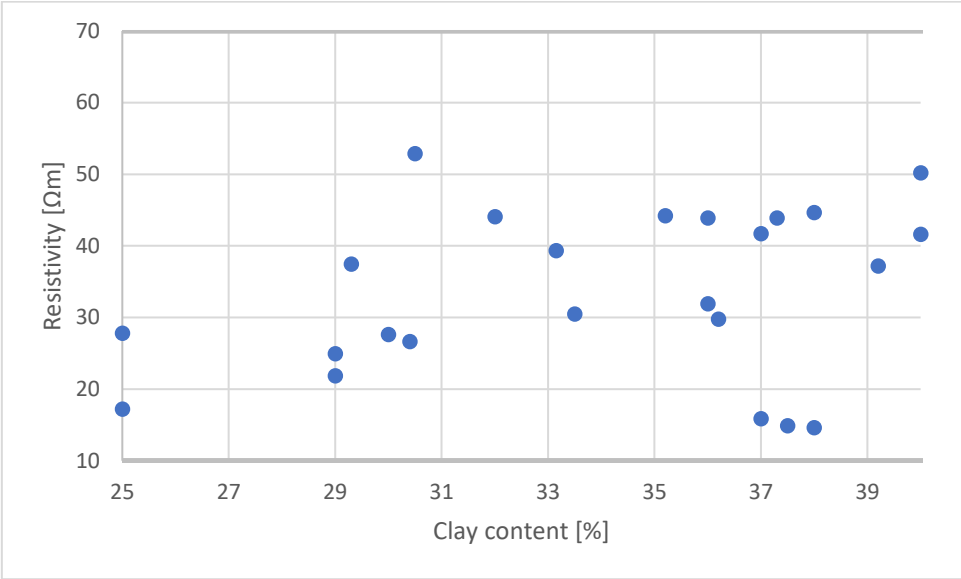


Figure 59. Clay content < 40 %

Upon closer examination, it becomes challenging to identify distinct and evident trends within the quadrant that contains the largest concentration of data points.

3.4.4 Salt content

Salt content was not routinely measured and was only controlled for a very limited number of samples in Gjerdrum. Torrance, (1974) suggests quick clay for salt contents below 2 g/l, which includes all these points. Salt content was carried out in two boreholes in Gjerdrum, see Figure 60.

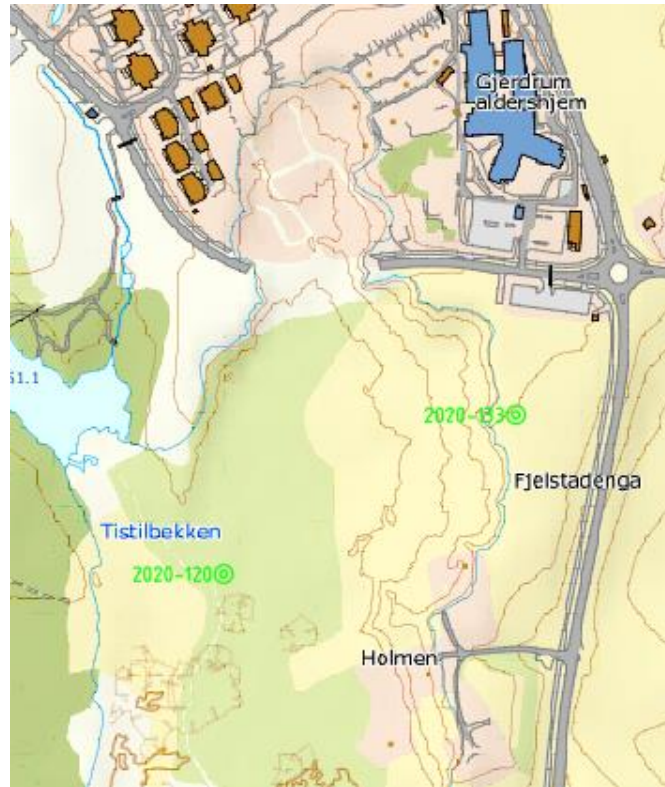


Figure 60. Salt content measurement locations

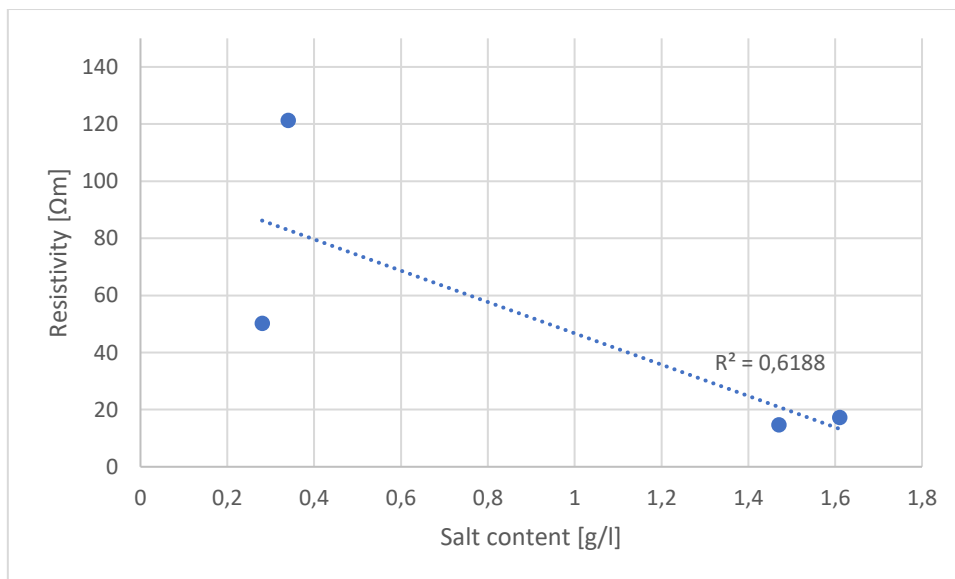


Figure 61. Salt content v. resistivity

Deposits characterized by higher salt content, ranging from 1.4 to 1.6, are predominantly found below 20 Ωm resistivity. Furthermore, it is observed that deposits with higher resistivity values also tend to exhibit lower salt content, aligning with the expected relationship between resistivity and salt content.

3.4.5 Other geotechnical parameters

Bulk density, water content and plasticity index are discussed in Appendix C: Other geotechnical parameters.

4 Discussion

4.1 Comparison with previous studies.

4.1.1 Resistivity-threshold

As discussed in 1.2, previous studies propose different resistivity thresholds for unleached clay, leached sensitive clay and dry crust. The consensus for Norwegian clays is summed up in Table 14.

Table 14. Resistivity-thresholds in Norway proposed by previous studies.

	Unleached clay deposits	Leached sensitive clay	Dry crust
Resistivity [Ωm]	< 10	10-100 10-80	> 100 80-200

The previous studies conducted in Norway have consistently reported similar resistivity thresholds, even when employing different combinations of geophysical approaches. This convergence among studies strongly suggests that these resistivity values are likely to be highly consistent and applicable to Norwegian clays. In the south-eastern region of Norway, several studies have examined resistivity thresholds for clay formations. Specifically, in the Smørgrav area, three studies (Bazin & Pfaffhuber, 2013; Donohue et al., 2012; Kalscheuer et al., 2013) have provided consistent findings. These studies concur on the identification of quick clay within the resistivity range of 10-90 Ωm , while unleached clays are typically characterized by resistivity values below 10 Ωm . In Hvitvingfoss, Sauvin et al., (2014) propose quick clay between 10-100 Ωm , but experience resistivity-values up to 150 Ωm for areas that exhibit siltier clays. Close to Trondheim, Solberg et al., (2012) suggests coarser materials such as moraine or bedrock and dry crust clay to possess values above 100 Ωm .

In this study, the following resistivity-threshold is proposed for the Gjerdrum landslide area, see 3.3:

Table 15. Resistivity-thresholds in Gjerdrum proposed by this study.

	Unleached clay deposits	Leached sensitive clay	Firm landslide mass
Resistivity [Ωm]	1-150	10-150	50-150

The leached sensitive clay identified in the Gjerdrum area exhibits a notable trend of generally higher resistivity values compared to what previous studies have proposed for clay formations in Norway. Earlier research suggest that quick clay is typically not encountered with resistivity values exceeding 100 Ωm . In this study, areas that are highly probable of being quick clay, have had readings up to 150 Ωm .

The unleached clay in the landslide area seems to vary a lot more than previous findings. In this research, the top clay layer and the lower unleached deposits within the study area

were considered as the same soil type, despite their occurrence in different layers. The resistivity measurements obtained from both layers revealed a wide range of values, spanning from 1 to 150 Ωm . Earlier studies consistently concluded that unleached clay is typically associated with resistivity values below 10 Ωm . However, the current research presents contrasting observations, indicating a notable divergence from the established understanding.

The presence of dry crust, which typically forms a firm and cohesive layer on the soil surface, was notably absent. This absence can be attributed to the significant displacement caused by the landslide event, which resulted in the removal of most of the top-layering within the pit-area. The present top-layer, referred to as landslide mass, has been interpreted and corresponds to values between 50-150 Ωm . Previous studies conclude with dry crust having values higher than that of quick clay, typically above 100 Ωm . The firmer landslide mass identified in this research displays resistivity values that are somewhat lower than those associated with dry crust clay.

Coarser layers in Gjerdrum exhibit values above 100 Ωm , which matches well with results from previous research. The tTEM data are often accurate in predicting transitions to these coarser materials. In several instances, rotary pressure soundings (RPS) ceased at assumed moraine or bedrock depths, aligning with the indications provided by the tTEM data. However, it is worth noting that there also were specific points where the tTEM data disagreed with the findings from RPS measurements. This discrepancy highlights the potential value of the tTEM method in guiding further geotechnical investigations. By incorporating insights from tTEM, drill crews can gain valuable information to guide their drilling operations, potentially uncovering additional geological features. Total soundings can prove bedrock by drilling to a depth of 3 meters. The tTEM data usually agrees with the total soundings with decent accuracy. However, in some points, the tTEM cannot resolve the data in these depths.

The geoelectrical data obtained in Gjerdrum exhibit generally higher resistivity values compared to what is documented in previous studies for similar soil types. This discrepancy can be attributed to several factors that influence the resistivity measurements in this particular area. There are multiple sources of noise in the area that can contribute to weakening the surveys. Especially in the northern part of the landslide area, close to housing and infrastructure. Construction machinery, pipes, containers, etc. were present when these surveys were carried out and contributed to weakening the signal-to-noise ratio. Even though the landslide mass in the area supposedly was cleaned of most of the landslide debris, there might have been parts left in the uppermost unleached clay. As addressed in 3.3.2, the high resistivity in the uppermost layer, weakens the signal of the geoelectrical surveys and reduces the accuracy as the signal continues deeper. However, it is expected that the data would offer the most reliable readings in the depth range of 5-25 meters, where the leached and unleached clays are predominantly present within the study area.

The fill mass utilized for leveling the landslide area should be regarded as unconsolidated material, leading to a greater void space between the grains. Consequently, this results in an increased presence of air within these layers. As air is very resistive, the lack of consolidation in these materials will contribute to increase their resistivity. Various other geotechnical parameters such as water content, grain shape and salinity can also contribute to increase resistivity, this will be further discussed in 4.1.3. Sauvin, (2014)

proposes a higher amount of silt to be influential in increasing resistivity for quick clay. Acquired data of grain distribution, presented in 3.4.3, do not support this trend.

The groundwater level exhibits variation throughout the landslide pit. For the profiles interpreted in this thesis the maximum depth below current terrain is about 5 meters. Beneath the groundwater level the resistivity should be lower as the conductivity increases where water is present in the soil. Shallower, unleached clay in Gjerdrum does exhibit larger resistivity than the deeper unleached clays. This observation supports the notion that the groundwater table exerts an influence on the resistivity characteristics in the study area. For the profiles, resistivity below 10 Ωm occurs in depths varying from 7 to 25 meters, i.e., consistently beneath the groundwater table.

For unleached clay, the values are inconsistent and do not match that of previous studies. Notably, clay that has surpassed its quick state demonstrates elevated resistivity levels, despite being categorized as non-sensitive, and has been used as an explanation for this trend in previous studies (Bazin & Pfaffhuber, 2013; Solberg et al., 2008, 2012). One possible explanation for the higher resistivity values observed in the uppermost layer of unleached clay is the potential presence of a mixture of landslide debris, stones, and other materials. These inclusions could contribute to an increase in resistivity readings. However, this explanation cannot be extended to account for the higher resistivity values observed in the deeper layers of the unleached clay.

Resistivity exhibits a complex behavior in both rocks and minerals, as well as in loose deposits, due to various factors such as soil moisture content, mineral types present, clay mineral shape and size, conductivity of the brine filling pores, and cementation. These factors can vary significantly and exert a significant influence on resistivity. Consequently, the creation of local resistivity thresholds may prove inaccurate. Therefore, a more appropriate approach might be to treat each case individually, taking into account the specific characteristics and conditions of the site.

4.1.2 Consistency of geoelectrical surveys

The geoelectrical surveys used in previous studies consist mostly of ERT and RCPTU. These methods have proven to be valuable in assessing subsurface conditions and characterizing soil properties. In more recent studies, additional attention has been given to the application of ATEM equipment. Other geophysical surveys like refraction seismic, GPR (ground penetrating radar) and RMT (radio-magnetotellurics) are also used in a few studies. The different geoelectrical surveys are known to provide comparable results. Especially ERT and RCPTU show good coherence according to previous studies (Bazin & Pfaffhuber, 2013; Kalscheuer et al., 2013; Long et al., 2012). Other studies have verified the consistency between the data obtained from ATEM and the results derived from ERT and RCPTU. However, it is worth noting that certain distinct trends can be observed when comparing electromagnetic (EM) data with ERT results.

Baranwal et al., (2017); Solberg et al., (2016) in their studies from Byneset, and Long et al., (2017) in their study from Kløfta, have identified a consistent trend in the geoelectrical data, where the values obtained from ERT initially exceed those derived from ATEM surveys. With increasing depth, the ERT shows a slower increase compared to ATEM data. This trend is not consistent with the findings of Löfroth et al., (2017); With et al., (2022) studies from Sweden, as their results do not support the notion of ERT having greater initial values. However, the ATEM data generally exhibit a faster increase in values compared to ERT, supporting the previously established trend. The Rydman, (2021) study

from Sweden presents findings that highlight the comparability of ATEM- and tTEM data. Given the demonstrated comparability between ATEM and tTEM in his study, the tTEM data obtained in the current research will be compared to previous ATEM data, allowing for a meaningful analysis and cross-validation of the results.

The study conducted by Anschütz et al., (2015) from E18-Kløfta/Kongsvinger shows that the ATEM effectively identified coarser layers prior to the ERT. Here, the ATEM data revealed the presence of bedrock or moraine at approximately 50 meters depth. This finding contrasts with the ERT data, which suggests the occurrence of bedrock or moraine at a greater depth of 90 meters. The depth of boreholes were assumed to coincide with the bedrock interface, which aligns well with observations from the ATEM. In certain areas of the study, notable discrepancies were observed between ERT- and ATEM data. Specifically, the ERT exhibited exceptionally high resistivity values ($>200 \Omega\text{m}$) within the first few meters, whereas the ATEM consistently indicated much lower values ranging from 7 to $30 \Omega\text{m}$. Further investigation revealed that this inconsistency could be attributed to the inherent limitations of the ATEM in resolving subsurface structures within the very near surface.

In Profile D, ERT data is compared to tTEM data, see 3.1.1. Intriguingly, consistent observations revealed a noticeable disparity within the first 5 meters of the stratigraphy. ERT data suggested resistivity reaching up to $500 \Omega\text{m}$ in specific areas, while the tTEM did not exceed $100 \Omega\text{m}$ in the same locations. Once past the initial few meters, the ERT and tTEM demonstrate a strong agreement in Profile D. The resistivity values obtained from both methods consistently fall within the range of $10\text{-}100 \Omega\text{m}$. In certain sections of the profile, both the ERT and tTEM surveys exhibit resistivity values below $10 \Omega\text{m}$. Although the two methods do not precisely coincide in identifying the exact locations of these low resistivity patches, they generally concur on the approximate areas where they are observed. This suggests a certain level of agreement in the overall interpretation of subsurface conditions, despite some minor discrepancies in the precise delineation of these low resistivity zones.

In the studied profiles, there is a notable discrepancy between the interpretations of the tTEM and ERT surveys regarding the probable location of the transition to bedrock. In profile D-3, the ERT data exhibits a perfect match with the location where the total sounding confirms the presence of bedrock at a depth of 40 meters. The tTEM signal generally reaches a depth of approximately 25 to 35 meters. In profile D-1, tTEM suggest resistivity of 150 to $500 \Omega\text{m}$ at depths where all rotary pressure soundings also suggest transition to coarser material. In this area, the ERT suggests bedrock to be located about 25 meters lower. The two surveys often disagree on where transition to bedrock is probable. These inconsistencies are often significant, making it challenging to favor one survey over the other in this purpose based solely on their agreement with geotechnical results.

This study aligns with the findings reported by Anschütz et al., (2015). In both studies, the ATEM data consistently anticipate the transition to coarser material earlier than indicated by the ERT data. The boreholes end at the same depth as the ATEM data, which substantiates the ATEM data for this profile. Baranwal et al., (2017); Solberg et al., (2016) and Long et al., (2017) present a trend where ERT initially show higher values, while ATEM gradually increases with depth, to a higher resistivity than the ERT. This current research study aligns with this observed trend, further corroborating the previous findings.

Like ATEM, the tTEM also faces challenges in resolving structures in the upper portions of the profiles. This limitation can be attributed to the presence of an immediate gravel layer, which proves difficult to resolve for the lower transmitter moment utilized in tTEM surveys. The tTEM is also susceptible to EM disturbance from housing, construction equipment, etc. in the northern part of the profile. The ERT has provided accurate values for the gravel layer based on Figure 2. However, it should be noted that the ERT measurements indicate a layer thickness of up to 5 meters, whereas the expected thickness of the gravel layer is around 1 meter. This discrepancy suggests that factors other than the actual thickness of the gravel layer may be influencing the resistivity values obtained from the ERT measurements. One possible explanation for the observed resistivity values is the presence of vertical drains which may introduce additional electrical pathways or alter the flow of current within the subsurface, thereby influencing the resistivity measurements. Another possible explanation is that the resolution of the ERT survey is unable to sufficiently capture and resolve abrupt changes in resistivity associated with the gravel layer.

The two methods provide matching results in homogeneous layers, but struggle to determine specific areas with resistivity values below 10 Ωm . The data might vary here because of different anomalies or subsurface features that give rise to distinct electrical properties. Another potential explanation is the existence of a different regime for changes in resistivity with depth.

The tTEM indicates coarser material at a lower depth than the ERT. This observation can be attributed to the inherent limitations of the tTEM method in distinguishing resistivity values above 200 Ωm (Personal com. Boufidis, 2023). Consequently, the tTEM data tend to exhibit a rapid increase in resistivity values after surpassing the threshold of 150 Ωm . The presence of conductive minerals in the bedrock is an important consideration, as highlighted by Solberg et al., (2008, 2016), when using 2D resistivity for depth indications. Certain minerals possess high electrical conductivity and can contribute to increase the conductivity and consequently decrease the resistivity in the data. However, this trend is not observed in Gjerdrum.

In this study, it was observed that the ERT signal generally reaches depths of approximately 40 meters, while the DOI for the tTEM is ranging from 25 to 35 meters. Based on earlier discussions and expectations, it was anticipated that the tTEM signal would penetrate deeper into areas where the presence of high-resistive layering was absent. In order to further investigate the impact of the high-resistivity top layer on the depth of signal penetration, a comparison was made between profile D-3, where gravel is present, and profile D-4, where gravel is not present. Surprisingly, it was observed that the DOI of the tTEM was approximately 30 meters in both profiles. This observation suggests that the presence of a high-resistivity top layer may have a relatively limited impact on the depth of signal penetration.

4.1.3 Correlation study

Long et al., (2012) propose a notable correlation between clay content and resistivity, where an increase in clay content corresponded to a decrease in resistivity. Specifically, they found that points with clay content higher than 40% tended to exhibit lower resistivity values. However, some points with clay content below 20% showed resistivity values exceeding 100 Ωm . Sauvin, (2014) has observed that sites with relatively high silt content and low clay content can exhibit resistivity values of up to 150 Ωm . Swedish studies suggests quick clay for values as low as 3 Ωm (With et al., 2022). Dahlin et al., (2013) conclude that the measured resistivity and clay content comply for every sampling point.

The study findings consistently demonstrate that as the clay content decreases, the resistivity values tend to increase. Sandven et al., (2015) suggest that this lower limit can be attributed to the presence of a thicker Swedish clay, which subsequently leads to a higher clay content. Rankka et al., (2004) have reported the clay content of Swedish clay, specifically in the Jonaker and Ugglum areas, to range from 50 % to 60 %.

In the study area of Gjerdrum, the clay content ranges from 15 % to 45 % (see Figure 58) which is slightly lower than the data analyzed by Long et al., (2012). The relationship between clay content and resistivity in Gjerdrum shows a trend that contradicts the findings of the aforementioned studies. Resistivity values above 100 Ωm vary between 29 % and 45 % clay content, giving no indication that higher clay content leads to lower resistivity as proposed by Sauvin, (2014).

The clay in Gjerdrum, see 3.4.3, does not exhibit distinctively low clay content compared to the data analyzed in the study conducted by Long et al., (2012). Consequently, it is challenging to attribute the high resistivity observed in Gjerdrum clay solely to this characteristic, although it may still play a role. The acquired samples do not show clear signs of being influenced by landslide mass or debris, although this can be a possible reason for why the trend deviates from previous studies.

Long et al., (2012) put forward a trend suggesting a decrease in resistivity with increasing plasticity index (I_p), which aligns with the understanding that I_p tends to increase with higher clay content. This observation is in accordance with the concept that clay-rich materials exhibit higher plasticity and lower resistivity. Notably, samples with resistivity values below 10 Ωm were found across the entire range of I_p values, indicating no clear trend for differentiating unleached and leached clays.

Data collected in Gjerdrum shows that there are no samples with resistivity below 10 Ωm for I_p values above 15% (medium plasticity), see Appendix C: Other geotechnical parameters. This finding suggests that the quick clay in Gjerdrum exhibits a higher degree of plasticity. The resistivity values corresponding to different plasticity index (I_p) values exhibit significant variability, making it challenging to discern a clear trend for the entire dataset. This lack of consistency is expected since I_p is influenced by clay content, which also showed a weak correlation with resistivity.

Long et al., (2012) found a strong link between salt content and resistivity. Their findings indicated that an elevated salt content had a significant impact on reducing resistivity values. The resistivity values tend to converge at around 5 Ωm when the clay samples exhibit a salt content greater than 8 g/l. Furthermore, the data indicate that no samples with a salt content below 4 g/l have resistivity values below 10 Ωm . This suggests no quick clay for samples with salt content higher than 4 g/l. The findings of Solberg et al., (2016) support the correlation between salt content and resistivity. In their study, they observed that resistivity values below 10 Ωm were associated with a salt content of approximately 2.5 g/l. Interestingly, their data also revealed that every reading below 2 g/l had resistivity values equal to or higher than 10 Ωm . This observation match well with the conclusion drawn by Torrance, (1974) regarding the presence of quick clay below the threshold of 2 g/l salt content.

In Gjerdrum, salt content was obtained from 14 samples. However, only four of these were able to be given a reasonable resistivity-value based on the location of the data. All these exhibited salt contents below 2 g/l, indicating quick clay. As anticipated based on previous research, none of these points displayed resistivity values below 10 Ωm . Consistent with

the findings of Long et al., (2012), the plot of salt content against resistivity indicated a trend where higher salt content corresponded to lower resistivity.

Long et al., (2012) present a distinct correlation between increasing remoulded shear strength and decreasing resistivity. This finding is in line with the understanding that remoulded shear strength is closely linked to the salt content of clay formations. The study provides further support to the notion that as clay undergoes leaching, the S_{ur} is reduced. Upon closer examination of the data, it is evident that all the data points below 0.5 kPa of remoulded shear strength also fall within a range of 10-70 Ωm . This observation holds true when considering the majority of the data, excluding certain data points from areas with relatively high silt content (below 20 % clay content), which exhibit resistivity values up to 150 Ωm . The findings of Solberg et al., (2016) show that all data below 0.5 kPa are exclusively above 10 Ωm . However, there are plenty of data that lies between 10-60 Ωm while also exhibiting values above 0.5 kPa, making this interval unexclusive to quick clay. In contrast to the clear tendency observed in the plot presented by Long et al. (2012), the findings of this study do not replicate the same pattern. The measurements obtained in this research consistently demonstrate resistivity values below 60 Ωm , indicating relatively low levels of silt content. The analysis of clay content in this study reveals variations within the range of 30-40 %, which differs slightly from the observations made by Long et al. (2012), where variations were primarily observed within the range of 30-50 %.

The data obtained from Gjerdrum, see 3.4.2, do not exhibit a clear trend in the plot. However, an interesting observation is that all data points below 0.5 kPa, indicating non-quick clay, are consistently above 10 Ωm . This consistency is valuable in distinguishing areas characterized as non-quick clay. On the other hand, numerous data points above 100 Ωm are observed for quick clay, as observed throughout this study.

Long et al., (2012) established a linear relationship between increasing sensitivity and resistivity. Specifically, they found that all sensitivity values above 30, which are indicative of potential quick clay, were associated with resistivity values above 10 Ωm . This finding supports the notion that resistivity can serve as an effective indicator of the presence of quick clay. Rankka et al., (2004) presents a Swedish study which indicated that resistivity higher than 5 Ωm is possibly quick clay. In accordance with this finding, the analysis revealed that all samples exhibiting sensitivity values above 30, also exhibited resistivity values surpassing the 5 Ωm threshold.

The data obtained from our study exhibits similarities to the findings of Long et al., (2012). Notably, none of the points indicated as quick clay based on sensitivity values have resistivity values below 20 Ωm . This corresponds well with the conclusion drawn from the remoulded shear strength. It is important to note that the determined resistivity threshold for quick clay in Gjerdrum slightly exceeds the limits reported in previous studies.

Long et al., (2012) proposed that resistivity would decrease with increasing unit weight due to the particles being forced closer together. However, our study did not give clear observations supporting this hypothesis, see Appendix C: Other geotechnical parameters. The resistivity data below 20 Ωm exhibited variations ranging from 16 to 21 kN/m³, while the resistivity data above 20 Ωm showed variations ranging from 18.8 to 20.3 kN/m³. This suggests a slightly higher unit weight for quick clay in the area. However, it is crucial to emphasize that the link between unit weight and resistivity in quick clay formations is very weak based on the data analyzed in this study. Similarly to unit weight, Long et al., (2012) find no clear pattern between resistivity and water content. The plotted water content values in their study vary from 20 % to 50 %, regardless of the corresponding resistivity

values. In the case of Gjerdrum, the water content of the samples ranges from 25 % to 35 %, and there is no apparent correlation between water content and resistivity.

4.1.4 Reliability and relevance

The results presented in this study are based on a comprehensive dataset collected within the Gjerdrum landslide area. It is important to note that the quantity of data obtained in this particular area may not be representative of a typical project setting or applicable to quick clay mapping efforts on a broader scale. In contrast to many previous studies, the present study incorporates an extensive number of geotechnical boreholes, providing a significantly higher level of subsurface layering information. This increased geotechnical basis enhances the reliability and accuracy of the assessment of the two geoelectrical surveys conducted.

The study of landslide areas presents unique challenges when it comes to conducting geoelectrical surveys, primarily due to the presence of various sources of noise and uncertainties inherent to these dynamic environments. Geoelectrical methods are known to excel in areas characterized by homogeneous subsurface conditions, where resistivity changes gradually and predictably. As explained in 2.1.2, the landslide pit is highly influenced by various safety measures, while also potentially containing some debris in the upper layers. These changes decrease the accuracy of the geoelectrical surveys for our main purpose, differentiating leached and unleached clay. As a consequence, the findings of this study may have limited relevance when compared to undisturbed sites. In addition, uncertainties arise regarding the accuracy of geotechnical surveys due to the parallel implementation of safety measures. This temporal overlap makes it difficult to ascertain the exact conditions of the area when the boreholes were drilled. However, it is important to note that these uncertainties primarily pertain to the upper layers.

4.1.5 Significance

The findings presented in this research contribute to the reinforcement of certain conclusions put forward by previous studies. The results are significant for the mapping of quick clay in landslide-affected areas, demonstrating the utility of geoelectrical data in characterizing regions that exhibit inhomogeneity and are influenced by significant noise factors. This study has provided valuable insights into the tTEM equipment, which has not received extensive prior investigation, showcasing its potential as a cost-effective and efficient electromagnetic method for geological and geotechnical applications. Further research and exploration of the tTEM survey technique for quick clay mapping hold great significance for geotechnical engineers and other professionals involved in ensuring stability.

4.2 Solving research questions

Research questions proposed in 1.3:

- Provide resistivity-thresholds for non-leached clay, leached clay, and landslide mass in the area, based on geotechnical boreholes.

The variability of resistivity thresholds in the study area makes it challenging to establish separate thresholds for the three soil types, see Table 15. However, based on the analyzed profiles, it can be concluded that quick clay rarely is found below 10 Ω m.

- Explore the innovative geophysical method tTEM's ability to differentiate leached from unleached clay.

The tTEM data collected in the landslide area do not exhibit clear consistency in differentiating leached from unleached clay. This lack of differentiation is attributed to the fact that the leached and unleached clay layers occupy similar intervals of resistivity values. As a result, the tTEM method alone is insufficient to reliably distinguish between these two clay types in the studied area.

- Assess the effectiveness of tTEM in conjunction with the geophysical method ERT to explore its utility for mapping of quick clay.

The two geoelectrical surveys conducted in the study area demonstrate relatively good agreement in regions where they are less susceptible to noise influence. The presence of multiple surveys increases the likelihood of obtaining reliable information from at least one of the methods. In areas where the surveys exhibit discrepancies, there are justifiable reasons for the observed differences, such as the presence of safety measures or debris, which can affect the accuracy of the surveys. However, in regions where the surveys align and provide consistent results, the data proves valuable and reliable for further analysis and interpretation.

- Provide correlations between geotechnical parameters and resistivity.

Despite the lack of a clear correlation between resistivity and parameters such as S_{ur} and S_t , meaningful conclusions can still be drawn from the analysis. Based on an analysis of all samples in the area and considering empirical geotechnical limits, it can be concluded that no indications of quick clay are observed below a resistivity threshold of $10 \Omega m$. This finding suggests that a resistivity value of $10 \Omega m$ or higher can serve as a reliable indicator for the absence of quick clay in the studied region. The study reveals promising findings regarding the relationship between salt content and clay characteristics, although it should be noted that these conclusions are based on a very limited number of samples.

- Investigate how CPTU data using Mayne-method reproduce against other soundings and sampling, see Appendix B: CPTu-interpretation (Mayne), for results.

The application of the Mayne method in this study demonstrates its potential as a reliable technique for assessing the presence of quick clay. The results obtained from the Mayne method exhibit a high degree of agreement with data derived from other methods such as RPS, TOT and conventional soil sampling. However, it should be noted that in certain areas, the Mayne method occasionally misidentifies clay as quick clay, whereas subsequent soil sampling reveals its non-quick clay nature. This suggests the need for careful interpretation and validation of the results from the Mayne method in such specific areas to ensure accurate identification of quick clay occurrences.

4.3 Impact of the proposed findings

The results reveal that there is high uncertainty related to separating leached and unleached clay using tTEM in Gjerdrum. However, the use of geoelectrical surveys alone and in combination has proven useful in linking up boreholes that are far from each other. Even though the landslide area is highly influenced by safety measures and changes in the upper stratigraphy, the results show resemblance of what was expected from previous research. This observation demonstrates that the geoelectrical surveys exhibit some

resilience against the high amounts of noise in this area. Geoelectrical methods have potential in reducing the number of boreholes needed in a project. The tTEM has through the HiGELIG project proven to be an effective and cheap survey to conduct, while providing data which resolution and accuracy are comparable to the well-known ERT. This confirms that the tTEM can be a valuable addition for soil investigation, especially in areas with lower variations in resistivity. The resistivity threshold values for different soil types in the area overlap with each other, highlighting the essential role of geotechnical investigations in distinguishing between the different soil types. However, empirical values obtained for the geotechnical parameters of quick clay indicate that resistivity values below 10 Ωm in Gjerdrum do not correspond to the presence of quick clay. This observation can be very useful to establish measurements below 10 Ωm as non-quick clay.

4.4 Assess the study

4.4.1 What could have been better?

To assess what could have been better for this study it is crucial to understand the factors that contribute to uncertainties in the collected data. By enhancing the consistency and certainty in the employed methods, it is possible to achieve clearer and more reliable results. Conducting the research in an undisturbed area would have resulted in less noise influencing the data and a more homogeneous stratigraphy, thereby facilitating easier interpretation. However, the exploration of these surveys in a challenging environment has provided valuable insights into their resilience and applicability.

Having access to data from before the occurrence of the landslide could possibly have enhanced the study. However, due to the presence of obstacles and hindrances in the area at this time, ERT profiles could not have been projected as far. In hindsight, expanding the coverage of ERT profiles in the area following the landslide would have been beneficial. Specifically, the inclusion of a profile perpendicular to profile D would have provided additional spatial information and enabled a more comprehensive comparison between the two data sets. To enhance the signal-to-noise ratio in the geoelectrical survey, an alternative electrode configuration such as the Wenner configuration could have been employed. The Wenner configuration is known to offer improved sensitivity to subsurface variations but would have come at the cost of reduced survey efficiency, approximately tripling the time required to complete the data acquisition process. Due to limitations in the accessibility and challenging terrain of the landslide area, it was not feasible to extend the coverage of the tTEM survey beyond the areas already surveyed. Furthermore, the ATV used for data collection was already operating at a reduced speed due to the demanding terrain, ensuring the acquisition of the highest possible signal-to-noise ratio given the constraints of the field conditions.

In the investigated landslide area, a significant number of boreholes were drilled without accompanying sampling, which resulted in a lack of secure data for the study. For the specific objectives of this study, the inclusion of sampling would have provided more reliable data compared to the geotechnical soundings, ensuring a more robust understanding of the subsurface conditions. However, it is important to note that sampling can be costly, which often imposes limitations on its use. Also, in some of the boreholes, only CPTU data was available, which is not a preferred method for identifying sensitive layers. Moreover, considering the significance of salt content in the context of quick clay,

it would be highly valuable to expand the sampling efforts in Gjerdrum to include a larger number of samples.

4.4.2 Strong and weak sides of the study

This study presents a comprehensive collection of geotechnical data within a relatively confined area, providing a robust foundation for calibration and validation of the geoelectrical data. Substantial amounts of sampling were conducted across the entire study area and routine laboratory tests were performed on the majority of these samples, which has provided a solid basis for the correlation study. The utilization of tTEM equipment is another notable strength of this study, as it has demonstrated to provide valuable data, for a geotechnical perspective.

One limitation of this study is the presence of high levels of noise in the area, primarily attributed to various safety measures implemented in the landslide pit. The geotechnical investigations were conducted simultaneously with these actions, while the geoelectrical surveys took place after the completion of all safety measures. The noise generated by these activities could have introduced uncertainties and affected the accuracy of the geoelectrical data, thereby posing challenges to the interpretation and analysis of the results. Due to the critical role of geotechnical data in the safety assessment, it was necessary to collect this information prior to conducting the geoelectrical surveys. However, this chronological order of data collection might have resulted in some inconsistencies between the geotechnical and geoelectrical data, as the geological conditions and characteristics of the site changed during the implementation of safety measures.

4.5 Conclusions and recommendations

The ultimate objective of this thesis was to further investigate and evaluate the suitability of resistivity measurements for quick clay mapping. Throughout this study, various tasks were undertaken to address this objective and examine its feasibility. It was found that:

1. The resistivity thresholds for unleached and leached clays in the Gjerdrum area exhibit greater variability than initially anticipated. Based on the analysis of eight profiles conducted across the landslide area, this study concludes that quick clay exhibits a resistivity range of 10-150 Ωm , while non-quick clay shows a wider range of resistivity from 1-150 Ωm . These findings indicate that the reliable differentiation of sensitive possible quick clay from unleached deposits using geoelectrical surveys is only possible when measurements fall below 10 Ωm .
2. Correlation between resistivity and geotechnical parameters indicates that the threshold for quick clay in Gjerdrum may be slightly narrower, ranging between 10-100 Ωm . Patterns observed in sensitivity and remoulded shear strength plots against resistivity provide valuable insights, affirming that proven quick clay is never found below 10 Ωm in the study area. The analysis of clay content, bulk density, water content, and plasticity index in relation to resistivity did not reveal any significant correlation or discernible patterns.
3. A comparative analysis between electrical resistivity tomography (ERT) and towed transient electromagnetics (tTEM) reveals a high degree of agreement in resistivity measurements. However, it is noted that ERT is more effective in resolving the resistivity values in the upper stratigraphy, whereas tTEM struggles to provide detailed information about these structures. Notably, the tTEM consistently exhibits a rapid increase in resistivity readings with depth compared to ERT.
4. It should be noted that in the challenging landslide area, the DOI of the tTEM method only reached 25 meters in some areas. In contrast, the ERT method, while less effective overall, demonstrated the ability to penetrate to greater depths. Therefore, the combination of both surveys has proven to be effective, as they can compensate for some of each other's limitations and can be considered highly reliable where the data sets show agreement.
5. The tTEM method has demonstrated its effectiveness and cost-efficiency, providing valuable data including indications of bedrock or moraine depth and the ability to rule out the presence of quick clay in areas characterized resistivity below 10 Ωm in Gjerdrum.

References

- ABEM. (2016). *Terrameter LS 2—User manual*.
- Agaiby, S. S., & Mayne, P. W. (2021). CPTU identification of regular, sensitive, and organic clays towards evaluating preconsolidation stress profiles. *AIMS Geosciences*, 7(4), 553–573. <https://doi.org/10.3934/geosci.2021032>
- Anschütz, H., Bazin, S., & Pfaffhuber, A. (2015). *Towards Using AEM for Sensitive Clay Mapping—A Case Study from Norway*. <https://doi.org/10.3997/2214-4609.201413863>
- Auken, E., Foged, N., Larsen, J. J., Lassen, K. V. T., Maurya, P. K., Dath, S. M., & Eiskjær, T. T. (2019). TTEM — A towed transient electromagnetic system for detailed 3D imaging of the top 70 m of the subsurface. *GEOPHYSICS*, 84(1), E13–E22. <https://doi.org/10.1190/geo2018-0355.1>
- Bache, B. K. (2021). *Stabilisering av nordre del av skredgrova* (Nr. 20200909-14-TN).
- Baranwal, V. C., Rønning, J. S., Solberg, I.-L., Dalsegg, E., Tønnesen, J. F., & Long, M. (2017). *Investigation of a Sensitive Clay Landslide Area Using Frequency-Domain Helicopter-Borne EM and Ground Geophysical Methods*.
- Bargel, T. H. (2005). *Gråsteinen nr 10—2005*.
- Bastani, M., Persson, L., Löfroth, H., Smith, C. A., & Schälin, D. (2017). *Analysis of Ground Geophysical, Airborne TEM, and Geotechnical Data for Mapping Quick Clays in Sweden*.
- Bazin, S., & Pfaffhuber, A. A. (2013). Mapping of quick clay by electrical resistivity tomography under structural constraint. *Journal of Applied Geophysics*, 98, 280–287. <https://doi.org/10.1016/j.jappgeo.2013.09.002>
- Bjerrum, L., & Landva, A. (1965). *Direct Simple-Shear Tests on a Norwegian Quick Clay*. <https://doi.org/10.1680/geot.1966.16.1.1>

- Christensen, C. W., Harrison, E. J., Pfaffhuber, A. A., & Lund, A. K. (2021). A machine learning-based approach to regional-scale mapping of sensitive glaciomarine clay combining airborne electromagnetics and geotechnical data. *Near Surface Geophysics*, 19(5), 523–539. <https://doi.org/10.1002/nsg.12166>
- Dahlin, T., Löfroth, H., Schälin, D., & Suer, P. (2013). Mapping of quick clay using geoelectrical imaging and CPTU-resistivity. *Near Surface Geophysics*, 11. <https://doi.org/10.3997/1873-0604.2013044>
- Dahlin, T., & Zhou, B. (2006). Multiple-gradient array measurements for multichannel 2D resistivity imaging. *Near Surface Geophysics*, 4(2), 113–123. <https://doi.org/10.3997/1873-0604.2005037>
- DiBiagio, A. J. (2021). *Akuttbilstand skred Ask, Gjerdrum* (Nr. 20200909-01-R).
- DiBiagio, A. J., & Heyerdahl, H. (2022). *Sikringstiltak i nordre skredgrop* (Nr. 20200909-16-TN).
- Donohue, S., Long, M., O'Connor, P., Eide Helle, T., Aspmo Pfaffhuber, A., & Rømoen, M. (2012). Multi-method geophysical mapping of quick clay. *Near Surface Geophysics*, 10(3), 207–219. <https://doi.org/10.3997/1873-0604.2012003>
- Grønvold, K. (2022). *Geoelectrical methods for quick clay mapping in Gjerdrum* (s. 36).
- Hovind, M. (2021). *Kvikkleireskred Ask Gjerdrum* (Nr. 10223695-02-RIG-RAP-002).
- Kalscheuer, T., Bastani, M., Donohue, S., Persson, L., Aspmo Pfaffhuber, A., Reiser, F., & Ren, Z. (2013). Delineation of a quick clay zone at Smørgrav, Norway, with electromagnetic methods under geotechnical constraints. *Journal of Applied Geophysics*, 92, 121–136. <https://doi.org/10.1016/j.jappgeo.2013.02.006>
- L'Heureux, J.-S., Høydal, Ø. A., Paniagua Lopez, A. P., & Lacasse, S. (2018). *Impact of climate change and human activity on quick clay landslide occurrence in Norway*.

- Long, M., Donohue, S., L'Heureux, J.-S., Solberg, I.-L., Rønning, J. S., Limacher, R., O'Connor, P., Sauvin, G., Rømoen, M., & Lecomte, I. (2012). Relationship between electrical resistivity and basic geotechnical parameters for marine clays. *Canadian Geotechnical Journal*, *49*(10), 1158–1168. <https://doi.org/10.1139/t2012-080>
- Long, M., Pfaffhuber, A., Bazin, S., Kåsin, K., Gylland, A., & Montafia, A. (2017). Glacio-marine clay resistivity as a proxy for remoulded shear strength: Correlations and limitations. *Quarterly Journal of Engineering Geology and Hydrogeology*, *51*, qjegh2016-136. <https://doi.org/10.1144/qjegh2016-136>
- Longva, O. (1987). *Ullensaker 1915 II*.
- Lundstrøm, K., Larsson, R., & Dahlin, T. (2009). *Mapping of quick clay formations using geotechnical and geophysical methods*.
- Lysdahl, A., Pfaffhuber, A. A., Anschütz, H., Kåsin, K., & Bazin, S. (2017). *Helicopter Electromagnetic Scanning as a First Step in Regional Quick Clay Mapping*.
- Löfroth, H., Lundstrøm, K., Persson, L., Bastani, M., Ekström, J., Smith, C. A., & Schälin, D. (2017). *Development of a Methodology for Quick Clay Mapping*.
- Mayne, P. W., Paniagua, P., L'Heureux, J.-S., Lindgård, A., & Emdal, A. (2019). *Analytical CPTu model for sensitive clay at Tiller-Flotten site, Norway*. 8.
- Moholdt, R., & DiBiagio, A. J. (2021a). *Avlastning av skredkanten i nordre skredgrop* (Nr. 20200909-15-TN).
- Moholdt, R., & DiBiagio, A. J. (2021b). *Avlastning av skredkanten sør for Gjerdrum bo- og behandlingssenter* (Nr. 20200909-11-TN).
- NGF. (1982). *NGF-melding 2*.
- NGF. (2019). *Veiledning for detektering av sprøbruddmateriale*.
- NGI, Geomap Norge, VFK, AGI, & EE. (2022). *HIGELIG project reports—O1 and O2*.
- NGU. (2023). *Løsmasser—NADAG*.

- NS 8002. (1982). *Geoteknisk prøving Laboriemetoder Konusflytegrensen.*
- NS 8003. (1982). *Geoteknisk prøving Laboriemetoder Plastisitetsgrensen.*
- NS 8005. (1990). *Geoteknisk prøving Laboriemetoder Kornfordelingsanalyse av jordprøver.*
- NS 8015. (1988). *Geoteknisk prøving—Laboriemetoder—Bestemmelse av udrenert skjærstyrke ved konusprøving.*
- OED. (2021, september 29). *Årsakene til kvikkleireskredet i Gjerdrum 2020* [Rapport].
Regjeringen.no; regjeringen.no. <https://www.regjeringen.no/no/dokumenter/arsakene-til-kvikkleireskredet-i-gjerdrum-2020/id2872948/>
- Olerud, S. (1982). *Berggrunnskart; Nannestad; 19153; 1:50 000.*
- Palacky, G. J. (1988). *Electromagnetic Methods in Applied Geophysics: Volume 1, Theory. I Resistivity Characteristics of Geologic Targets.*
- Penna, I., & Solberg, I.-L. (2021). *Landscape changes and bedrock reconstruction in Gjerdrum area. Methodological approach and main results.*
- Pfaffhuber, A., Bazin, S., & Helle, T. E. (2014). *An Integrated Approach to Quick-Clay Mapping Based on Resistivity Measurements and Geotechnical Investigations.*
- Rankka, K., Andersson-Sköld, Y., Hultén, C., Larsson, R., Leroux, V., & Dahlin, T. (2004). *Quick clay in Sweden.*
- Reutz, E. H. (2022). *Akuttbistand skred Ask, Gjerdrum* (Nr. 20200909-02-R).
- Robertson, P. K. (2010). *Soil behaviour type from the CPT: an update.* 8.
- Rydman, O. (2021). *Integration of Borehole, Ground, and Airborne Data to Improve Identification of Areas With Quick Clays in Sweden.* <https://www.diva-portal.org/smash/get/diva2:1566426/FULLTEXT01.pdf>
- Rømoen, M., Pfaffhuber, A. A., Karlsrud, K., & Helle, T. E. (2010a). *Resistivity on marine sediments retrieved from RCPTUsoundings: A Norwegian case study.* 8.

- Rømøen, M., Pfaffhuber, A. A., Karlsrud, K., & Helle, T. E. (2010b). *Resistivity on marine sediments retrieved from RCPTUsoundings: A Norwegian case study.*
- Salas-Romero, S., Malehmir, A., & Snowball, I. (2016). *Combined Land and River High-resolution Reflection Seismic Imaging of an Area Prone to Quick-clay Landslides in Sweden.* <https://doi.org/10.3997/2214-4609.201601912>
- Sandven, R., Montafia, A., Gylland, A. S., Pfaffhuber, A. A., Kåsin, K., & Long, M. (2015). *NIFS* (Nr. 126–2015). NIFS.
- Sandven, R., Senneset, K., Emdal, A., Nordal, S., Janbu, N., Grande, L., & Amundsen, H. A. (2017). *Geotechnics Field and Laboratory Investigations.*
- Sauvin, G. (2014). *Integrated geophysics for mapping of quick-clay landslide-prone areas in Norway* [Doctoral thesis]. <https://www.duo.uio.no/handle/10852/39924>
- Sauvin, G., Lecomte, I., Bazin, S., Hansen, L., Vanneste, M., & L'Heureux, J.-S. (2014). On the integrated use of geophysics for quick-clay mapping: The Hvittingfoss case study, Norway. *Journal of Applied Geophysics*, *106*, 1–13. <https://doi.org/10.1016/j.jappgeo.2014.04.001>
- Shan, C., Bastani, M., Malehmir, A., Persson, L., & Engdahl, M. (2014). *Integrated 2D modeling and interpretation of geophysical and geotechnical data to delineate quick clays at a landslide site in southwest Sweden.*
- Sharma, P. V. (1997). *Environmental and Engineering Geophysics.* Cambridge University Press.
- Solberg, I.-L., Hansen, L., Rønning, J., Haugen, E., Dalsegg, E., & Tønnesen, J. (2012). Combined geophysical and geotechnical approach to ground investigations and hazard zonation of a quick clay area, mid Norway. *Bulletin of Engineering Geology and The Environment - BULL ENG GEOL ENVIRON*, *71*. <https://doi.org/10.1007/s10064-011-0363-x>

- Solberg, I.-L., Long, M., Baranwal, V. C., Gylland, A. S., & Rønning, J. S. (2016). *Geophysical and geotechnical studies of geology and sediment properties at a quick-clay landslide site at Esp, Trondheim, Norway.*
- Solberg, I.-L., Rønning, J. S., Dalsegg, E., Hansen, L., Rokoengen, K., & Sandven, R. (2008). Resistivity measurements as a tool for outlining quick-clay extent and valley-fill stratigraphy: A feasibility study from Buvika, central Norway. *Canadian Geotechnical Journal*, 45(2), 210–225. <https://doi.org/10.1139/T07-089>
- Tavakoli, S. (2011). *GEO4120: Near-Surface Geophysics.*
- Tavakoli, S., Geomap Norge, Viken fylkeskommune, Eskeland electronics, & Aarhus GeoInstruments. (2022). *HiGELIG - High resolution Geophysical mapping of the quick clays in Gjerdrum.*
- Torrance, J. K. (1974). *A laboratory investigation of the effect of leaching on the compressibility and shear strength of Norwegian marine clays.*
- Vest Christiansen, A., & Auken, E. (2012). A global measure for depth of investigation. *GEOPHYSICS*, 77(4), WB171–WB177. <https://doi.org/10.1190/geo2011-0393.1>
- With, C., Löfroth, H., Bastani, M., Persson, L., Rodhe, L., Hedfors, J., & Schoning, K. (2022). A methodology for mapping of quick clay in Sweden. *Natural Hazards*, 112(3), 2549–2576. <https://doi.org/10.1007/s11069-022-05278-y>
- Aarhus GeoInstruments. (2022). *TTEM 3x3 | Aarhus GeoInstruments.* Home. <https://www.aarhusgeoinstruments.dk/ttem-3x3>

Attachments

Appendix A: Profile drawings

Appendix B: CPTu-interpretation (Mayne)

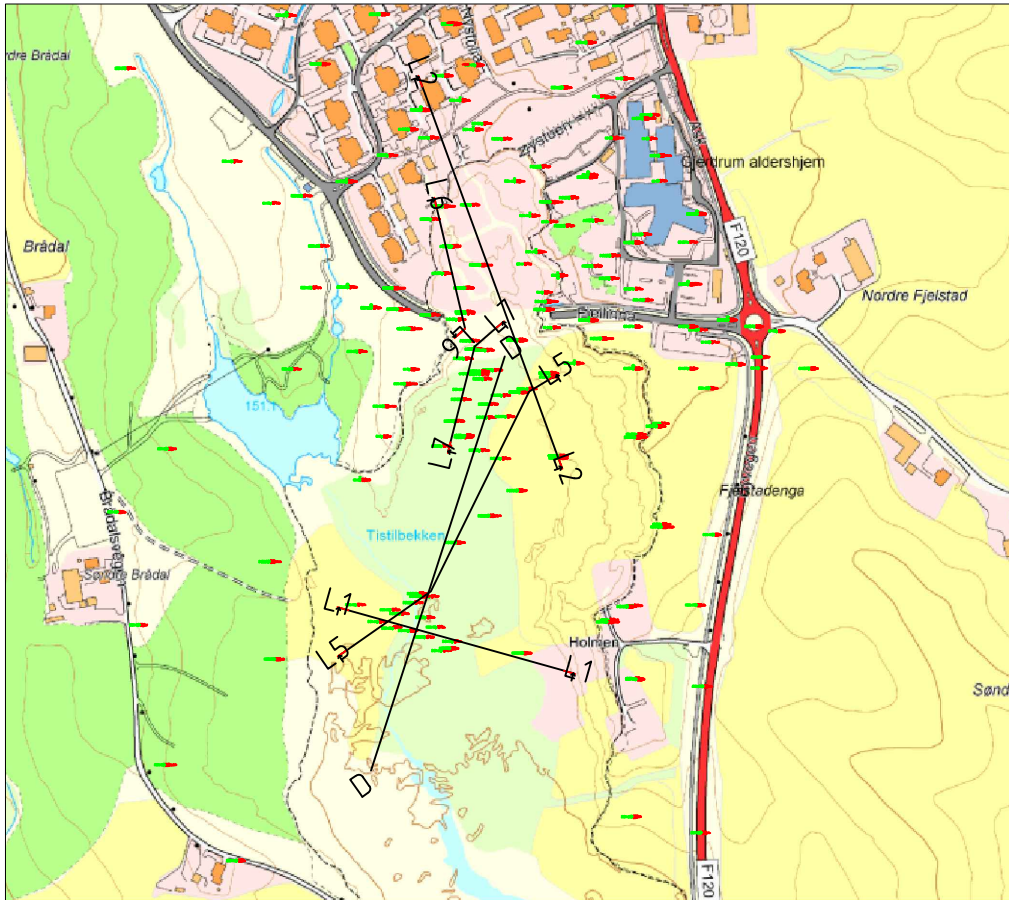
Appendix C: Other geotechnical parameters


Appendix D: Overview of interpreted boreholes

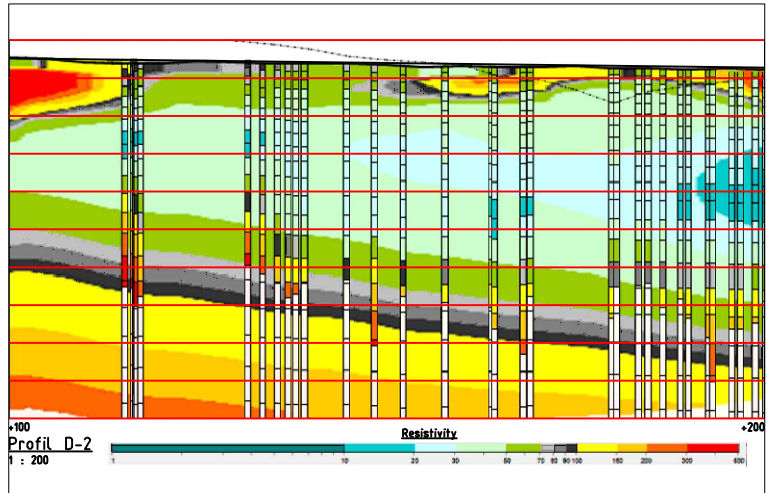
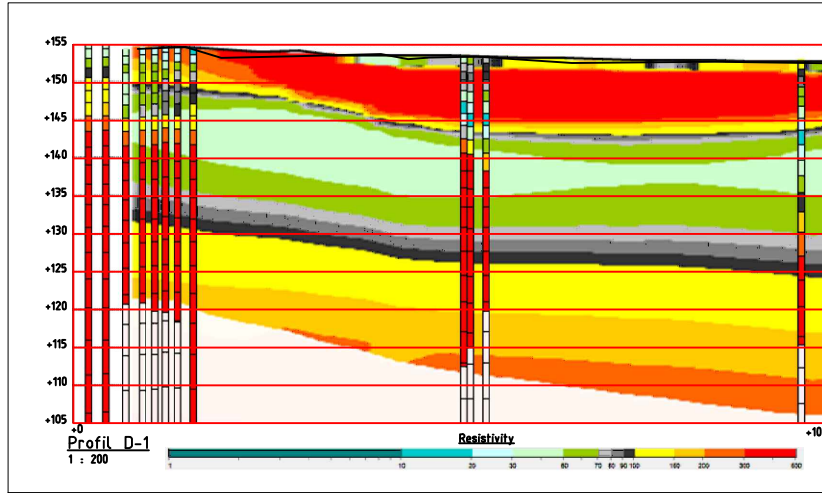
Appendix A: Profile drawings


Table 16. Profile drawings

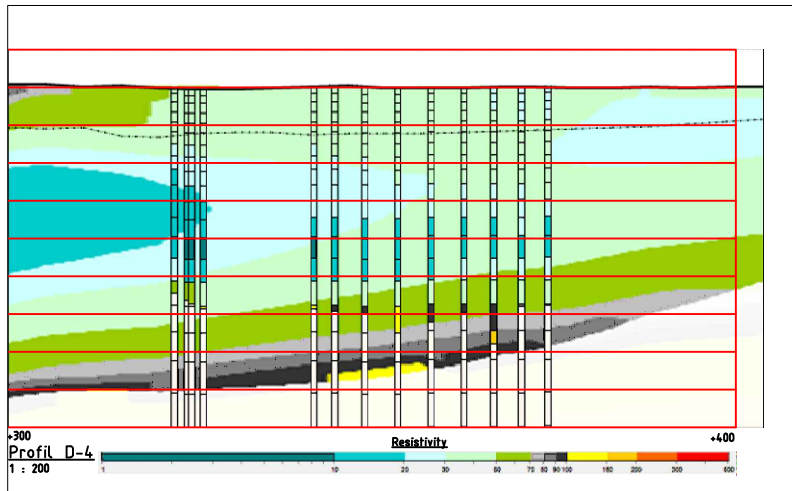
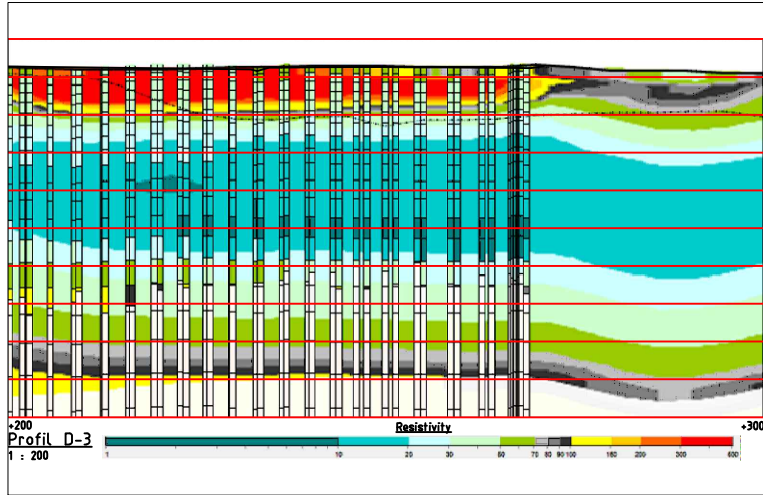
Drawing nr.	Name
1.	Overview profiles
2.	ERT and tTEM, D1,D2
3.	ERT and tTEM, D3,D4
4.	Profile D, geotechnical
5.	tTEM, D1,D2
6.	tTEM, D3,D4
7.	ERT, D1,D2
8.	ERT, D3,D4
9.	Profiles L1,L2,L6,L7
10.	Profile L5




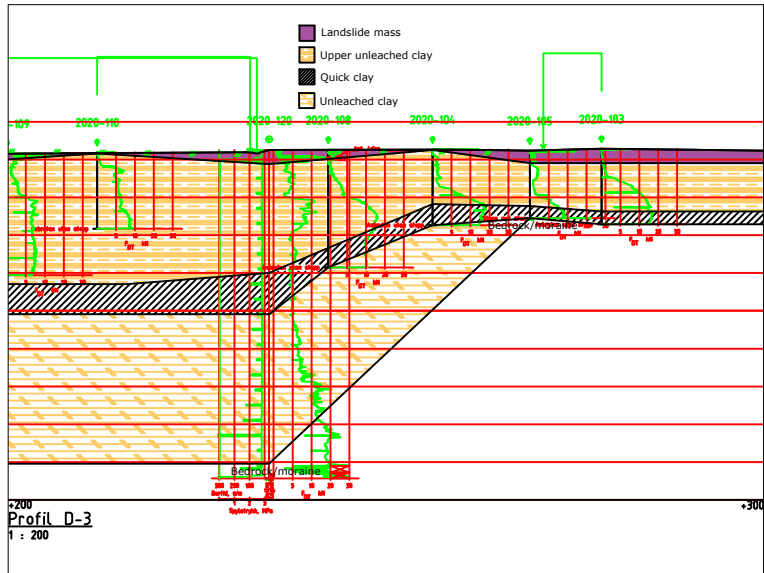
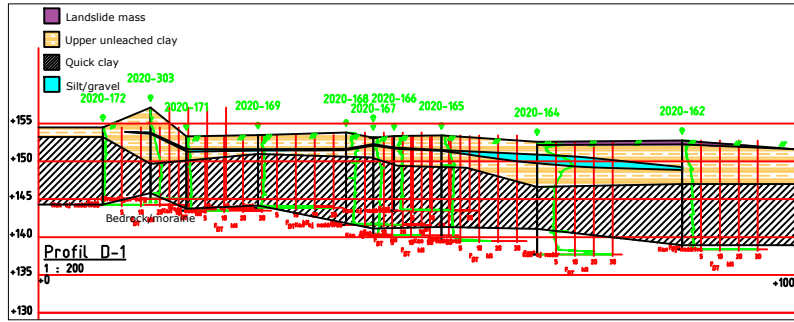
□ Overview profiles		Nr. 1
Drawer: KGr		 NTNU Norwegian University of Science and Technology
Scale:	Date: 16.05.2023	




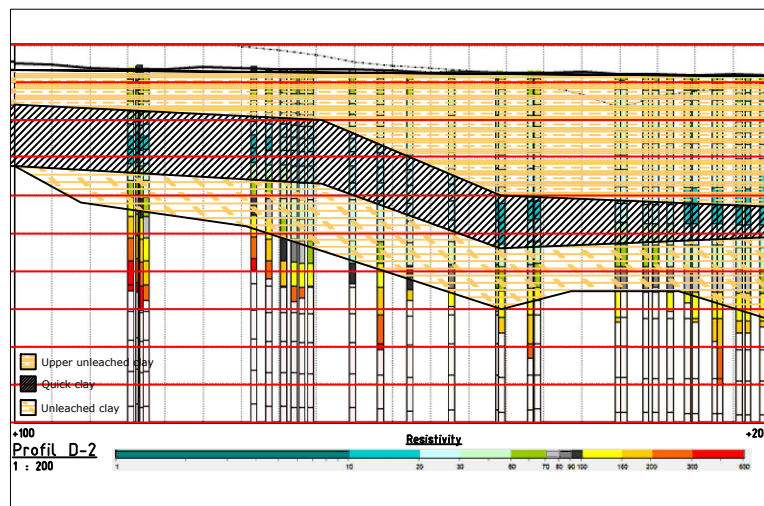
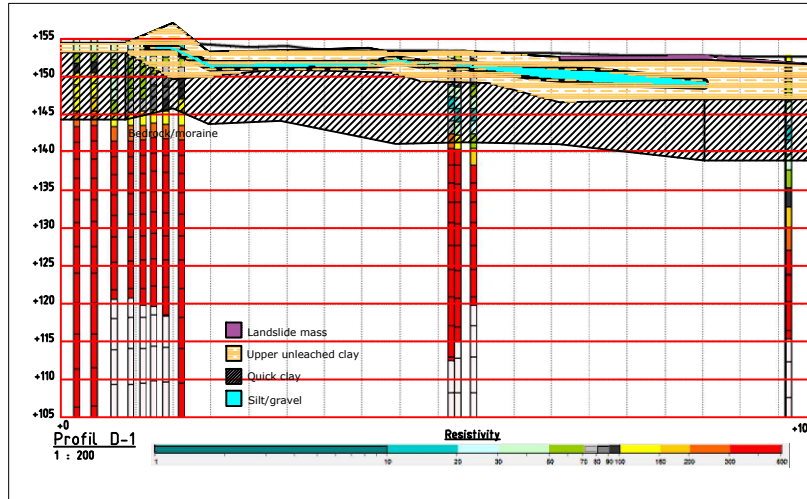
ERT and tTEM, D-1,D-2		Nr. 2
Drawer: KGr		 NTNU Norwegian University of Science and Technology
Scale:	Date: 16.05.2023	




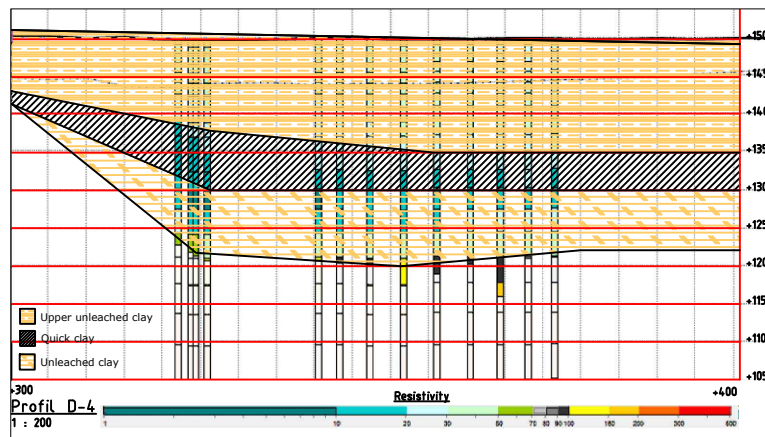
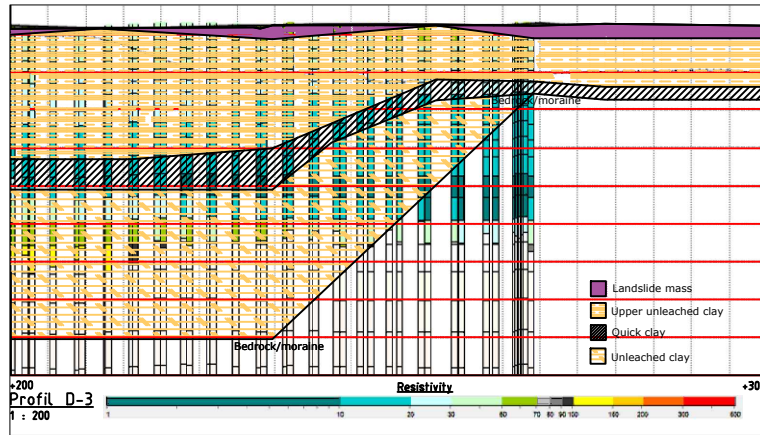
ERT and tTEM, D-3,D-4		Nr. 3
Drawer: KGr		 NTNU Norwegian University of Science and Technology
Scale:	Date: 16.05.2023	




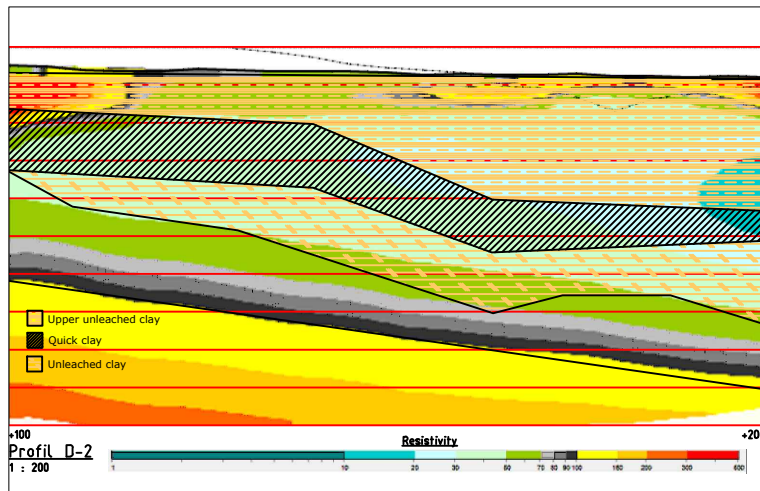
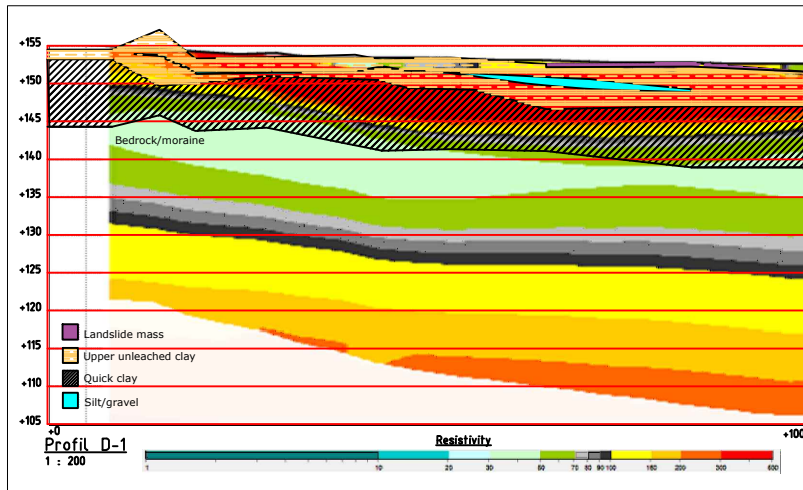
Profile D, geotechnical		Nr. 4
Drawer: KGr		 NTNU Norwegian University of Science and Technology
Scale:	Date: 16.05.2023	




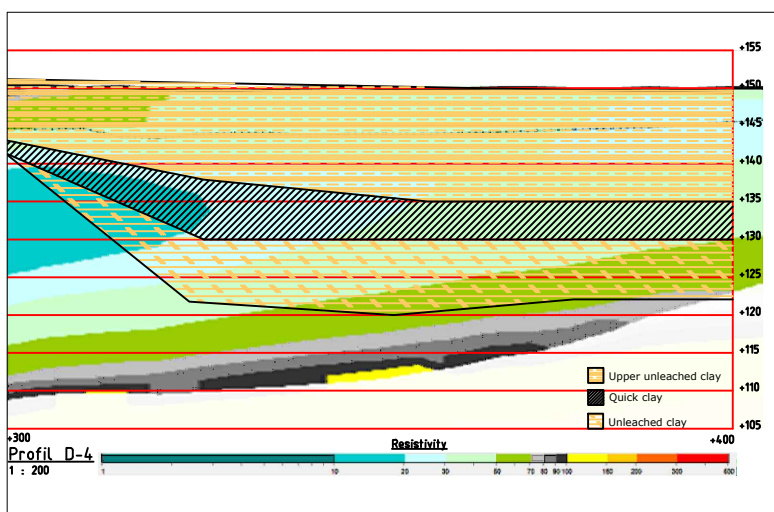
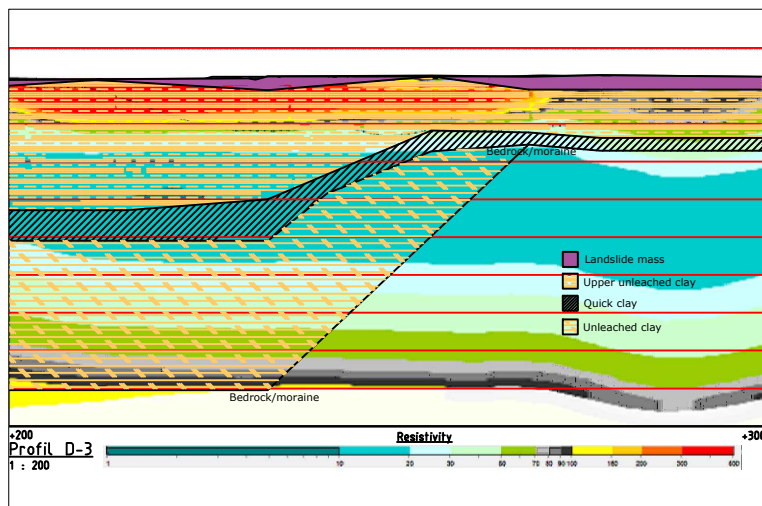
tTEM, D-1,D-2		Nr. 5
Drawer: KGr		 NTNU Norwegian University of Science and Technology
Scale:	Date: 16.05.2023	




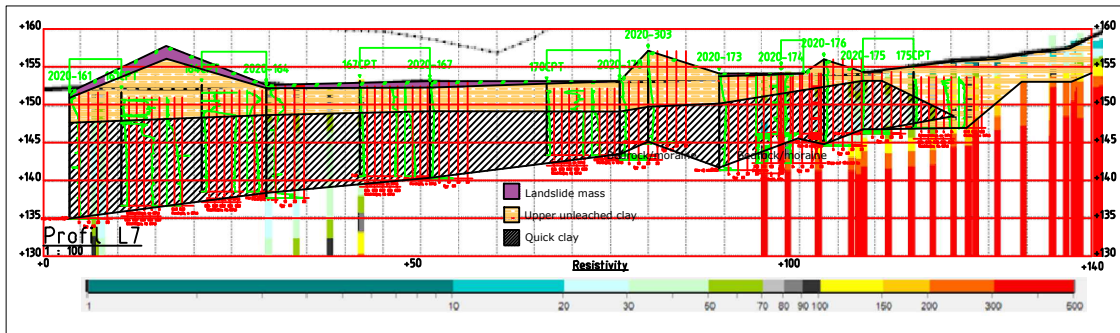
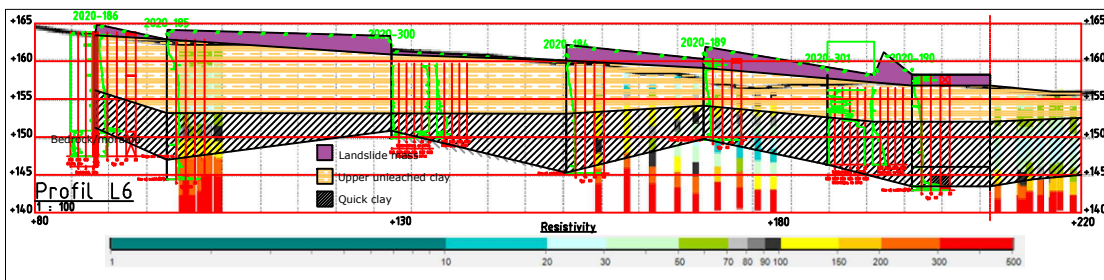
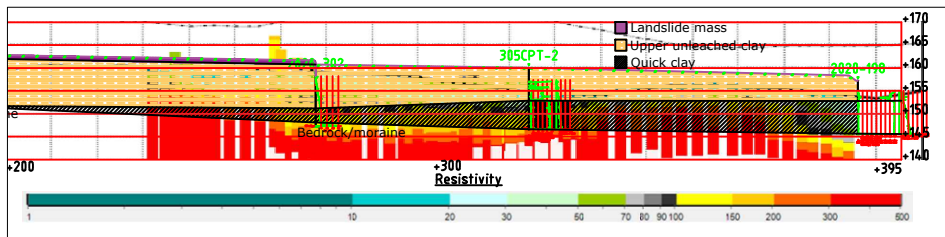
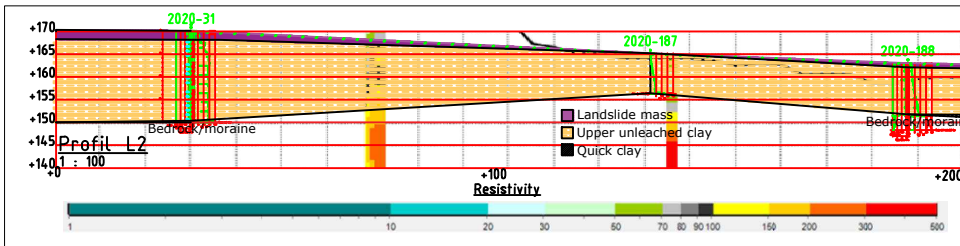
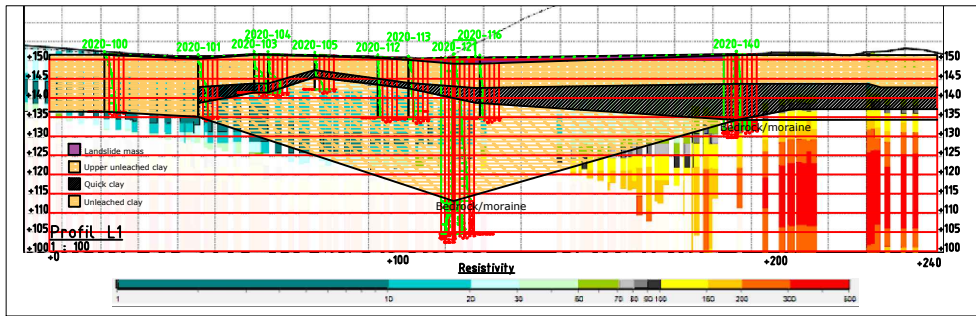
tTEM, D-3,D-4		Nr. 6
Drawer: KGr		 NTNU Norwegian University of Science and Technology
Scale:	Date: 16.05.2023	




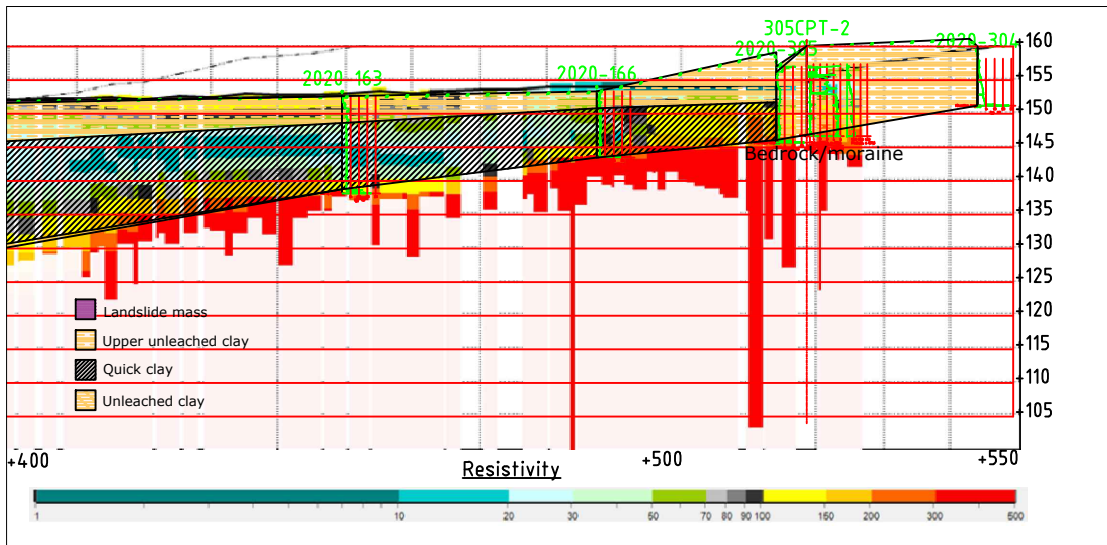
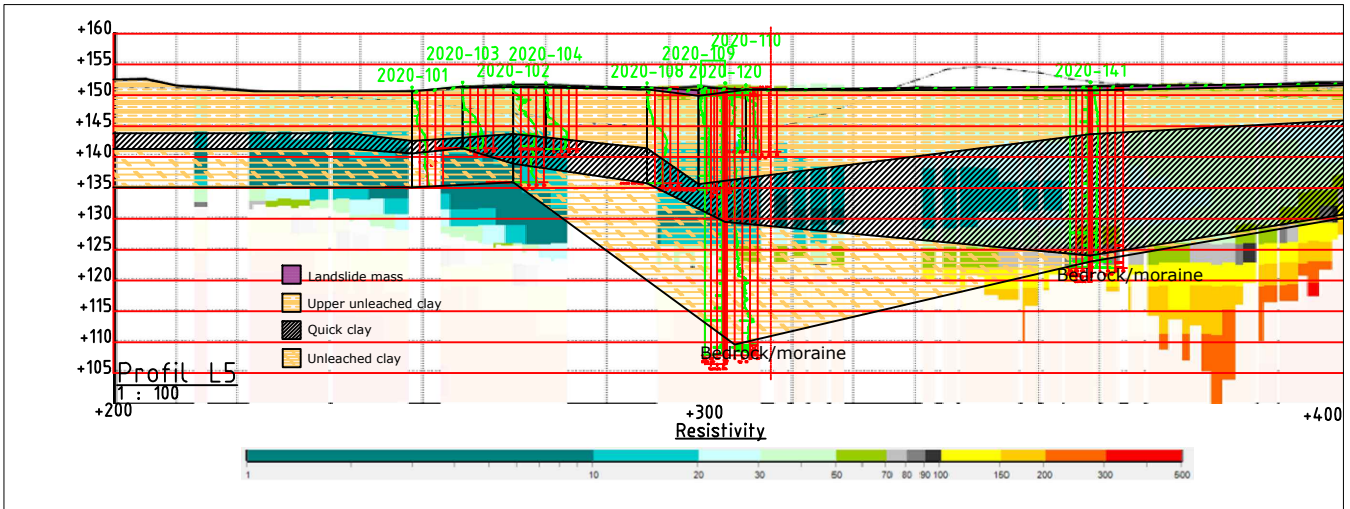
ERT, D-1,D-2		Nr. 7
Drawer: KGr		 NTNU Norwegian University of Science and Technology
Scale:	Date: 16.05.2023	




ERT, D-3,D-4		Nr. 8
Drawer: KGr		 NTNU Norwegian University of Science and Technology
Scale:	Date: 16.05.2023	



Profiles L1, L2, L6, L7		Nr. 9
Drawer: KGr		 NTNU Norwegian University of Science and Technology
Scale:	Date: 16.05.2023	



Profile L5		Nr. 10
Drawer: KGr		 NTNU Norwegian University of Science and Technology
Scale:	Date: 16.05.2023	

Appendix B: CPTu-interpretation (Mayne)

In this study, the boreholes most often consist of a rotary pressure or total sounding, and a CPTU in every point. However, a few points of interest only have CPTU data available. Because of this, CPTU data is also used to identify quick clay based on methods suggested in earlier study (see Mayne et al., 2019). To interpret sensitive layers with CPTU data, there exist several methods, see Grønvold, (2022) for examples. The Mayne approach (Agaiby & Mayne, 2021; Mayne et al., 2019) uses difference in preconsolidation stress to differentiate insensitive clay from quick clay. Mayne's method indicates sensitive clays when a following hierarchical sorting is present: $0,60 q_E < 0,33 q_{net} < 0,53 \Delta u_2$.

2020-140:

	DrT/TOT	Mayne	Agreement
Firm clay	0-7m	0-7,8m	Very good
Quick clay	7-17m	7,8-17m	

2020-141:

	DrT/TOT	Mayne	Agreement
Firm clay	0-7m	0-7,8m	Very good
Quick clay	7-27m	7,5-27m	

2020-164:

	Sample	DrT/TOT	Mayne	Agreement
Quick clay	4-12m	4-14m	4-14m	Very good

2020-120:

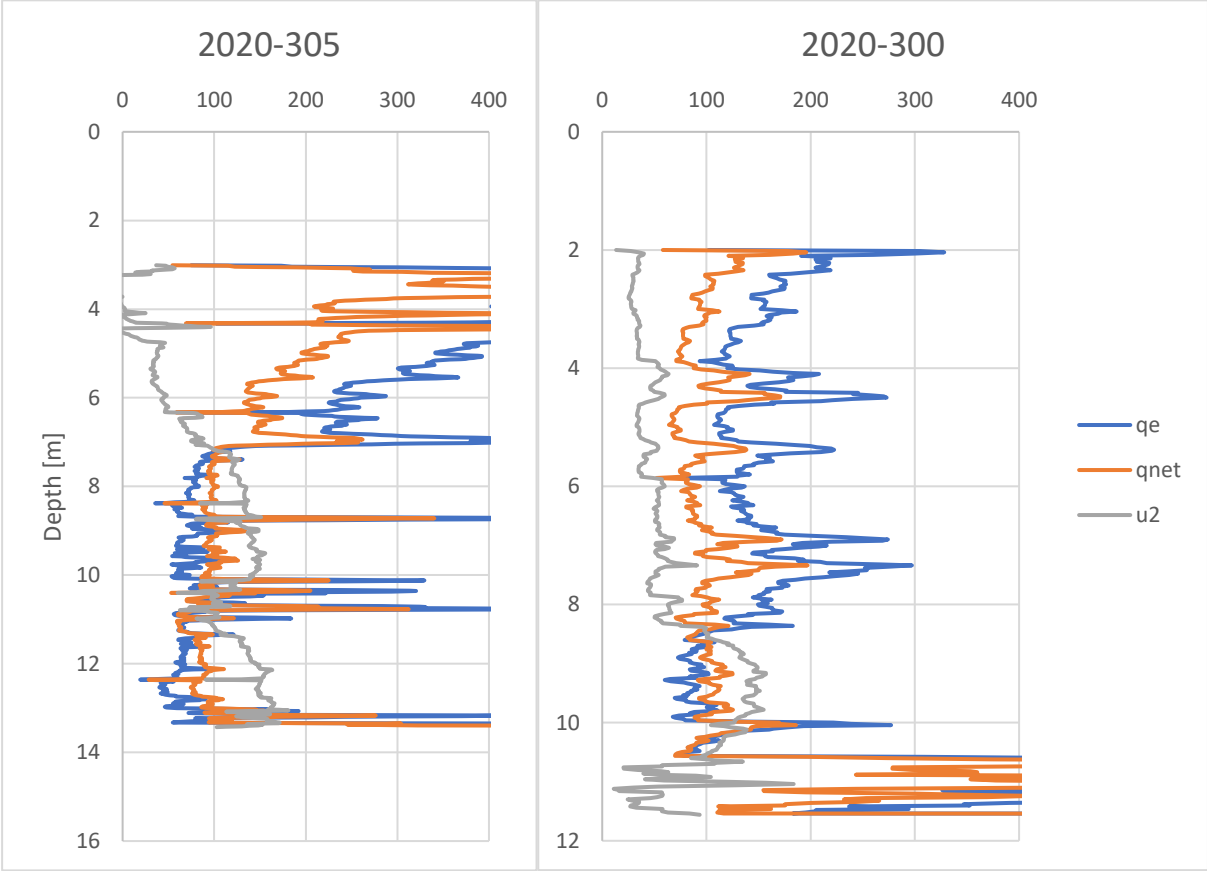
	Sample	DrT/TOT	Mayne	Agreement
Firm clay	6-16m	0-10m	2-10m	TOT vs Mayne: Very good.
Quick clay	-	10-22m	10-23m	
Firm clay	-	22-43m	-	Sample vs Mayne: Poor

2020-121:

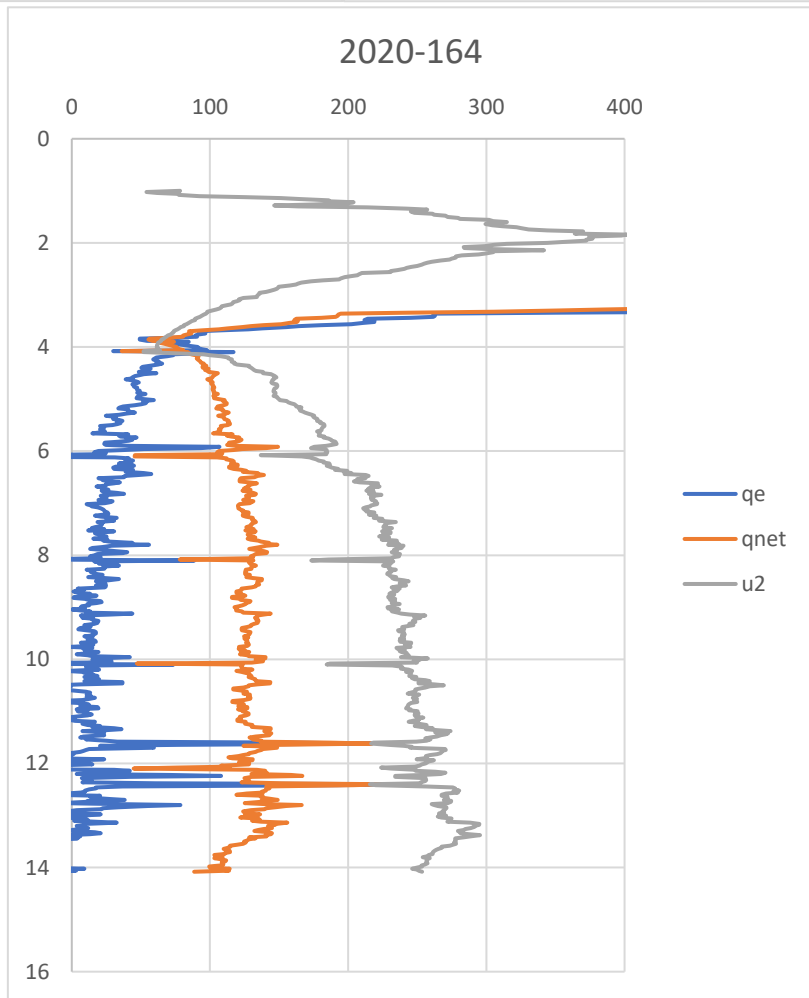
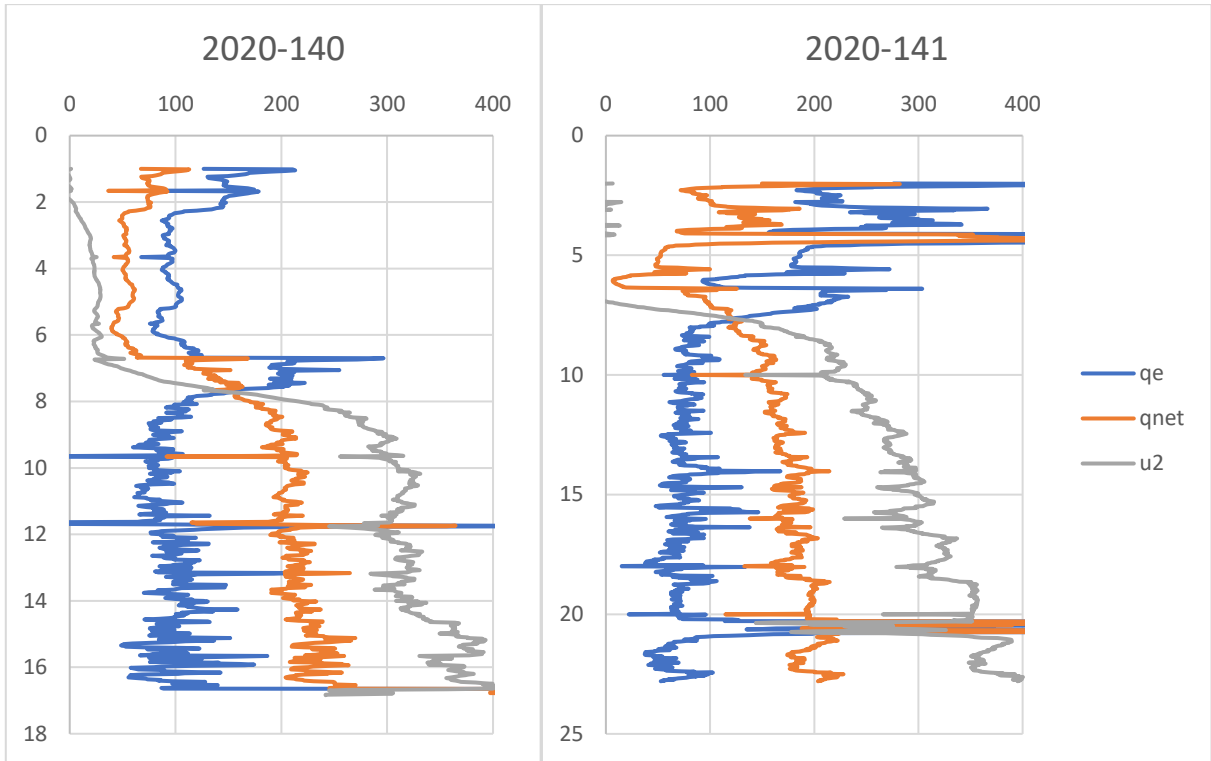
	Sample	DrT/TOT	Mayne	Agreement
Firm clay	6-7m	0-23m	2-9m	TOT vs Mayne: Poor Sample vs Mayne: OK
Quick clay	7-12m	-	9-23m	
Firm clay	12-16m	-	-	

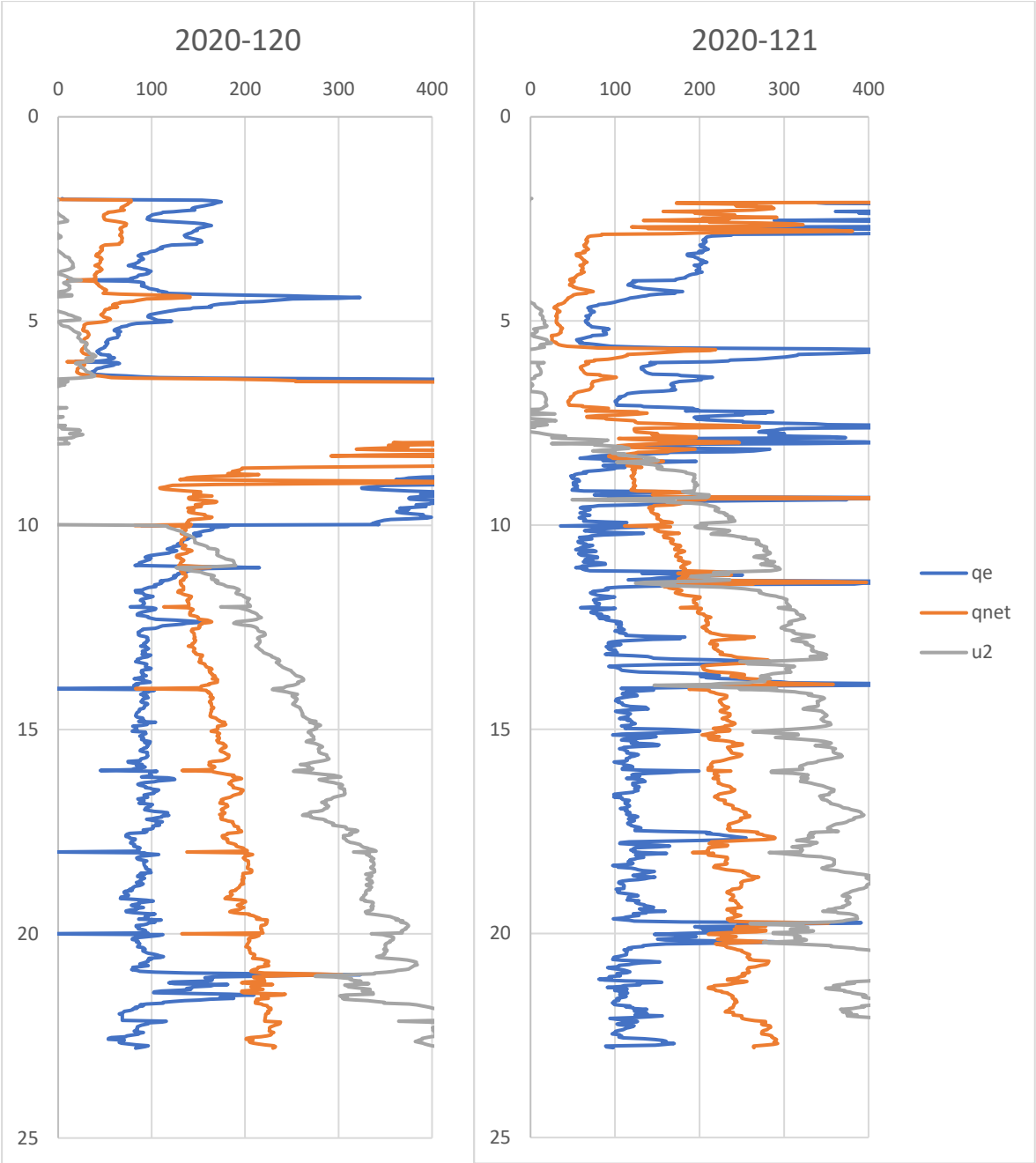
The Mayne approach often agrees well with total and rotary pressure soundings in the area. In 2020-164, the stress approach also matches up very well with the sample. However, in borehole 2020-120 and 2020-121, the sampling does not correlate well with Mayne.

Based on these results, the Mayne approach has been used to interpret the layering. In borehole 2020-300 and 2020-305, CPTu-data is the only data available. These boreholes are present in profiles L2, L5 and L6.



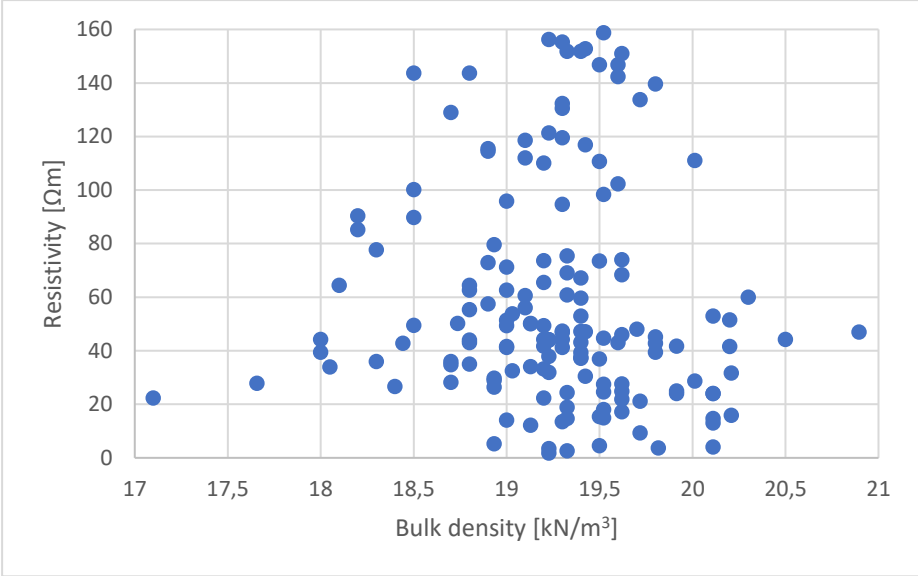
2020-305 indicate quick clay from 7-10m and from 11.5-13m, 2020-300 indicate quick clay from 8.5-10m.





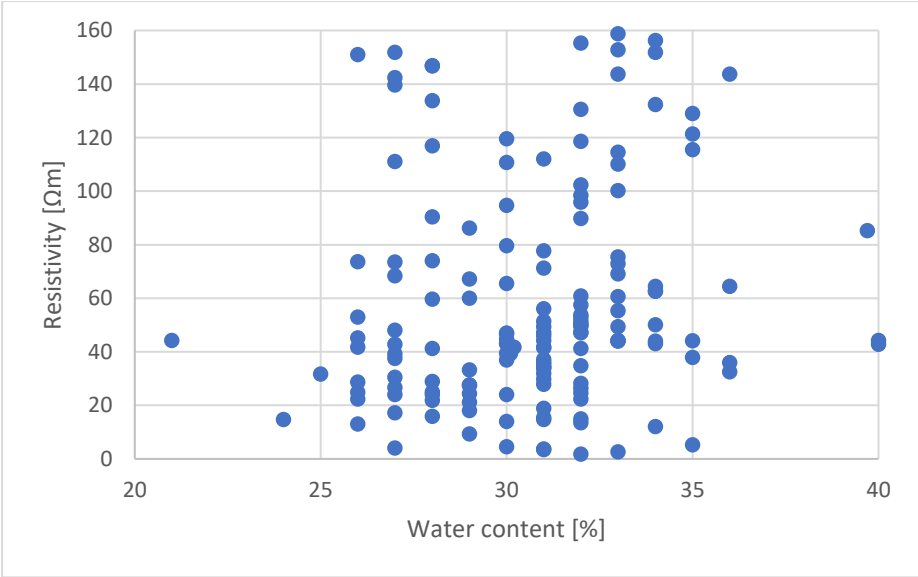
Appendix C: Other geotechnical parameters

Bulk density



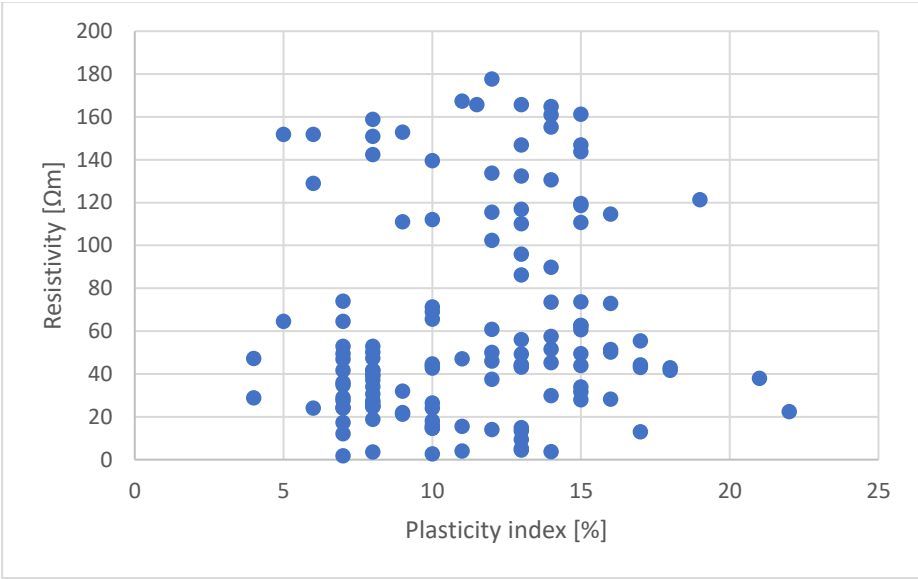
The bulk density of clay in the area varies from 17-21 kN/m³. Bulk density below 20 Ωm usually lies from 19-20,2 kN/m³, and is given somewhat higher values than samples with resistivity ranging from 20-100 Ωm.

Water content



Water content of clay in the area varies from 20-40 %. There are not really any clear trends in this plot.

Plasticity index



Plasticity index varies from 4-22. The plot shows no clear trends.

Appendix D: Overview of interpreted boreholes

Most of the boreholes available in Gjerdrum has been interpreted through this thesis to assist the HiGELIG project. An overview of all geotechnical data considered in this thesis is shown in Table 17.

Table 17. List of interpreted boreholes

Abbreviation	Report nr.	First borehole	Last borehole
NGI-01	20200909-01-R	2020-01	2020-54, G2-3
M-01	10223695-02-RIG-RAP-002	2020-71	2020-154
NGI-02	20200909-02-R	2020-161	2020-407
M1	-	M106	M110
M3	102351-1	M301	M306
M4	23802	M401	M406, MPR1
M5	8623-0	M500	M513
M8	111695	M801	M804
L1	08-56	L101	L128
L2	12-308	L201	L210
L3	13-12	L301	L307
L5	14-65	L501	L507
L6	15444	L601	L606
N1	20031570	N101	N104
N2	20071384	N201	N206
N3	20150630	N310	N312
N4	20150756	N401	N407
N5	63-63	N519	N526
N6	20021504	N601	N609

The boreholes are interpreted based on a simplified layering of the soil types that are most relevant in this area. These layers included are shown in Table 18. Boreholes are systemized in Microsoft Excel with their interpreted layering. After this, the excel-file can be read to Aarhus Workbench, systemizing the interpreted layering for comparison with geophysical data.

Table 18. Simplified layering

Soil types	Abbreviation	ID
Dry crust	D	1
Clay	C	2
Quick clay	Qc	3
Sand or silt	S	4
Moraine or gravel	M	5
Bedrock (intact)	R	6
Landslide mass	L	7



NTNU

Norwegian University of
Science and Technology